The University of Southern Mississippi

The Aquila Digital Community

Dissertations

Spring 5-2012

New Dual Initiators for Polyisobutylene-Based Block and Star Polymers

Yaling Zhu
University of Southern Mississippi

The University of Southern Mississippi

NEW DUAL INITIATORS FOR POLYISOBUTYLENE-BASED

BLOCK AND STAR POLYMERS

by

Yaling Zhu

Abstract of a Dissertation
Submitted to the Graduate School
of The University of Southern Mississippi
in Partial Fulfillment of the Requirements
for the Degree of Doctor of Philosophy

May 2012

ABSTRACT

NEW DUAL INITIATORS FOR POLYISOBUTYLENE-BASED

BLOCK AND STAR POLYMERS

by Yaling Zhu

May 2012

Polyisobutylene (PIB), available solely by living carbocationic polymerization (LCP), is a commercially important polymer with excellent thermal stability, good flexibility and extraordinary impermeability to gases. Due to these attractive properties, coupling PIB to other polymer blocks is expected to result in new and useful products. Two types of new dual initiators possessing initiating sites for both LCP and atom transfer radical polymerization (ATRP), have been designed for the preparation of AB linear and A_2B miktoarm star copolymers, where A is PIB-based block copolymer that grows cationically and B is polyacrylate or other radically-derived polymer block, without intermediate modification.

Mono-cationic mono-radical dual initiators, 3,3,5-trimethyl-5-chlorohexyl 2-bromopropionate (IB_2BP) and 3,3,5-trimethyl-5-chlorohexyl 2-bromo-2-methylpropionate (IB_2BMP) were synthesized and used to prepare AB linear polymers. PIBs obtained from both initiators showed high efficiency in ATRP initiations of methyl acrylate (MA), yielding polymers with targeted block length and narrow polydispersity index (PDI). However, IB_2BMP and IB_2BP displayed slow cationic initiation of isobutylene (IB) leading to moderate initiation efficiencies ($0.50 < I_{eff} < 0.80$) at low temperature (-70 °C) and low monomer/initiator ratio (82). 3,3,5,5,7-Pentamethyl-7-chlorooctyl 2-bromo-2-methylpropionate (IB_3BMP), which differs from IB_2BMP by the

inclusion of one additional isobutylene (IB) repeating unit, was then synthesized. It

showed quantitative initiation efficiency (I_{eff} ~1) in TiCl$_4$-co-initiated LCP of IB under

various reaction conditions. I_{eff} and PDI of the resulting PIBs were identical to those

obtained with the standard mono-cationic initiators. The superiority of IB$_3$BMP

compared to IB$_2$BMP in carbocationic initiation was attributed to elimination of

through-space interactions between the *tert*-chloride initiating site and the

TiCl$_4$:carbonyl complex at the ATRP initiating site.

Di-cationic mono-radical dual initiator 3-[3,5-bis(1-chloro-1-

methylethyl)phenyl]-3-methylbutyl 2-bromo-2-methylpropionate (DCCBMP) was

syntheized for the preparation of miktoarm star copolymers. Initiation efficiency of

DCCBMP was high (0.89 < I_{eff} < 0.98) for LCP of IB and it was comparable to the

standard di-cationic initiator. Using sequential monomer addition under LCP

conditions, narrow-polydispersity poly(styrene-*b*-isobutylene-*b*-styrene) (PS-PIB-PS)

triblock copolymers were prepared, yielding poly(acrylic acid-*b*-styrene-*b*-isobutylene)$_2$-

s-poly(acrylic acid) [(PAA-PS-PIB)$_2$-*s*-PAA] amphiphilic miktoarm star polymer after

ATRP of *tert*-butyl acrylate (*t*BA) and thermolysis of poly(*tert*-butyl acrylate) (P*t*BA)

block. Upon thermolyzing PS-PIB-PS macroinitiator, poly(styrene-*b*-isobutylene)$_2$-*s*-

poly(acrylic acid) [(PS-PIB)$_2$-*s*-PAA] stars were obtained in the same manner.

The University of Southern Mississippi

NEW DUAL INITIATORS FOR POLYISOBUTYLENE-BASED

BLOCK AND STAR POLYMERS

by

Yaling Zhu

A Dissertation
Submitted to the Graduate School
of The University of Southern Mississippi
in Partial Fulfillment of the Requirements
for the Degree of Doctor of Philosophy

Approved:

Robson F. Storey_____
Director

Sarah E. Morgan_____

Sergei I. Nazarenko_____

William L. Jarrett_____

Jeffrey S. Wiggins_____

Susan A. Siltanen_____
Dean of the Graduate School

May 2012

DEDICATION

To my father, Bingqiu Zhu,

for your endless love and support.

ACKNOWLEDGMENTS

TABLE OF CONTENTS

LIST OF TABLES

Table

LIST OF ILLUSTRATIONS

LIST OF ABBREVIATIONS

$<R_h>$	average hydrodynamic radius
2-PIB-furan	ω-furan functionalized PIB
AIBN	azobisisobutyronitrile
ATR	attenuated total reflectance
ATRP	atom transfer radical polymerization
b.p.	boiling temperature
BDPEP	2,2-bis[4-(1-phenylethenyl)phenyl]propane
BDTEP	2,2-bis[4-(1-tolylethenyl)phenyl]propane
bFPF	2,5-bis(2-furyl-2-propyl)furan
bis-DPE	bis-diphenylethylenes
BMP-PIB	PIB with 2-bromo-2-methylpropionate head group
BPPC	2,2-bis((2-bromo-2methyl)propionatomethyl)propionyl chloride
BP-PIB	PIB with 2-bromopropionate head group
bTPB	1,3-bis[2-(3-trimethylsilyl)propenyl]benzene
CMC	critical micelle concentration
DCBBMP	3-[3,5-bis(1-bromo-1-methylethyl)phenyl]-3-methylbutyl 2-bromo-2-methylpropionate
DCCBMP	3-[3,5-bis(1-chloro-1-methylethyl)phenyl]-3-methylbutyl 2-bromo-2-methylpropionate
DCOHBMP	3-[3,5-bis(1-hydroxy-1-methylethyl)phenyl]-3-methylbutyl 2-bromo-2-methylpropionate

DCOOHBMP   3-[3,5-bis(1-hydroperoxy-1-methylethyl)phenyl]-3-methylbutyl 2-bromo-2-methylpropionate

DHTMH   1,5-dihydroxy-3,3,5-trimethylhexane

DIPBMP   3-(3,5-diisopropylphenyl)-3-methylbutyl 2-bromo-2-methylpropionate

DMVBMP   3-(3,5-diisopropenylphenyl)-3-methylbutyl 2-bromo-2-methylpropionate

DPE   1,1-diphenylethylene

DSC   differential scanning calorimetry

DTE   1,1-ditolylethylene

DVB   divinylbenzene

EI   electron impact

$\overline{F}_n$ number average of functionality

FTIR   Fourier transform infrared spectroscopy

Hex   hexane

HRMS   high-resolution mass spectrometry

I   initiator

IB   isobutylene

IB_2BMP 3,3,5-trimethyl-5-chlorohexyl 2-bromo-2-methylpropionate

IB_2BP 3,3,5-trimethyl-5-chlorohexyl 2-bromopropionate

IB_3BMP 3,3,5,5,7-pentamethyl-7-chlorooctyl 2-bromo-2-methylpropionate

I_{eff} initiation efficiency

ISP   poly(isoprene-b-styrene-b-2-vinylpyridine)

LAP   living anionic polymerization

LCP   living carbocationic polymerization

M	monomer
m.p.	melting temperature
MA	methyl acrylate
MacroI	macroinitiator
MALLS	multi-angle laser light scattering
MATMS	2-methallyltrimethylsilane
MCHex	methylcyclohexane
MeCl	methyl chloride
MeVE	methyl vinyl ether
MMA	methyl methacrylate
$\overline{M}_n$	number average of molecular weight
N_{agg}	micelle aggregation number
NBS	*N*-bromosuccinimide
NHPI	*N*-hydroxyphthalimide
NMP	nitroxide-mediated polymerization
NMR	nuclear magnetic resonance
PAA	poly(acrylic acid)
PB	polybutadiene
PDI	polydispersity index
PDMS	polydimethylsiloxane
PEO	poly(ethylene oxide)
PI	polyisoprene
PIB	polyisobutylene

PIB-allyl-X   haloallyl end-functionalized PIB

PInd   polyindene

PM1H   2,4,4,6,6-pentamethyl-1-heptene

PMA   poly(methyl acrylate)

PMDETA   1,1,4,7,7-pentamethyldiethylenetriamine

PMeVE   poly(methyl vinyl ether)

PMHCl   2-chloro-2,4,4,6,6-pentamethylheptane

PMMA   poly(methyl methacrylate)

PS   polystyrene

P*t*BA   poly(*tert*-butyl acrylate)

PTHF   poly(tetrahydrofuran)

PTPB   1-(2-propenyl)-3-[2-(3-trimethylsilyl)-propenyl]benzene

RAFT   reversible addition-fragmentation chain transfer

RMC   rapid monomer consumption

ROP   ring opening polymerization

SEC   size exclusion chromatography

SIP   poly(styrene-b-isoprene-b-2-vinylpyridine)

*t*BA   tert-butyl acrylate

t-Bu-*m*-DCC   5-*tert*-butyl-1,3-(1-chloro-1-methylethyl)benzene

TEA   triethylamine

TEM   transmission electron microscopy

THF   tetrahydrofuran

TMCHA   3,3,5-trimethyl-5-chlorohexyl acetate

TMHDCl	1,5-dichloro-3,3,5-trimethylhexane
TMPCl	2-chloro-2-methyl-2,4,4-trimethylpentane
TMS	tetramethylsilane
TPE	thermoplastic elastomer
$\overline{X}_n$	degree of polymerization

CHAPTER I

SYNTHETIC STRATEGIES FOR POLYISOBUTYLENE-BASED POLYMERS

USING CONTROLLED/LIVING POLYMERIZATIONS

Polyisobutylene (PIB) is a commercially important polymer with a large number of applications due to its excellent UV and thermal-oxidative stability, good flexibility at low and ambient temperatures, high mechanical damping, high gas impermeability, as well as good biocompatibility. It was first invented by BASF Corp. in the late 1930s, and they have marketed a few PIB products such as Oppanol® and Glissopal®. Today, over 19 chemical companies, including many key and niche players such as Chevron Oronite Company LLC, Exxonmobil Corp, Lanxess Corp, and TPC group Inc., manufacture polyisobutylene or PIB-based products.

Low-molecular-weight PIBs ranging in form from viscous liquids to tacky semisolids are used for lubricating oil and fuel additives,[1] chewing gum base, caulks, and sealants.[2] High-molecular-weight PIBs are rubbery solids and are typically used as plasticizers and impact modifiers of thermoplastics. Butyl rubber, a copolymer consisting of isobutylene (IB) monomer with a few percent of isoprene comonomer, is produced at a rate of about 1 billion pounds annually in the United States.[3] It is widely used in the production of tubeless automobile and truck tires, tire innertubes, ball bladders, cable coatings, automotive parts, construction materials, adhesives, and consumer products. Besides these applications, PIB's biocompatibility and biostability, due to the fully saturated hydrocarbon backbone structure, make it ideal for the healthcare and medical devices fields.[4]

PIB-based Polymers via Living Carbocationic Polymerization (LCP)

The discovery of controlled/living polymerizations is credited to Michael Szwarc.[5] He demonstrated in 1956 that electron transfer from sodium naphthalenide to styrene resulted in stable dimeric dianions of styrene, which subsequently initiated styrene polymerization. Szwarc's research revealed that polymer continued to grow as more monomers were added and that the carbanion propagating center could only be terminated in the presence of terminating agents, such as water, alcohols, acids and esters. This was the first example of a polymerization that could proceed in the absence of termination and chain transfer reactions. Since then, investigateors have been dedicated to developing other controlled/living polymerization mechanisms, such as cationic and radical. Such processes can function without chain breaking side reactions and allow precise control over molecular weights, molecular weight distributions, end-functionalities, and architectures.

Extension of this mechanism to living cationic polymerizations was successfully demonstrated in the mid 1980s. Higashimura et al.[6,7] were the first to observe a living cationic polymerization process when polymerizing isobutyl vinyl ether monomer with a HI/I_2 initiating system in 1984. In 1987, living carbocationic polymerization (LCP) of isobutylene (IB) was reported for the first time by Faust and Kennedy using acetate-BCl_3 initiating systems.[8] The livingness of IB polymerzaiton was indicated by the linear increase in PIB molecular weight with monomer conversion during the course of polymerization.

To achieve living polymerizations with precise control over molecular weight and molecular weight distribution, initiators are carefully designed to begin

polymerization efficiently and fast. Initiators are commonly designed to generate carbocations structurally similar to that of the propagating center. For example, initiators for IB polymerization are often tertiary halides (or acetates) derived from isbutylene dimmer (2,4,4-trimethylphent-2-yl) or cumyl (Figure1). The choice of solvent and Lewis acid (or counterion) is also critical for LCP.[9] For a typical isobutylene polymerization induced by a tertiary alkyl chloride/$TiCl_4$ Lewis acid catalyst, the livingness of polymerization is achieved by introducing a dynamic equilibrium between the active propagating species (ion pairs) and dormant species (covalent chain ends), as shown in Figure 2. Solvent and Lewis acid that have been selected for a polymerization should be able to push the equilibrium to the left, thus reducing the effective concentration of the active propagating center. This decreases the risk of chain-breaking reactions and lowers the overall rate of polymerization, allowing greater synthetic control.

Quenching LCP of IB with hard nucleophiles such as methanol or ammonia yields PIBs with *tert*-chloride chain end functionalities.[10,11] This permits important functional groups such as *exo*-olefin (isobutenyl),[12,13] succinic anhydride,[14] hydroxyl,[15,16,17] phenol,[18] epoxide,[15,16,19,] sulfonic acid,[20] as well as carboxylic acid[21-27] to be added as end groups onto PIB chain end through post-polymerization modifications of the *tert*-chloride functional group. However, PIB propagating chains can also be functionalized *in situ* by quenching the living polymerization with various soft nucleophiles, which do not react (or react very slowly) with the Lewis acid. Successful classes of soft-nucleophilic quenching compounds include non-homopolymerizable olefins (to avoid multiple addtion),[16,28,29,30] sterically hindered

bases,[31,32,33] sulfides,[34,35] and ethers.[36] For example, Kennedy et al.[16,28] reporeted the direct end-capping of PIB carbocations using allyltrimethylsilane to yield an allyl-terminated PIB. In the same manner, quantitative addition of methallyltrimethylsilane[29] and 2-phenylallyltrimethylsilane[30] to the living PIB ends yielded methallyl and α-methylstyryl functional macromonomers, respectively. The one-pot synthesis of *exo*-olefin-terminated PIB[31,32] and halogen-free PIB[33] was accomplished in through β-proton abstraction with a hindered base and *in situ* hydride transfer from tributylsilane, respectively. Morgan et al.[34] quenched the LCPs of IB with mono- and disulfides to form PIB polymers with isopropyl thioether and 2-bromoethylsulfanyl chain ends, respectively.

Quantitative monoadditions of PIBs with 2-substituted furans,[37] bis-furan,[38] thiophene,[39] alkoxybenzenes,[40] and *N*-substitutedpyrroles,[41,42,43] have been achieved under appropriate conditions. Faust et al. reported the synthesis of haloallyl end-functionalized PIBs (PIB-allyl-X, X = Cl or Br) using the quantitative capping reaction of living PIB with 1,3-butadiene.[44,45] The latter authors used several methods to convert the allyl-X groups at the PIB chain ends into useful functionalities including hydroxy, amino, carboxy, azide, propargyl, methoxy, and thymine end groups.[46] More importantly, they studied the initiation behavior of PIBs with allyl halide end group as macroinitiators for atom transfer radical polymerization (ATRP),[47] which will be discussed later in this chapter.

Based on the excellent properties of PIB, coupling this thermally, oxidatively, and hydrolytically stable polymer to a variety of other polymer blocks is expected to produce many new and useful block copolymers. Kennedy and coworkers[48,49,50] were

the first to synthesize poly(styrene-*b*-isobutylene-*b*-styrene) (PS-*b*-PIB-*b*-PS) using a di-functional cationic initiator in the early 1990s. The polymer was produced by bi-directionally polymerizing isobutylene followed by styrene combining living carbocationic polymerization (LCP) and the technique of sequential monomer addition. These copolymers exhibit strong phase separation in the bulk state and constitute a group of useful thermoplastic elastomers (TPEs). These triblock copolymers show excellent low-temperature flexibility and elongation properties, imparted by the rubbery PIB center block, and possess elastic recovery and physical strength properties due to the glassy PS segments.[48-54] Compared to other well-known TPEs such as PS-*b*-polyisoprene (PI)-*b*-PS and PS-*b*-polybutadiene (PB)-*b*-PS, which contain unsaturated double bonds in the middle rubbery segments, PS-*b*-PIB-*b*-PS shows outstanding resistance to oxidation and has long lifetime of usage. Because of its biostability, PS-*b*-PIB-*b*-PS was approved in 2004 to sequester Paclitaxel® on the highly successful Taxus® drug-eluting coronary stent.[55,56]

Over the years, other cationically polymerizable monomers including α-methylstyrene,[57,58,59] *p*-methylstyrene,[60,61] *p*-chlorostyrene,[62] *p*-(*tert*-butyldimethylsiloxy)styrene[63] and vinyl ether[64-67] have also been copolymerized with PIB via sequential monomer addition. Faust et al.[68,69] developed synthesis methods for cases when the second monomer is significantly more reactive than isobutylene. Here good blocking efficiencies were obtained by adding a non-homopolymerizable olefin, such as 1,1-diphenylethylene (DPE) and 1,1-ditolylethylene (DTE), to living PIB to affect complete ionization of the chain ends, followed by adjusting the Lewis acidity prior to the introduction of the second monomer. Alkylfurans represent another class of

non-homopolymerizable monomers useful in preparing block copolymers. By capping

of living PIB chains with 2-alkylfurans instead of DPE or DTE, a stable carbocation is

generated which can initiate the polymerization of methyl vinyl ether (MeVE)

monomer, yielding poly(isobutylene-b-methyl vinyl ether) (PIB-b-PMeVE) diblock

copolymers.[37,70] A potential disadvantage of the capping technique is that it introduces

an additional step in the synthesis of block copolymers. This increases the possibility of

premature chain termination by impurities.

An alternative strategy for the synthesis of symmetric ABA linear triblock

copolymers involves the formation of living AB chains and subsequent coupling them

with an appropriate coupling agent. A number of non-homopolymerizable compounds,

such as bis-diphenylethylenes (bis-DPEs), bis(furanyl) derivatives and allylsilanes, have

been successfully utilized for the efficient coupling of cationic living chains. Cao et

al.[71] succeeded in preparing poly(α-methylstyrene-b-isobutylene-b-α-methylstyrene)

triblock copolymers by coupling living poly (α-methylstyrene-b-isobutylene) diblock

copolymers with 2,2-bis[4-(1-phenylethenyl)phenyl]propane (BDPEP). Faust and

coworkers reported the success for coupling living PIB polymer chains using

BDPEP,[72,73] 2,5-bis(2-furyl-2-propyl)furan (bFPF)[74] and 1,3-bis[2-(3-

trimethylsilyl)propenyl]benzene (bTPB).[30] More interestingly, this group also prepared

star polymers having an average of four PIB arms with high efficiency by the same

coupling strategy using 1-(2-propenyl)-3-[2-(3-trimethylsilyl)-propenyl]benzene

(PTPB).[30] In addition to the methods utilizing non-homopolymerizable olefin agents,

coupling ω-isopropenyl PIB with catalytic amounts of triflic acid (CF$_3$SO$_3$H) in

quantitative yields at -80 °C was reported by Coca and coworkers.[75]

Non-linear polymers are receiving increased attention because of their different rheological, solution, and mechanical properties compared to their linear counterparts. Kennedy and coworkers found that multi-arm PIB stars showed superior rheological behaviors as compared with linear PIBs, making them useful as motor oil additives.[76] The first star polymer prepared via cationic polymerization, although only with three PIB arms radiating from a phenyl ring core, was produced by Kennedy et al.[77] This PIB star polymer was not synthesized by true living polymerization methods, but rather via a transfer-dominated process involving a trifunctional initiator-transfer agent (inifer). Tri- and tetrafunctional initiators were synthesized later for the preparation of well-defined three- and four-arm PIB star polymers using living polymerization technique.[78-81] In 1996 Kennedy and coworkers[82] reported the synthesis of well-defined star polymers with eight PIB arms emanating from a calixarene core, which was produced from the cyclic condensation of a *para*-substituted phenol with formaldehyde. Growing the living polymer chains radically outward from a multifunctional initiator allows for the sequential addition of a second monomer, such as styrene,[51,83,84] or *p*-chlorostyrene,[85] producing versatile thermoplastic elastomers possessing multiple PIB-based block copolymer arms.

Coupling agents, such as cyclosiloxanes and divinylbenzene (DVB), have often been used in the synthesis of non-linear block copolymers, eventhough the number of arms produced by this method is not as controllable as those involving multifunctional initiators. Stars with multiple PS-*b*-PIB arms[84,86] or poly(isobutylene-*b*-indene) (PIB-*b*-PInd) arms[87] emanating from a cyclosiloxane core were synthesized by linking allylic end-functionalized PS-*b*-PIB or PIB-*b*-PInd prearms with cyclosiloxanes. In 1998,

Storey et al.[88] reported the synthesis of a series of gel-core, multi-arm star-branched PIBs via living carbocationic polymerization using a cumyl chloride/$TiCl_4$/pyridine initiating system and DVB as core-forming comonomer. Divinylbenzene (DVB) induced star-block PS-*b*-PIB polymers were also obtained by Kennedy and coworkers.[89] These multiarmed PS-*b*-PIB star block copolymers possess superior tensile properties, lower dynamic melt viscosity, and much lower sensitivity to diblock contamination than their linear triblock counterparts.[86,89]

Hetero-arm stars having a A_nB_m topology can also be prepared using these coupling agents, because the living sites are stoichiometrically retained in the coupled product. The resulting polymer can thus grow new chains outward upon addition of a second monomer.[90] Amphiphilic A_2B_2 star-block copolymers (A is PIB and B is PMeVE) were prepared by the coupling reaction of living PIB followed by the chain ramification polymerization of MeVE at the junction of the living coupled PIB using 2,2-bis[4-(1-tolylethenyl)phenyl]propane (BDTEP).[73] Similarly, A_3B_3 star-block copolymers were formed by reacting ω-furan functionalized PIB (2-PIB-furan), synthesized by end-capping living PIB with 2-Bu_3SnFu, with 1,3,5-tricumyl chloride, followed by polymerizing MeVE from the resulting tri-functional core.[91] The asymmetric star AA'B was obtained by the quantitative addition of 2-PIB-furan to living PIB (designated A' because it has a different molecular weight than 2-PIB-furan), thereby producing living coupled PIB-Fu$^+$-PIB'; this was then successfully employed in the subsequent chain ramification polymerization of MeVE.[70]

The disadvantage of producing A_nB_m hetero-arm stars with coupling agents is the possibly severe steric congestion at the linking site. This especially happens when

the number of arm attachment points is above four or five. Thus, this approach is limited to the synthesis of stars with small numbers of arms. In addition, the arm number is often not controllable with the second double bond causing loops fromation.[92]

PIB-based Polymers via the Combination of Controlled/Living Polymerizations

Block copolymers are able to self-assemble, in bulk as well as in selective solvents, into ordered nanostructures, with domain size and shape as well as the interdomain distance can be manipulated by changing the molecular weight, chemical structure, molecular architecture, and composition of the polymer.[93] Phase behavior for polymers with more than two monomer blocks, also depends on the sequence of the blocks in the chain (i.e., whether it is sequenced A-B-C, B-C-A, or C-A-B).[94,95] Therefore, it becomes increasingly important to develop new synthetic strategies to overcome the synthetic limitations of known techniques in order to simultaneously allow both efficient preparation and precise control over polymer compositions and architectures.[96,97]

Although the technique of sequential monomer addition is simple and direct, it is limited to those monomer combinations that can be polymerized by the same mechanism: anionic, cationic, radical, etc. To create block copolymers from monomers that cannot be polymerized by the same mechanism, one may couple existing prepolymers or combine different controlled/living polymerization methods. As shown in Figure 3, coupling, site transformation (mechanism transformation), and dual initiator approaches were developed to produce new and unique, otherwise unavailable, polymer architectures. Combining different living polymerization techniques, such as anionic or

radical, with LCP can significantly expand the existing synthetic methods, leading to complex but well-defined polymeric materials from new and existing monomers.

As previously discussed, living PIB cationic chains can be coupled using various non-homopolymerizable coupling agents. Similarly, homopolymer blocks prepared by different mechanisms can also be linked using either multifunctional coupling agents or highly efficient chemical reactions and/or physical interactions. This approach can produce well-defined polymer structures using monomers that can not be polymerized via the same mechanism easily and efficiently. Methods to synthesize such PIB-based block copolymers have focused on using various reactions or interactions such as ionic substitution[98,99] and click chemistry.[100,101] For example, Faust and coworkers[98] reported the synthesis of PIB-*b*-poly(methyl methacrylate) (PMMA) by reacting PIB-allyl-Cl, prepared by quenching living PIB with 1,3-butadiene, with living anionic PMMA$^-$Li$^+$. Hirao et al.[99] synthesized new A_2B, A_4B, and A_8B asymmetric star polymers, as well as A_2BA_2, A_4BA_4, and A_8BA_8 star polymers (A is PMMA, B is PIB), by reacting PIB having either 2, 4, or 8 benzyl bromide moieties at each chain terminus with living anionic PMMA$^-$Li$^+$. The multiple benzyl bromide moieties were fitted to the termini in a successive generational fashion similar to the synthesis of dendrimers. Starting from allyl halide-terminated PIB, the terminal halide groups were reacted with an anionic end-capping compound based on 1,1-diphenylethylene (DPE). The DPE end-capper was then fitted with two new benzyl bromide moieties. This sequence could be repeated multiple times, with the number of primary halide groups doubled with each successive generation. Binder et al.[100] prepared a star block copolymer with three equivalent

poly(ethylene oxide) (PEO)-*b*-PIB arms by linking a three-arm azido-telechelic PIB star with three equivalents of alkyne-terminated PEO via the azide/alkyne ''click'' reaction.

Site transformation approaches that combine two or more living polymerization mechanisms is an easy route to synthesize polymers with various monomer components and structures. Here a stable but potentially reactive functional group is introduced at the chain ends. This modified chain end can then provide a means for another polymerization mode to be used.

The pioneering work in this area was reported by Burgess et al.,[102] who prepared PS-*b*-poly(tetrahydrofuran) (PTHF) diblock copolymers by combining anionic and cationic polymerization mechanisms. In 1995, Endo and coworkers[103,104] reported a direct transformation from cationic to anionic living polymerization. However, in many cases, indirect transformations involving multiple steps are required to switch reaction schemes.

Site transformation is used to convert the growing chain ends of a cationically-derived polymer into an initiating site for other polymerization processes including LAP,[39,105,106,107] ATRP,[108-114] reversible addition-fragmentation chain transfer (RAFT) polymerization,[115,116] anionic olefin polymerization[39,117,118] and anionic ring opening polymerization (ROP).[26,119] For example, Muller and coworkers[106] reported the first synthesis of PIB-*b*-poly(*tert*-butyl methacrylate) diblock copolymer, with high blocking efficiency, by transforming the polymerization from LCP to LAP. In this instance they capped living PIB chains with DPE then quenched with methanol/ammonia to form PIB with a methoxydiphenylmethyl terminus. Quantitative metalation with K/Na alloy, Cs metal, or Li in THF at room temperature produced an anionic macroinitiator that was

used to polymerize *tert*-butyl methacrylate. By transforming LCP to a radical

polymerization mechanism, hydroxyl-tailed PIBs were functionalized with

bromoisobutylryl (or bromopropionyl) groups. This yielded PIB marcroinitiators with

classical bromoester functional groups for ATRP.[120] It is interesting to note that ATRP

and LCP of styrene share the same dormant chain end, *sec*-benzylic chloride; thus site

transformation may be theoretically performed in either direction with equal facility.

For example, Masar and coworkers[121,122] synthesized PIB-*b*-PS-*b*-PMMA-*b*-PS-*b*-PIB

pentablock copolymers by radically polymerizing MMA and then styrene, followed by

mechanism transformation to the LCP of IB. In contrast, Storey et al.[110] prepared P*t*BA-

b-PS-*b*-PIB-*b*-PS-*b*-P*t*BA in the reverse order by applying sequential cationic

polymerization of IB and then styrene, followed by transformation to ATRP to add *tert*-

butyl acrylate (*t*BA).

The key in producing block copolymers via mechanism transformation is to

quantitatively functionalize the chain ends and to ensure the initiating site can begin the

second polymerization efficiently and fast. Matyjaszewski et al.[47] studied the ATRP

initiation performance of PIB-allyl-X systems (X = Cl or Br), prepared by capping

living PIB with 1,3-butadiene.[44,45] Results showed that PIB-allyl-Br performed better

then PIB-allyl-Cl, with the efficiency of initiation and cross-propagation in ATRP

depending strongly on the structure of the dormant species.

Another synthetic scheme to produce block copolymers involves the use of dual

initiators containing initiating sites for two or more different polymerization processes.

The different sites must be able to survive the first polymerization process while

initiating the second polymerization in a selective and independent manner. In addition,

unwanted intermediate transformation such as deprotection/activation steps or the use of multifunctional coupling agents must be avoided.

Sogah et al.[123,124] first reported the synthesis of multifunctional initiators possessing initiating sites for different types of polymerization and the synthesis of block and graft copolymers. This concept was further developed by Hawker et al.[125] who performed dual living polymerizations from a single initiating molecule without the requirement of additional reactions. Lim et al.[126,127] managed to perform two mechanistically distinct polymerizations in one step using a palladium complex. Copolymers prepared through this method showed narrow polydispersities and controllable molecular weights on each individual block. To date, polymers synthesized from dual initiators include combinations such as nitroxide-mediated polymerization (NMP)-ROP,[123,124,125,128] ROP-ATRP,[129-141] ATRP-NMP,[142,143] and ROP-ATRP-NMP.[144,145] For some dual initiators, the order of reaction is not specific; for example synthesis could be arranged in an alternating order.[125,132,134,136,141] Also, more complex molecular architectures such as graft copolymers,[123] and ABC,[144,145] A_2B,[129,130] A_2B_2,[131,133] and A_3B_3[141] miktoarm star copolymers have been prepared using dual initiators.

Dual Initiators for PIB-based Polymers via the Combination of LCP and ATRP

As discussed previously, new strategies combining living carbocationic polymerization (LCP) with different controlled/living polymerization mechanisms have been developed to expand the number of PIB-based block copolymers. Compared to coupling and site transformation methods, dual initiators provide a more attractive approach to combine normally inconvertible monomers into one polymer. They

maintain the livingness of polymer chain ends after each step and allow different polymerizations be performed consecutively without any post-polymerization modifications or coupling reactions.

Among the various controlled/living polymerization mechanisms, ATRP is recognized to be versatile with regard to monomer type and tolerant to a wide variety of functional groups, such as allyl, amino, epoxy, hydroxy and vinyl; ATRP is also easy to implement due to the availability and/or relative ease of synthesis of ATRP initiators.[146] The first reports of ATRP appeared in 1995 by Sawamoto,[147] Matyjaszewski[148] and Percec[149] each using different initiators. They all demonstrated the living characteristics of ATRP. A variety of monomers, all with substituents that can stabilized the propagating radials, have been successfully polymerized via ATRP. These include styrenes, (meth)acrylates, (meth)acrylamides, and acrylonitrile.[149-159] ATRP allows good control over polymer architecture (stars, combs, branched),[160-164] comonomer sequence, composition (block, gradient, alternating, statistical), and end group functionality.[165,166,167]

The ATRP reaction is initiated by a halogenated organic species, whose concentration determines the concentration of growing polymer chains. Propagation involves a reversible redox process in the presence of a metal halide species M_t^n-Y, as shown in Figure 4. Because M_t^n-Y species is typically not very soluble in organic solvents, a ligand is added to improve the solubility. In a well-controlled ATRP, the rate of chain terminations is low to allow all chains to propagate uniformly. The latter condition is usually accomplished through careful selection of the initiator. Homolysis of the carbon-halide bond should produce a relatively stable radical, preferably with a

structure similar to that of the growing chain end, so that the rate of initiation is equal to or greater than the rate of propagation.[168,169] Any alkyl halide with activating substituents on the α-carbon, such as aryl and carbonyl groups shown in Figure 5, can be used as ATRP initiators.[167]

Inherent in the mechanism of ATRP is the incorporation of the halogen at the chain ends. The alkyl halide end functionalities can be transformed by standard organic procedures into other functionalities, including azide and amine groups,[170,171,172] hydroxyl end groups,[173] acetate and phosphonium end groups,[174] allyl end groups.[175,176] Monomers such as allyl alcohol and 1,2-expoxy-5-hexene,[177] silyl enol ethers[178] and bicylic olefin[179] have also been used to modify the halogen end groups.

Few dual initiators have been reported to contain a cationic polymerization initiating site. Du Prez et al. reported the compound 2-bromo-(3,3-diethoxy-propyl)-2-methylpropanoate, which contains an acetal function for initiation of the cationic polymerization of MeVE and a 2-bromo-2-methylpropionate functional group to initiate the ATRP of *t*BA, styrene or methacrylate monomers.[180] The same group[132,137] also reported the compound 4-hydroxybutyl 2-bromo-2-methylpropionate with the same ATRP initiating site as well as a primary hydroxyl group to serve as an initiator for the cationic ROP of THF. Schubert et al.[181] used 2-bromo-2-methylpropionyl bromide for the cationic ROP of 2-ethyl-2-oxazoline and subsequent ATRP of styrene.

In 2006, Storey et al.[182] reported synthesis of the latent dual initiator, 3,3,5-trimethyl-5-chlorohexyl acetate (TMCHA), a carbocationic initiator containing a blocked hydroxyl group, which can be subsequently converted to an ATRP initiator. This compound was first used as a cationic initiator to create PIB-*b*-PS block

copolymers. The primary acetoxy group remained intact throughout the carbocationic

polymerization process and was easily converted back to a primary hydroxyl group

served as an ATRP initiator by reacting with 2-bromopropionyl bromide. The resulting

macroinitiator was used to produce poly(*tert*-butyl acrylate) (P*t*BA) under ATRP

conditions, which was then hydrolyzed into poly(acrylic acid) (PAA) to form

amphiphilic triblock copolymers PAA-*b*-PIB-*b*-PS with PAA attached directly to the

PIB chain. Disadvantages of TMCHA were its low initiation efficiency (I_{eff}) during

cationic polymerization and the tedious two-step site transformation reaction prior to

ATRP. Although the authors did not fully understand the cause for low I_{eff}, it was

speculated to be related to the complexation of the ester carbonyl group with the Lewis

acid TiCl$_4$. This was postulated by Takacs and Faust[183] in the case of a similar initiator.

Besides linear triblock copolymers, star polymers PAA$_2$-*s*-PIB-PS were also prepared

from the same TMCHA initiator by functionalizing the protected primary hydroxyl with

a branching agent 2,2-bis((2-bromo-2methyl)propionatomethyl)propionyl chloride

(BPPC) after cationic polymerization of IB and then styrene. This molecule placed two

bromoester groups into the polymer head to initiate ATRP.[184]

Phase Separation of Block and Star Polymers

The increasing importance and interest in block copolymers arises mainly from

their unique phase separation properties in solution and the solid state.[185-188] The driving

force for microphase separation is the incompatibility between the covalently linked

blocks within block copolymers. The formation of ordered periodic phases, sphere,

cylinder, gyroid, or lamellae morphologies, with sizes comparable to the chain

dimensions, as shown in Figure 6, is largely controlled by the inherent block

incompatibility, block length, and the volume fraction of the components.[189,190,191] The

morphological structure of linear triblock copolymers depends not only on the molecular

weight and the fraction of each block, but also on the chain block sequence.[94,95] For

example, a lamellar morphology was observed for poly(isoprene-*b*-styrene-*b*-2-

vinylpyridine) (ISP) of a given composition,[192] whereas a hexagonally ordered coaxial

cylindrical phase is obtained for poly(styrene-*b*-isoprene-*b*-2-vinylpyridine) (SIP) with

the same composition.[193]

Molecular architecture affects the morphology and physical behavior of block

copolymers. A variety of experimental research as well as molecular dynamics

simulations[194] have compared the difference between linear and A_2B,[195] ABC miktoarm

star,[196] H and π-shaped,[197] and highly branched polymers.[198] For example, miktoarm

star copolymers, in which three or more different blocks are linked at one junction point,

require that these junction points lie on the mutual intersections of different domains. It

was confirmed by Yamaguchi and coworkers[199] by showing the energy-filtering

transmission electron microscopy (TEM) images taken from a miktoarm star polymer

composed of PI, PS, and polydimethylsiloxane (PDMS). This topological requirement

effectively suppresses the formation of concentric domains and leads to novel

morphological features with promising potential applications in nanotechnology, which

were never thought possible for linear polymers.[199-203] However, in contrast to the

substantial studies on AB diblock and linear ABC triblock copolymers, there is still

limited understanding concerning the morphology of branched copolymers because of

the experimental difficulties in synthesizing these materials with the desired well-

characterized structures.

Using the tunable phase separation property of block copolymers to produce selective membrane materials continues to be of interest, including protective clothing for military personnel and first-responders.[204] In this application the selective membrane material would allow the transport of perspiration moisture through its thickness while still completely blocking harmful chem-bio agents. This would provide significant advantages over conventional materials, which have often been constructed of impermeable rubbers, such as butyl rubber. One promising selective membrane material is a TPE discussed earlier, PS-*b*-PIB-*b*-PS. Water transport through this triblock copolymer films was enabled by sulfonating the PS phase.[205-208] However, thermodynamic driving forces during processing tend to strongly orient the PS phase in the film plane, limiting the thru-thickness transport. Latter studies showed the attachment of the hydrophilic polymer PAA to both ends of PS-*b*-PIB-*b*-PS, yielded a pentablock terpolymer, PAA-*b*-PS-*b*-PIB-*b*-PS-*b*-PAA, having diffusion pathways for water by forming effective triphasic morphologies illustrated in Figure 7.[209] Increasing the weight percentage of PAA from 11.6% to 43.8% changes the PAA phase morphology from non-continuous rods located along the centering of PS cylinders, to continuous rods, to coaxial cylinders within PS cylinders, and finally, PAA lamellae containing PS cylinders alternating with PIB lamellae. Simultaneously, water sorption increased from 1.3% to 163.0% due to increasingly larger and more extended hydrophilic PAA domains formed in the film. In this way, the crosslinking and diffusion characteristics were decoupled into separate blocks, thereby allowing for more freedom in tailoring these materials.

Compared with phase separation behavior of block copolymers in solid state, the use of selective solvents creates polymer micellar aggregates with addtional controlling parameters such as solvent-polymer interactions and polymer concentration.[186,210] Because of their stability, variety of sizes, and core-shell structure, micelles are used in numerous applications, such as colloidal stabilization, compatibilization of polymer blends, controlled drug delivery, water purification, gene therapy, phase transfer catalysis, and viscosity and surface modification.[211-216] The micellization of block copolymers using selective solvents for one of the blocks was first described by Merret in 1954.[217] Futher studies show that structural parameters of amphiphilic block copolymer micelles such as critical micelle concentration (CMC), micelle aggregation number (N_{agg}), average hydrodynamic radius ($<R_h>$), micelle shape, and colloidal stability are mainly determined by the solution conditions (pH, temperature, and ionic strength), relative block lengths (composition), and molecular weights.[164,210,218-224]

Recent research results suggest polymer architectures also play an important role in controlling the solution self-assembly behavior. For example, ABC triblock linear polymers[225-228] can segregate into multicompartment micelles with two or more separated compartments in the core. However, this is contingent on the two blocks composing the core being large enough and thermodynamically incompatible.

Branching points within a polymer reduce the conformational entropy and lead to self-assembled nanostructures that differ from its linear counterparts.[229-233] For example, PS_8PI_8 star polymers showed a lower aggregation number than corresponding consecutive diblocks or diblocks of similar total molecular weights and composition.[234] Micelles formed by dissolving PS-s-PI_2, PS_2-s-PI miktoarm stars in a selective solvent

for PI exhibit different aggregation numbers, hydrodynamic radii, and thicknesses as compared with PS-*b*-PI linear polymer aggregates.[195] Liu and coworkers[129] observed analogous results by comparing the aqueous self-assembly of well-defined amphiphilic AB$_2$ and A$_2$B stars with AB linear diblock copolymer; here A is poly (ε-caprolactone) and B is poly(2-(dimethylamino)ethyl methacrylate). Lodge, Hillmyer and coworkers have been very productive in developing various sets of amphiphilic ABC miktoarm stars and charactering their multicompartment micelle morphology in aqueous solution.[235,236,237]

One type of architecturally asymmetric linear polymer, ABCA tetrablock copolymers, has gained special attention, because they can form vesicles with asymmetric membranes. Bates et al.[238] reported vesicles composed of PEO-*b*-PS-*b*-PB-*b*-PEO tetrablock copolymers contained an asymmetric bilayer hydrophobic core, with the PB blocks located along the inside surface at weight percentages of the hydrophilic block PEO was less than 0.50. As shown in Figure 8, increasing the weight percentage of the outer block PEO to over 0.50 transformed the core into a complex in-plane structure having a bicontinuous or hexagonally arranged state of segregation that exposes both PB and PS domains. Balsara and coworkers[239] reported the platelet self-assembly of an amphiphilic tetrablock copolymer poly(sulfonated styrene-*b*-methylbutylene-*b*-ethylene-*b*-sulfonated styrene) in water. The vesicle formation process of ABCA linear polymers in solvents that were selective for block A was studied using Monte Carlo simulations.[240] Results showed that the chain length ratio and the hydrophobicity of the hydrophobic blocks B and C are two key factors determining the hydrophobic layer structure of the vesicles.
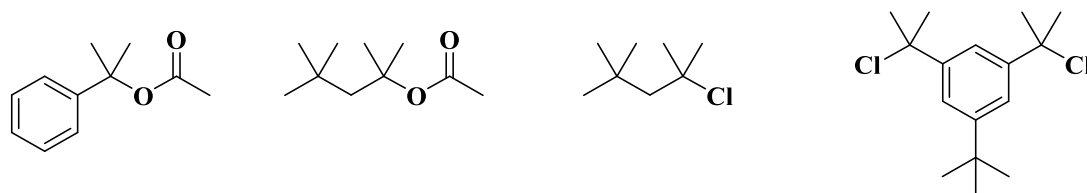
Figure 1. Typical initiators for living carbocationic polymerization (LCP) of
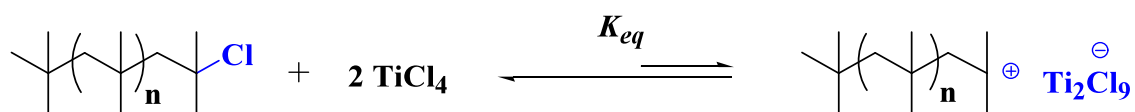
isobutylene (IB).

Figure 2. Reversible termination process in living carbocationic polymerization (LCP)

of isobutylene (IB).
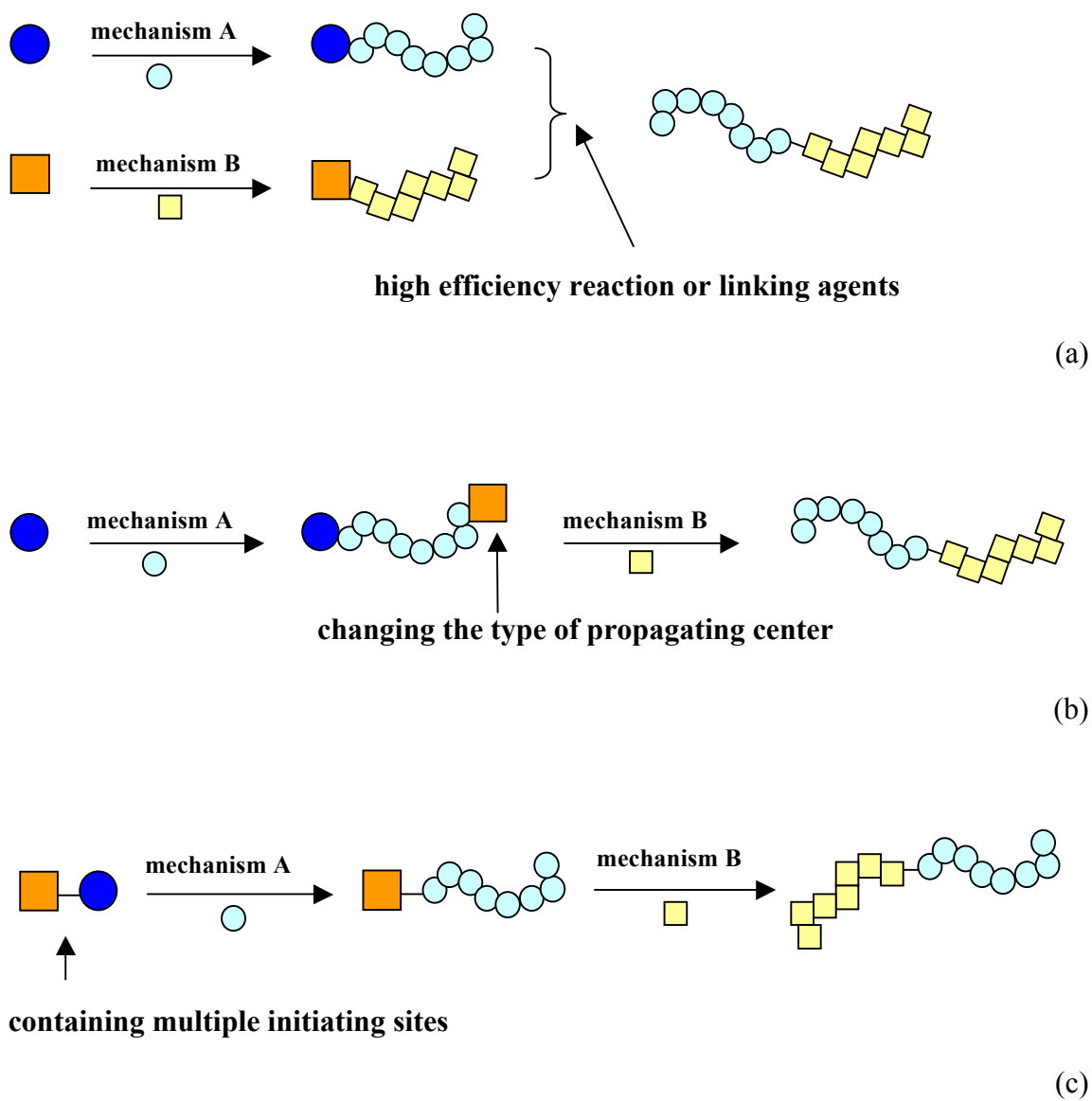
Figure 3. Schematic illustration of AB diblock copolymer synthesis: (a) coupling of polymer blocks prepared from different mechanisms; (b) transforming the chain end functionality from one polymerization mechanism to another; (c) use of a dual initiator consisting of two distinct initiating fragments.

$$P_n\text{-}X \quad + \quad M_t^n\text{-}Y/\text{Ligand} \quad \underset{k_{da}}{\overset{k_a}{\rightleftharpoons}} \quad P_n^{\bullet} \quad + \quad X\text{-}M_t^{n+1}\text{-}Y/\text{Ligand}$$

monomer   termination
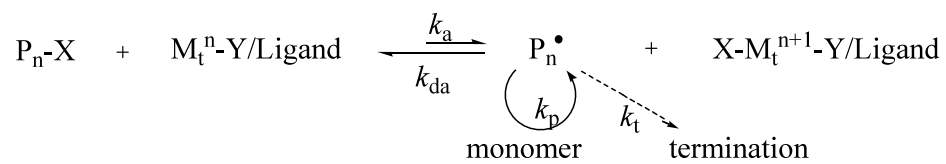
Figure 4. Mechanism of transition-metal-catalyzed atom transfer radical polymerization (ATRP).

R = H, CH3
X = Br, Cl   X = Br, Cl
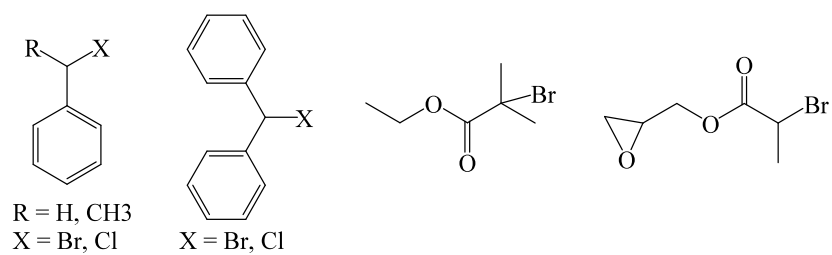
Figure 5. Structures of representative ATRP initiators.

Spheres Cylinders Bicontinuous Perforated Layers Lamellae

increasing the volume fraction of polyisoprene (white)
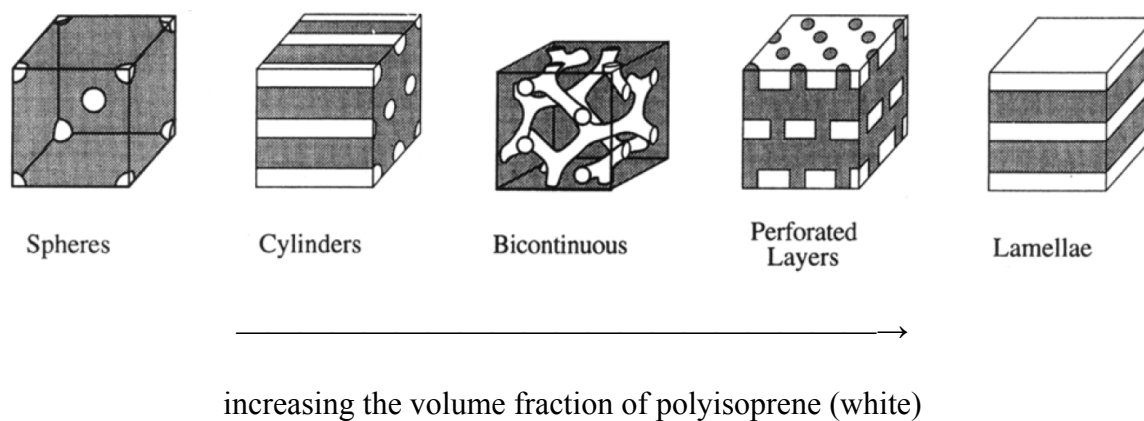
Figure 6. Schematic representations of the morphologies obtained for polystyrene-*b*-polyisoprene (PS-*b*-PI) diblock copolymer melts when increasing the volume fraction of PI. Reproduced with permission from ref 189. Copyright 1995 American Chemical Society.
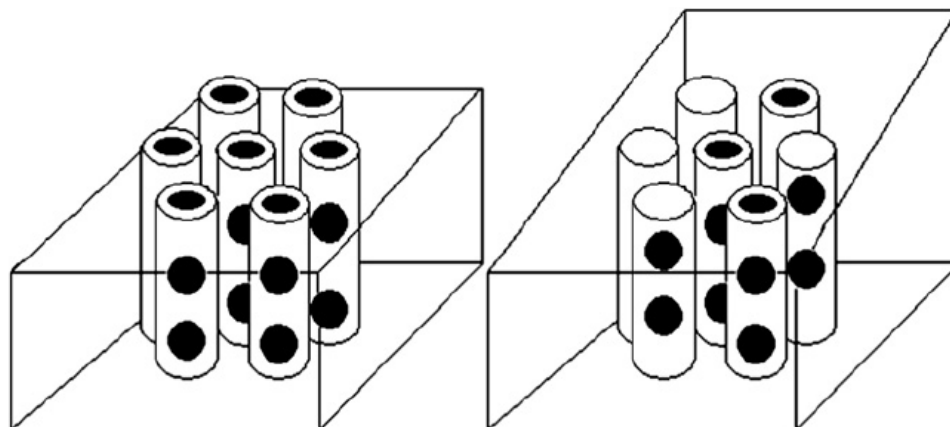
Figure 7. Schematic morphology of PAA-*b*-PS-*b*-PIB-*b*-PS-*b*-PAA pentablock

terpolymers with dark non-continuous rod-like PAA packed in ordered PS cylinders in a

continuous PIB phase. Reproduced with permission from ref 209. Copyright 2008

Elsevier Ltd.
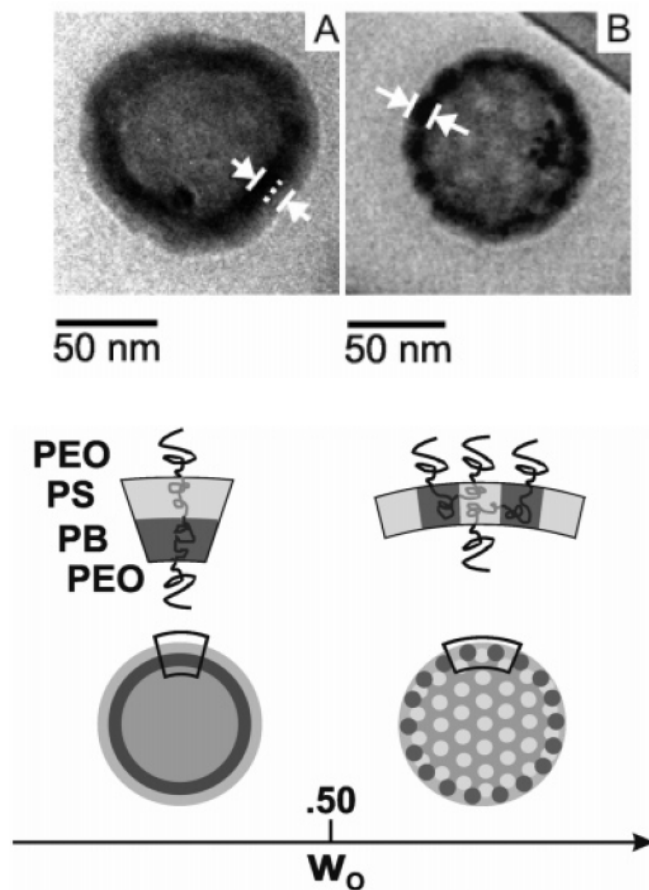
Figure 8. Structural models of vesicles formed by PEO-*b*-PS-*b*-PB-*b*-PEO tetrablock

copolymers in aqueous solution. Dark and light regions correspond to PB and PS

regions, respectively. Reproduced with permission from ref 238. Copyright 2004

American Chemical Society.

CHAPTER II

DESIGN AND SYNTHESIS OF MONO-CATIONIC MONO-RADICAL DUAL

INITIATORS TO COMBINE LIVING CARBOCATIONIC POLYMERIZATION

AND ATOM TRANSFER RADICAL POLYMERIZATION

Objective

As mentioned in the previous chapter, a latent dual initiator, TMCHA, was

synthesized for the purpose of synthesizing P*t*BA-*b*-PIB-*b*-PS triblock copolymers via

the combination of LCP and ATRP.[182] This study showed that after cationic

polymerization of IB followed by sequential addition of styrene, the acetate head group

of the resulting PIB-*b*-PS could be deprotected and converted to a 2-bromopropionate

function, with retention of high head-group functionality, guaranteeing effective

initiation in the consecutive ATRP process. However, this 2-step site transformation

reaction was tedious, and high reaction conversion was required at each step. Another

drawback with TMCHA was low cationic initiation efficiency (I_{eff}). This phenomenon

has been discussed by Takacs and Faust,[183] who suggested that this was caused by

interaction of the carbonyl group with the Lewis catalyst, $TiCl_4$. In order to alleviate

these issues, especially the 2-step transformation procedure, we have developed two new

dual initiators, 3,3,5-trimethyl-5-chlorohexyl 2-bromopropionate (IB_2BP) and 3,3,5-

trimethyl-5-chlorohexyl 2-bromo-2-methylpropionate (IB_2BMP). Figure 9 shows the

structure of these two initiators and an overview of their synthesis. These compounds

have a cationic initiating site identical to that of TMCHA, but the acyl groups contain a

bromine atom bonded to the α carbon and are thus ATRP-ready. The bromide function

is predicted to be essentially inert toward the strong Lewis acids used in carbocationic

polymerization since ionization would place a positive charge on a carbon that is α to a

carbonyl group, which would be extremely unstable. The bulkiness and electron

withdrawing nature of bromine is also predicted to diminish the tendency toward

interaction of the carbonyl oxygen with Lewis acids, thus potentially improving I_{eff}.

Comparing the two compounds, the 2-bromo-2-methylpropionate group of IB$_2$BMP

would be less resistant toward ionization, but it would be more bulky, providing more

steric suppression of complexation.

We have demonstrated the utility of these new initiators by synthesizing PIB-*b*-

PMA diblock copolymers. Methyl acrylate (MA) was chosen as a model ATRP

monomer since its methoxy group provides a well-separated, easily quantifiable signal

in ^{1}H NMR. The general synthesis of the PIB-*b*-PMA diblock copolymer is illustrated

in Figure 10. It involves first the LCP of IB from the *tert*-chloride function of the

initiator, followed by ATRP of MA from the resulting macroinitiaor yielding PIB-*b*-

PMA diblock copolymer. The synthesis can be easily extended to form ABC triblock

copolymers such as PS-*b*-PIB-*b*-PMA.

<div align="center">Experimental</div>

Materials

Methyl 3,3-dimethyl-4-pentenoate was used as received from TCI America.

Methyl magnesium bromide (3 M solution in diethyl ether), borane–tetrahydrofuran

(THF) complex (1 M solution in THF), hydrogen peroxide (30 wt% solution in water),

2-bromopropionyl bromide (97%), 2-bromo-2-methylpropionyl bromide (98%),

triethylamine (99.5%), silica gel (70-230 mesh, 60Å, for column chromatography),

hexane (anhydrous, 99%), 2,6-lutidine (99+%), TiCl$_4$ (99.9%, packaged under N$_2$ in

Sure-Seal bottles), Cu(I)Br (99.999%), aluminum oxide (activated, neutral, Brockmann I,

~ 150 mesh, 58 Å), 1,1,4,7,7-pentamethyldiethylenetriamine (PMDETA), toluene

(anhydrous, 99.8%) and deuterated chloroform were used as received from Sigma-

Aldrich, Inc. Diethyl ether (spectranalyzed), methylene chloride (99.9%),

tetrahydrofuran (HPLC grade), heptane (HPLC grade), sodium chloride, potassium

carbonate, sulfuric acid, magnesium sulfate, calcium chloride, sodium bicarbonate, and

sodium hydroxide were used as received from Fisher Chemical Co. Isobutylene (IB)

(99.5%, BOC Gases) and CH_3Cl (MeCl) (99.5%, Alexander Chemical Co.) were dried

through columns packed with $CaSO_4$ and $CaSO_4$/4 Å molecular sieves, respectively.

Methyl acrylate (MA) (99%, Sigma-Aldrich) was passed through a K_2CO_3 and

aluminum oxide column to remove inhibitor.

Instrumentation

Molecular weights and polydispersity index (PDI) of polymers were determined

using a size exclusion chromatography (SEC) system consisting of a Waters Alliance

2695 Separations Module fitted with on-line multi-angle laser light scattering (MALLS)

detector (MiniDAWN^{TM}, Wyatt Technology, Inc.), interferometric refractometer

(Optilab rEX^{TM}, Wyatt Technology Inc.), and on-line differential viscometer

(ViscoStar^{TM}, Wyatt Technology, Inc.), all operating at 35 °C, and either two mixed E

(3 μm beadsize) or two mixed D (5 μm beadsize) PL gel (Polymer Laboratories Inc.)

SEC columns connected in series. Freshly distilled THF served as the mobile phase and

was delivered at a flow rate of 1.0 mL/min. Samples were prepared by dissolving 10-12

mg polymer into 1.5 g freshly distilled THF, and the injection volume was 100 μL. The

detector signals were recorded using ASTRA^{TM} software (Wyatt Technology Inc.) and

PIB homopolymer molecular weights were determined using an assumed *dn/dc* given by

the following equation:[241] $dn/dc = 0.116 \times (1-108/\overline{M}_n)$ ($\overline{M}_n$ = number average

molecular weight). PIB-*b*-PMA diblock copolymers were analyzed using a *dn/dc*

calculated from the interferometric refractormeter detector response and assuming 100%

mass recovery from the columns.

Solution ^{1}H nuclear magnetic resonance (NMR) spectra were obtained on a

Varian Mercury[plus] NMR spectrometer operating at a frequency of 300.13 MHz, using 5

mm o.d. tubes with sample concentrations of 5-7% (w/v) in deuterated chloroform

(CDCl$_3$) (Aldrich Chemical Co.) containing tetramethylsilane (TMS) as an internal

reference. All shifts were referenced automatically by the software (VNMR 6.1C) using

the resonance frequency of TMS (0 ppm).

A ReactIR 4000 reaction analysis system (light conduit type), equipped with a

DiComp (diamond composite) insertion probe, a general-purpose platinum resistance

thermometer, and CN76000 series temperature controller (Omega Engineering,

Stamford, CT), was used to collect spectra of the polymerization components and

monitor reaction temperature in real time. The light conduit and probe were contained

within a drybox (MBraun Labmaster 130) equipped with a thermostatted

hexane/heptane cold bath.

Initiator Synthesis

The overall synthesis of IB$_2$BP and IB$_2$BMP is illustrated in Figure 9. The

Grignard and hydroboration-oxidation reactions were carried out as previously

described.[182] Esterification of 1,5-dihydroxy-3,3,5-trimethylhexane (DHTMH) was

performed using 2-bromopropionyl bromide or 2-bromo-2-methylpropionyl bromide.

After applying column chromatography to remove impurities, dry, gaseous HCl was bubbled through a solution of the purified ester in CH_2Cl_2 to chlorinate the tertiary hydroxyl group.

Esterification

To a 500 mL three-neck, round-bottom flask, equipped with magnetic stirrer, and nitrogen inlet/outlet, were charged triethylamine (2.2 mL, 0.016 mol) and DTHMH (2.5 g, 0.016 mol) dissolved in 20 mL THF. 2-Bromopropionyl bromide (3.9 g, 0.018 mol) dissolved in 10 mL THF was added dropwise via syringe, and a light orange precipitant appeared. The reaction was allowed to proceed for 5 h. Then 100 mL diethyl ether was added to the flask, and the mixture was washed thrice with deionized water (DI H_2O) and dried over magnesium sulfate. After removing the solvent, the crude product, 5-hydroxy-3,3,5-trimethylhexyl 2-bromopropionate, was obtained as a yellow liquid in 89% yield (4.1 g).

5-Hydroxy-3,3,5-trimethylhexyl 2-bromo-2-methylpropionate was synthesized similarly using 2-bromo-2-methylpropionyl bromide (crude yield 95%).

Column Chromatography

Before chlorination, crude 5-hydroxy-3,3,5-trimethylhexyl 2-bromopropionate (4.1 g) was passed through a 15 cm silica gel column, using 9/1 (v/v) heptane/THF (9/1, v/v) cosolvents as the eluent. A clear, yellow liquid was obtained in 53% yield (2.4 g). ^{1}H NMR ($CDCl_3$): δ = 1.06 (s, 6H, 3-Me), 1.30 (s, 6H, CH_3COH), 1.53 (s, 2H, 4-H), 1.76 (t, 2H, 2-H), 1.82 (d, 3H, C$\underline{H}_3$CHBr), 4.25 (t, 2H, 1-H), 4.35 (q, 1H, CH_3C$\underline{H}$Br) ppm. ^{13}C NMR: δ = 21.60 ($\underline{C}H_3$CHBr), 29.11 (3-Me), 32.09 (C6), 33.32 (C3), 40.19 (CHBr), 40.95 (C2), 53.31 (C4), 63.66 (C1), 72.22 (C5), 171.32 (CO) ppm. 5-Hydroxy-

3,3,5-trimethylhexyl 2-bromo-2-methylpropionate was treated similarly and obtained as a colorless liquid in 47% yield. ^{1}H NMR (CDCl$_3$): δ = 1.09 (s, 6H, 3-Me), 1.32 (s, 6H, CH$_3$COH), 1.56 (s, 2H, 4-H), 1.78 (t, 2H, 2-H), 1.93 (s, 6H, CH$_3$CBr), 4.27 (t, 2H, 1-H) ppm. ^{13}C NMR: δ = 29.04 (3-Me), 30.67 (CH$_3$CBr), 31.99 (C6), 33.28 (C3), 40.98 (C2), 53.32 (C4), 55.80 (CBr), 63.65 (C1), 72.12 (C5), 171.70 (CO) ppm.

Chlorination

Dry, gaseous HCl, formed by dripping sulfuric acid over sodium chloride, was bubbled through a solution of 5-hydroxy-3,3,5-trimethylhexyl 2-bromopropionate (2.4 g, 8.1×10^{-3} mol) in 30 mL methylene chloride for 5 h. The liquid product, IB$_2$BP was obtained in 91% yield (2.8 g). ^{1}H NMR (CDCl$_3$): δ = 1.11 (s, 6H, 3-Me), 1.68 (s, 6H, CH$_3$CCl), 1.79 (t, 2H, 2-H), 1.83 (d, 3H, CH$_3$CHBr), 1.89 (s, 2H, 4-H), 4.26 (t, 2H, 1-H), 4.35 (q, 1H, CH$_3$CHBr) ppm. ^{13}C NMR: δ = 21.61 (CH$_3$CHBr), 28.76 (3-Me), 34.22 (C3), 35.00 (C6), 40.16 (CHBr), 41.14 (C2), 55.66 (C4), 63.29 (C1), 70.84 (C5), 171.32 (CO) ppm. IB$_2$BMP was obtained in the same way. ^{1}H NMR (CDCl$_3$): δ = 1.12 (s, 6H, 3-Me), 1.68 (s, 6H, CH$_3$CCl), 1.79 (t, 2H, 2-H), 1.91 (s, 2H, 4-H), 1.93 (s, 6H, CH$_3$CBr), 4.25 (t, 2H, 1-H) ppm. ^{13}C NMR: δ = 28.72 (3-Me), 30.73 (CH$_3$CBr), 34.21 (C3), 35.01 (C6), 41.32 (C2), 55.72 (C4), 55.85 (CBr), 63.31 (C1), 70.81 (C5), 171.70 (CO) ppm.

PIB Synthesis

The following procedure was employed for polymerizations of IB initiated by IB$_2$BP or IB$_2$BMP within an inert atmosphere drybox equipped with a hexane/heptane cold bath. FTIR (ReactIR 4000) was used to monitor isobutylene conversion by observing the olefinic =CH$_2$ wag (887 cm^{-1}) of IB.[242] The DiComp probe was inserted

into a 250 mL 4-necked round bottom flask equipped with a temperature probe and a stirring shaft with a Teflon paddle. The reactor was placed into the cold bath and allowed to equilibrate to -70 °C. Into the flask were charged 57.9 mL prechilled hexane, 38.6 mL prechilled MeCl, 2,6-lutidine (0.0489 mL, 4.23×10^{-4} mol), and IB_2BMP (0.4224 g, 1.29×10^{-3} mol). The mixture was allowed to stir for 10 min to reach thermal equilibrium after which a background spectrum was collected. Prechilled IB (8.50 mL, 0.106 mol) was added to the flask, and then about 15 spectra were obtained to establish the average intensity at 887 cm^{-1}, A_0, corresponding to the initial monomer concentration. Then $TiCl_4$ (0.565 mL, 5.16×10^{-3} mol) was injected into the flask. The molar concentrations of reagents were $[IB]_0 = 1.00$ M; $[I]_0 = 12.2$ mM; $[2,6\text{-lutidine}]_0 = 4.00$ mM; $[TiCl_4]_0 = 48.8$ mM. Once the monomer was fully consumed, which was indicated by the 887 cm^{-1} absorbance approaching an asymptotic value, A_r, 20 mL prechilled CH_3OH was added to quench the polymerization. After warming to room temperature and loss of MeCl, the hexane layer was washed with CH_3OH and DI H_2O and dried over magnesium sulfate. PIB samples were then precipitated from MeOH and dried under vacuum to yield a colorless viscous liquid.

Monomer concentration at a given reaction time, $[M]_t$, was calculated from the intensity of the 887 cm^{-1} absorbance at that time, A_t, using the following equation, where $[M]_0$ is the original monomer concentration:

$$[M] = [M]_b \frac{A_t - A_r}{A_o - A_r} \qquad (1)$$

PIB-b-PMA Synthesis

ATRP of MA was performed using Cu(I)Br as a catalyst, PMDETA as a ligand, and PIB with 2-bromo-2-methylpropionate (BMP-PIB) or 2-bromopropionate head

group (BP-PIB) as the macroinitiator (MacroI).[182,243] Polymerizations were performed with molar ratio $[MacroI]_0 : [CuBr]_0 : [PMDETA]_0 = 1 : 1 : 1$ in toluene with $[MacroI]_0$ = 0.05 M at 70 °C, targeting $\overline{X}_n$ of 60, 90, or 120. The number average molecular weight for the BP-PIB via SEC was 5,570 g/mol; the PDI was 1.04, and $\overline{X}_n$ = 89 by NMR. The number average molecular weight for the BMP-PIB via SEC was 4,650 g/mol; the PDI was 1.02, and $\overline{X}_n$ = 77 by NMR.

The following procedure was employed for ATRP of MA. A dry Schlenk flask was charged with BMP-PIB (0.93 g, 1.7×10^{-4} mol), MA (1.8 mL, 2.0×10^{-2} mol), CuBr (0.029 g, 2.0×10^{-4} mol), and 4 mL anhydrous toluene. After three freeze-pump-thaw cycles, PMDETA (0.042 mL, 2.0×10^{-4} mol) was added to the reaction mixture via a deoxygenated syringe. Then the reaction mixture was immersed in an oil bath at 70 °C. Aliquots were taken every half hour, and the progress of polymerization was monitored by observing diminution of the olefinic resonances of monomer in the ^{1}H NMR spectrum. The polymerization was allowed to proceed for several hours to reach a monomer conversion of about 60%. After polymerization, the polymer solution was passed through an Al_2O_3-packed column to remove the copper salt. Then 15-20 mL THF was added to completely dissolve the polymer, and the resulting solution was passed through a filter with pore size 0.2 μm to remove Al_2O_3. PIB-*b*-PMA samples were then precipitated into MeOH and dried under vacuum to yield a solid product.

<div align="center">Results and Discussion</div>

Initiator Synthesis

New initiators, IB_2BP and IB_2BMP, for LCP of IB were synthesized via the route shown in Figure 9. Synthesis of the common intermediate, DTHMH, has been

reported.[182] Esterification to attach either the 2-bromopropionoyl or the 2-bromo-2methylpropionoyl moiety was carried out in each case using the acid bromide in THF solution with triethylamine as acid scavenger. Upon esterification of DTHMH with 2-bromopropionyl bromide or 2-bromo-2-methylpropionyl bromide, the products were contaminated by impurities, which could not be simply eliminated by extraction. However, by passing either crude product through a silica gel column and eluting with heptane/THF (9/1, v/v) cosolvents, pure product was obtained in approximately 50% yield.

Figure 11 shows ^{1}H NMR spectra of 5-hydroxy-3,3,5-trimethylhexyl 2-bromopropionate (upper) and 5-hydroxy-3,3,5-trimethylhexyl 2-bromo-2-methylpropionate (lower) after column chromatography. For both compounds, the methylene protons formerly next to the primary hydroxyl group shifted downfield to 4.2 ppm (peak g). In addition, a new doublet at 1.8 ppm (peak h) and a quartet at 4.3 ppm (peak i) appeared for the methyl and methine protons in the newly incorporated 2-bromopropionoyl group, as shown in the upper spectrum. Likewise, a singlet at 1.9 ppm (peak j) appeared for the methyl protons in the 2-bromo-2-methylpropionoyl group, as shown in the lower spectrum. For both spectra, the integrated peak areas were in excellent agreement with the theoretical values.

The last step of the synthesis was substitution of the tertiary hydroxyl group by chlorine for both intermediates. As this reaction increased deshielding of adjacent methyl and methylene protons in both products, their proton NMR peaks shifted downfield to 1.6 ppm (peak a) and 1.9 ppm (peak b), as shown in Figure 12.

PIB Synthesis

Various PIBs with α-bromoester head groups were prepared from both initiators via LCP (Tables 1-4). Figure 13 shows ^{1}H NMR spectra of representative PIBs initiated by IB₂BP (upper) and IB₂BMP (lower). Large peaks for the methyl and methylene protons in the isobutylene repeat units were observed at 1.1 ppm (peak c) and 1.4 ppm (peak d), respectively. Peaks due to the methyl groups within the α-bromoacyl groups at 1.82 ppm (doublet, h, IB₂BP) and 1.93 ppm (singlet, j, IB₂BMP) and the triplet due to the methylene protons next to the ester linkage at about 4.2 ppm (peak g) were present in both spectra, indicating that the α-bromoester head groups survived intact during LCP. For both polymers, as determined by integration of peak g relative to the combined peaks characteristic of the tail group of the polymer[31] (*tert*-Cl plus possible fractions of *exo*- and *endo*-olefin[244]), the number of α-bromoester head groups was approximately equal to the number of total polymer chains, indicating that protic initiation and transfer to monomer were absent and all chains contained the desired ATRP initiating sites.

To optimize polymerization conditions for LCP of IB, parameters that control the active chain end concentration, including the initial concentration of TiCl₄ catalyst ([TiCl₄]₀), polymerization temperature, polarity of cosolvent mixture, and targeted number average molecular weight ($\overline{M}_{n\,\text{theo}}$) were examined systematically for both initiators.

The influence of TiCl₄ concentration was first investigated (Table 1). LCPs of IB (1.0 M) were performed at -70 °C using IB₂BMP as the initiator, 2,6-lutidine as Lewis base in 60/40 (v/v) Hex/MeCl cosolvents, targeting $\overline{M}_{n\,\text{theo}}$ = 4,900 g/mol. Polymerization time listed in the tables is the observed time to reach 6 half-lives (98.4%

IB conversion) as determined from ReactIR data; the actual time from catalyst addition to reaction termination was typically between 6.2 and 9 half-lives. As shown in equation (2), number average degree of polymerization ($\overline{X}_{n\,PIB}$) was determined by ^{1}H NMR spectroscopy using the ratio of the integrated peak area, A_{Me}, of the methyl protons in the isobutylene repeat unit (peak **c**, 1.1 ppm) to that of the sum of all chain ends, A_{CE}, the sum of the integrated peak areas of characteristic resonances representing the various polymer chain ends, defined by equation (3). In quation (3), A_{exo} is the area of the upfield *exo*-olefinic resonance at 4.64 ppm, A_{endo} is the area of the single *endo*-olefinic resonance at 5.15 ppm, and $A_{tert\text{-}Cl}$ is the area of the resonance at 1.96 ppm due to the methylene protons of the *tert*-chloride end group. $A_{coupled}$ was calculated by equation (4), where $A_{4.75\text{-}5.0}$ is the integrated area of the convoluted peaks from 4.75-5.0 ppm associated with the downfield *exo*-olefinic proton and the two identical protons of the coupled product. Number average molecular weight ($\overline{M}_{n\,PIB}$) and polydispersity index (PDI) were determined by SEC/MALLS using a *dn/dc* calculated as *dn/dc* = 0.116×(1-108/$\overline{M}_n$).[241] I_{eff} was calculated as $\overline{X}_{n\,theo}/\overline{X}_{n\,PIB}$ and $\overline{M}_{n\,theo}/\overline{M}_{n\,PIB}$, from NMR and SEC/MALLS data, respectively. As shown in Table 1, I_{eff}'s determined by the two methods were in fair agreement and low relative to a single-cationic-site initiator such as 2-chloro-2-methyl-2,4,4-trimethylpentane (TMPCl).

$$\overline{X}_{n\,PIB} = \frac{A_{Me}/6}{A_{CE}} - 1 \qquad (2)$$

$$A_{CE} = A_{exo} + A_{endo} + A_{tert\text{-}Cl}/2 + 2A_{coupled} \qquad (3)$$

$$A_{coupled} = \frac{\left(A_{4.75\text{-}5.0} - A_{exo}\right)}{2} \qquad (4)$$

For the 5 runs in Table 1, PDIs were narrow (≤ 1.15). As $[TiCl_4]_0$ was raised from 36.6 mM to 85.4 mM, the polymerization time decreased from over 6 h to about 0.5 h. This increase in polymerization rate reflects a progressive shift in the ionization equilibrium toward a higher concentration of active propagating species, controlled by the effective equilibrium constant, $K_{eq}[TiCl_4]^2$. However, I_{eff} was consistently < 1 and did not change significantly with increasing $[TiCl_4]_0$. Faust et al.[245] reported I_{eff} < 1 for the related initiator, 5-chloro-3,3,5-trimethylhexyl methacrylate, which also contains an ester group, and these authors suggested that complexation of $TiCl_4$ with the carbonyl group was the likely cause of low I_{eff}. Breland, Murphy, and Storey[182] observed low initiation efficiency with the acetate ester of this compound and likewise attributed low I_{eff} to complexation with the Lewis acid. However, if complexation were the cause, one would reasonably expect initiation efficiency to steadily diminish with increasing $[TiCl_4]_0$. However, initiation efficiency was insensitive to $[TiCl_4]_0$ based on the data in Table 1, and this suggests that complexation, is not the reason, or least not the principal reason, for low initiation efficiency.

ReactIR provided a means to monitor real-time [IB] during the polymerization. Figure 14 compares $\ln([M]_0/[M])$ vs. polymerization time plots for polymerizations initiated by IB_2BMP and TMPCl, at the same reaction conditions. Polymerization initiated by IB_2BMP was slower, and the first-order plot showed upward curvature, indicating the overall polymerization rate increased as reaction continued. This behavior is consistent with slow initiation for IB_2BMP initiated polymerizations. In fact, initiation was not only slow; it was incomplete at this monomer/initiator ratio, as supported by the detection of unreacted IB_2BMP in the MeOH wash. Slow initiation by

IB_2BMP produced an asymmetric peak in the SEC trace, with a characteristic low molecular weight tail, as shown in Figure 15.

As $[TiCl_4]_0$ did not influence I_{eff} significantly, the value of $[TiCl_4]_0$ was chosen to complete polymerizations within a reasonable amount of time for all the experiments discussed below.

The influence of polymerization temperature on I_{eff} was next investigated over the range -70 to -50 °C, employing IB_2BMP as the initiator. Polymerization conditions and results are listed in Table 2. In general, polymerization rate decreased with increasing temperature, consistent with the well-known negative apparent activation energy for IB polymerization under these conditions.[246] At the same time, number average molecular weight, characterized by SEC, decreased from 155% to 114% of theoretical. This clearly shows that I_{eff} increases with increasing polymerization temperature, which is consistent with the fact that the apparent activation energy for ionization by $TiCl_4$ is greater than that for propagation, i.e., run number decreases with increasing temperature.[247]

The influence of solvent polarity was next investigated at -70 °C, employing IB_2BMP as the initiator. These experiments were conducted in part to eliminate the possibility that low I_{eff} resulted from incompletely dissolved initiator. Polymerization conditions and results are listed in Table 3. Reaction time decreased from 2 h to about 10 min as the volume percentage of MeCl in the cosolvents was increased from 40 to 80. However, I_{eff} was essentially unchanged with increasing medium polarity, which confirmed that initiator solubility is not the cause of low I_{eff}.

The effect of IB_2BMP initiator concentration (at constant [IB] = 1 M) was

investigated at several temperatures, targeting. $\overline{M}_n$ s of 3,000 g/mol (3k), 5,000 g/mol (5k), and 10,000 g/mol (10k). Polymerization conditions and results are listed in Table 4. Different $[TiCl_4]_0$ were applied to adjust the polymerization time. At -70 °C, as the targeted $\overline{M}_n$ was increased from 3k, 5k, to 10k, I_{eff} (SEC) increased from 53%, 58%, to 83%, as expected. The same trend was observed for the polymerizations performed at -60 °C, consistent with slow initiation. At -50 °C, the I_{eff} for 5k and 10k was about same, approximately 87%.

All polymerizations discussed above were initiated by IB_2BMP. Polymerizations of IB were also performed using IB_2BP as the initiator, targeting $\overline{M}_n$ s of 3k, 5k, and 10k. Polymerization conditions and results are listed in Table 5. Different $[TiCl_4]_0$ were used to adjust the polymerization time. At -70 °C, as the targeted $\overline{M}_n$ was raised from 3k, 5k, to 10k, I_{eff} (SEC) increased from 58%, 65%, to 83%, revealing the same tendency as IB_2BMP. SEC elution curves (see representative curve in Figure 15) showed low molecular weight tailing, indicating slow initiation. In general, under the same conditions, IB_2BP produced slightly higher I_{eff} compared to IB_2BMP.

PIB-b-PMA Synthesis

ATRP was demonstrated from both α-bromoester functionalized PIB macroinitators (BP-PIB and BMP-PIB) using methyl acrylate (Table 6). Polymerizations were monitored and terminated at 60% conversion in order to avoid termination or chain transfer reactions. Figure 16 shows ^{1}H NMR spectra of BP-PIB-*b*-PMA$_{60}$ (upper) and BMP-PIB-*b*-PMA$_{60}$ (lower), which are representative. Peaks due to the PMA block appeared at 3.6 (peak k), 2.3 (peak j), and 1.4-2.0 ppm (peak i).

Tacticity effects caused the PMA methylene protons to exist in three different chemical environments, and thus exhibit 3 major peaks in the range 1.4 to 2.0 ppm.[248]

Compositions of block copolymers listed in Table 6 were calculated from both ^{1}H NMR spectroscopy and SEC, considering the IB_2BMP or IB_2BP residue as part of the PIB block. $\overline{X}_{n\,PMA}$ was calculated from the ratio of the integrated peak area of the methyl hydrogens of the PMA block, $A_{3.6ppm}$, to that of the *gem*-dimethyl hydrogens of the PIB block, $A_{1.1ppm}$, via equation (5). Weight percentage of PMA in the block copolymer was calculated using equation (6), where M_{IB}, M_{MA}, and M_I are the molecular weights for IB, methyl acrylate, and the initiator, respectively. $\overline{M}_{n\,PIB\text{-}b\text{-}PMA}$ and PDI of block copolymers were obtained by SEC-MALLS using two mixed D columns and a *dn/dc* calculated from the refractive index detector response and assuming 100% mass recovery from the columns. Number average molecular weight of the PMA block, $\overline{M}_{n\,PMA}$, and copolymer composition were calculated from SEC data using equation (7) and (8), respectively. PIB-*b*-PMA diblock copolymer compositions characterized by these two methods were comparable.

$$\overline{X}_{n\,\text{PMA}}(\text{NMR}) = \frac{A_{3.6ppm}}{A_{1.1ppm}\Big/2} \times (\overline{X}_{n\,\text{PIB}} + 1) \tag{5}$$

$$wt\%\ \text{PMA(NMR)} = \frac{\overline{X}_{n\,\text{PMA}} \times M_{MA}}{\overline{X}_{n\,\text{PIB}} \times M_{IB} + \overline{X}_{n\,\text{PMA}} \times M_{MA} + M_I} \times 100\% \tag{6}$$

$$\overline{M}_{n\,\text{PMA}}(\text{GPC}) = \overline{M}_{n\,\text{PIB-}b\text{-PMA}} - \overline{M}_{n\,\text{PIB}} \tag{7}$$

$$wt\%\ \text{PMA(GPC)} = \frac{\overline{M}_{n\,\text{PMA}}}{\overline{M}_{n\,\text{PIB-}b\text{-PMA}}} \times 100\% \tag{8}$$

SEC characterization (Figure 17) showed that low PDI diblock polymers were

obtained and that no unreacted MacroI was present. This indicated that the α-bromoester functional groups of both IB$_2$BP and IB$_2$BMP remained intact during LCP and that ATRP initiation was quantitative. As the target degree of polymerization of the PMA block increased, SEC elution peaks shifted to the left, as expected. However, for systems targeting the highest PMA degree of polymerization, radical-radical coupling occurred, as evidenced by a high molecular weight shoulder in the SEC curve (see BMP-PIB-*b*-PMA$_{120}$ in Figure 17).

Conclusions

New dual initiators, IB$_2$BMP and IB$_2$BP, containing both a cationic polymerization initiating site and an ATRP initiating site, were designed for the preparation of PIB-based AB diblock and ABC triblock copolymers. Both initiators were successfully synthesized in four steps, as confirmed by ^{1}H NMR spectroscopy. When used for the LCP of IB, low initiation efficiencies (I_{eff}), caused by slow initiation, were observed for both initiators. To optimize the conditions for LCP and to examine the cause for low I_{eff}, polymerization conditions including the initial concentration of catalyst ([TiCl$_4$]$_0$), temperature, solvent polarity, and targeted number average of molecular weight ($\overline{M}_n$) were examined. The observed I_{eff} for all reactions were less than 1 for both initiators within the range of conditions examined. However, increasing polymerization temperature significantly improved I_{eff}, and at -50 °C, about 90% efficiency was achieved for IB$_2$BMP at a target molecular weight of 5k, i.e., for [IB]$_0$/[IB$_2$BMP]$_0$ = 82. As expected, I_{eff} increased with increasing target molecular weight. Changes in [TiCl$_4$] and solvent polarity caused negligible changes in I_{eff}. Complexation between TiCl$_4$ and the carbonyl oxygen of 3,3,5-trimethyl-5-chlorohexyl

esters has been proposed[182,244] as a reason for low I_{eff}, but this seems inconsistent with the absence of any correlation between I_{eff} and [TiCl$_4$].

Further investigations directed to the origin and solution of low I_{eff} will be presented in the next chapter. However, the following points can be presently made for optimal use of either initiator. If the initiator is being used to create low molecular weight PIB, then a relatively high polymerization temperature, e.g. -60 to -50 °C, is advantageous since the lower propagation run number[248] boosts I_{eff} and lowers PDI. If the initiator is being used to create high molecular weight PIB, the high monomer/initiator ratio will ensure $I_{eff} \cong 1.0$ and low PDI regardless of temperature, and therefore a lower temperature such as -80 °C is preferred to maximize livingness.

PIBs with 2-bromo-2-methylpropionate (BMP-PIB) or 2-bromopropionate (BP-PIB) head groups were successfully used for ATRP of MA. Targeted $\overline{M}_n$ and narrow PDIs were obtained for both macroinitiators. No macroinitiator residue was observed via SEC, indicating that the α-bromoester functional groups remained intact during LCP.

Table 1. Effect of $[TiCl_4]_0$ on IB_2BMP-Initiated Living Carbocationic Polymerizations (LCP) of isobutylene (IB)[a]

Run	$\dfrac{[TiCl_4]_0}{[I]_0}$	Time[b] (min)	NMR			SEC			
			$\overline{X}_{n\,PIB}$	$\overline{X}_{n\,theo}$	I_{eff}	$\overline{M}_{n\,PIB}$ (g/mol)	$\overline{M}_{n\,theo}$ (g/mol)	I_{eff}	PDI
1	3	370	102	82	0.80	6750	4900	0.73	1.08
2	4	120	128	82	0.64	8410	4900	0.58	1.05
3	5	110	118	82	0.70	7680	4900	0.64	1.11
4	6	40	123	82	0.67	7570	4900	0.65	1.11
5	7	35	120	82	0.68	7300	4900	0.67	1.09

Note. [a]60/40 Hex/MeCl cosolvents (v/v); -70 °C; $[IB]_0 = 1.00$ M; $[IB_2BMP]_0 = 12.2$ mM; $[2,6\text{-lutidine}]_0 = 4.00$ mM

[b]Time required to reach 6 half-lives for monomer consumption (98.4% IB conversion)

Table 2. Effect of Temperature on IB_2BMP-Initiated Living Carbocationic Polymerizations (LCP) of isobutylene (IB)[a]

| | | | NMR | | | SEC | | | |
Run	Temp. (°C)	Time[b] (min)	$\overline{X}_{n\,PIB}$	$\overline{X}_{n\,theo}$	I_{eff}	$\overline{M}_{n\,PIB}$ (g/mol)	$\overline{M}_{n\,theo}$ (g/mol)	I_{eff}	PDI
4	-70	40	123	82	0.67	7570	4900	0.65	1.11
6	-60	85	107	82	0.77	7230	4900	0.68	1.10
7	-50	170	91	82	0.90	5610	4900	0.81	1.15

Note. [a]60/40 Hex/MeCl cosolvents (v/v); $[IB]_0 = 1.00$ M; $[IB_2BMP]_0 = 12.2$ mM; $[TiCl_4]_0 = 73.2$ mM; $[2,6\text{-lutidine}]_0 = 4.00$ mM

[b]Time required to reach 6 half-lives for monomer consumption (98.4% IB conversion)

Table 3. Effect of Solvent Polarity on IB_2BMP-Initiated Living Carbocationic

Polymerizations (LCP) of isobutylene (IB)[a]

Run	Hex/MeCl (v/v)	Time[b] (min)	NMR			SEC			
			$\overline{X}_{n\,PIB}$	$\overline{X}_{n\,theo}$	I_{eff}	$\overline{M}_{n\,PIB}$ (g/mol)	$\overline{M}_{n\,theo}$ (g/mol)	I_{eff}	PDI
2	60/40	120	128	82	0.64	8410	4900	0.58	1.05
8	50/50	50	119	82	0.69	8060	4900	0.61	1.07
9	20/80	10	121	82	0.68	7770	4900	0.63	1.15

Note. [a]-70 °C; $[IB]_0$ = 1.00 M; $[IB_2BMP]_0$ = 12.2 mM; $[TiCl_4]_0$ = 48.8 mM; $[2,6\text{-lutidine}]_0$ = 4.00 mM

[b]Time required to reach 6 half-lives for monomer consumption (98.4% IB conversion)

Table 4. Effect of $[IB_2BMP]_0$ on Living Carbocationic Polymerizations (LCP) of isobutylene (IB) at Several Temperatures[a]

| Run | $[IB_2BMP]$ (mmol/L) | Temp. (°C) | Time[b] (min) | NMR | | | SEC | | | |
				$\overline{X}_{n\,PII}$	$\overline{X}_{n\,the}$	I_{eff}	$\overline{M}_{n\,PIB}$ (g/mol)	$\overline{M}_{n\,theo}$ (g/mol)	I_{eff}	PDI
10	20.8	-70	70	94	48	0.51	5630	3000	0.53	1.10
2	12.2	-70	120	128	82	0.64	8410	4900	0.58	1.05
11	6.1	-70	160	201	164	0.82	11370	9500	0.84	1.06
12	12.2	-60	290	107	82	0.77	7070	4900	0.69	1.06
13	6.1	-60	450	200	164	0.82	11060	9500	0.86	1.10
7[c]	12.2	-50	170	91	82	0.90	5610	4900	0.87	1.15
14[d]	6.1	-50	320	201	164	0.82	10880	9500	0.87	1.09

Note. [a]60/40 Hex/MeCl cosolvents (v/v); $[IB]_0 = 1.00$ M; $[TiCl_4]_0 = 48.8$ mM; $[2,6\text{-lutidine}]_0 = 4.00$ mM

[b]Time required to reach 6 half-lives for monomer consumption (98.4% IB conversion)

[c]$[TiCl_4]_0 = 62.5$ mM

[d]$[TiCl_4]_0 = 73.2$ mM

Table 5. Effect of $[IB_2BP]_0$ on Living Carbocationic Polymerizations (LCP) of isobutylene (IB)[a]

Run	$[IB_2BP]$ (mmol/L)	Time[b] (min)	NMR			SEC			
			$\overline{X}_{n\,PIB}$	$\overline{X}_{n\,theo}$	I_{eff}	$\overline{M}_{n\,PIB}$ (g/mol)	$\overline{M}_{n\,theo}$ (g/mol)	I_{eff}	PDI
15[c]	20.8	35	82	48	0.59	5160	3000	0.58	1.06
16	12.2	110	117	82	0.70	7590	4900	0.65	1.12
17	6.1	250	183	164	0.90	11460	9500	0.83	1.10

Note. [a] 60/40 Hex/MeCl cosolvents (v/v); -70 °C; $[IB]_0$ = 1.00 M; $[TiCl_4]_0$ = 48.8 mM; $[2,6\text{-lutidine}]_0$ = 4.00 mM

[b] Time required to reach 6 half-lives for monomer consumption (98.4% IB conversion)

[c] $[TiCl_4]_0$ = 62.5 mM

Table 6. Atom Transfer Radical Polymerization (ATRP)[a] of Methyl Acrylate (MA) Initiated from PIB Macroinitiators[b]

Run	NMR		SEC		
	$\overline{X}_{n\ PMA}$	wt% PMA	$\overline{M}_{n\ PMA}$ (g/mol)	PDI	wt% PMA
BP-PIB-b-PMA$_{60}$	68	52.4	5780	1.06	50.9
BP-PIB-b-PMA$_{90}$	80	56.5	7020	1.04	55.8
BP-PIB-b-PMA$_{120}$	112	64.5	12900	1.14	69.8
BMP-PIB-b-PMA$_{60}$	62	53.5	6020	1.04	56.4
BMP-PIB-b-PMA$_{90}$	90	62.5	8970	1.04	65.9
BMP-PIB-b-PMA$_{120}$	126	70.0	13760	1.05	74.7

Note. [a][MacroI]$_0$: [CuBr]$_0$: [PMDETA]$_0$ = 1:1:1 ([MacroI]$_0$ = 0.05 M) in toluene at 70 °C; 0.60[MA]$_0$/[MacroI]$_0$ = 60, 90, or 120

[b]BP-PIB: $\overline{M}_n$ = 5,570 g/mol and PDI = 1.04 (SEC); $\overline{X}_n$ = 89 by NMR. BMP-PIB: $\overline{M}_n$ = 4,650 g/mol and PDI = 1.02 (SEC); $\overline{X}_n$ = 77 by NMR
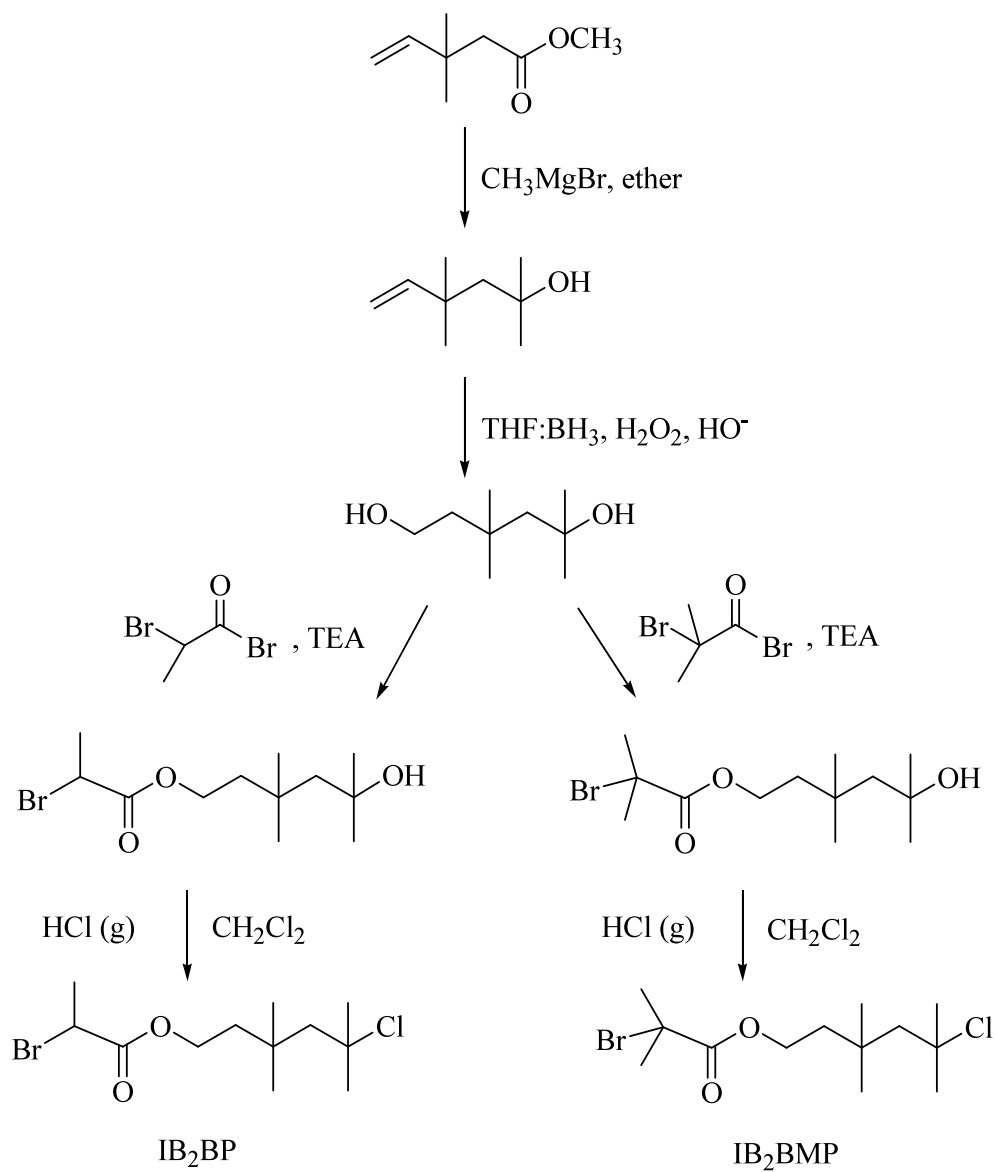
Figure 9. Synthesis of LCP-ATRP dual initiators 3,3,5-trimethyl-5-chlorohexyl 2-bromopropionate (IB$_2$BP) and 3,3,5-trimethyl-5-chlorohexyl 2-bromo-2-methylpropionate (IB$_2$BMP).
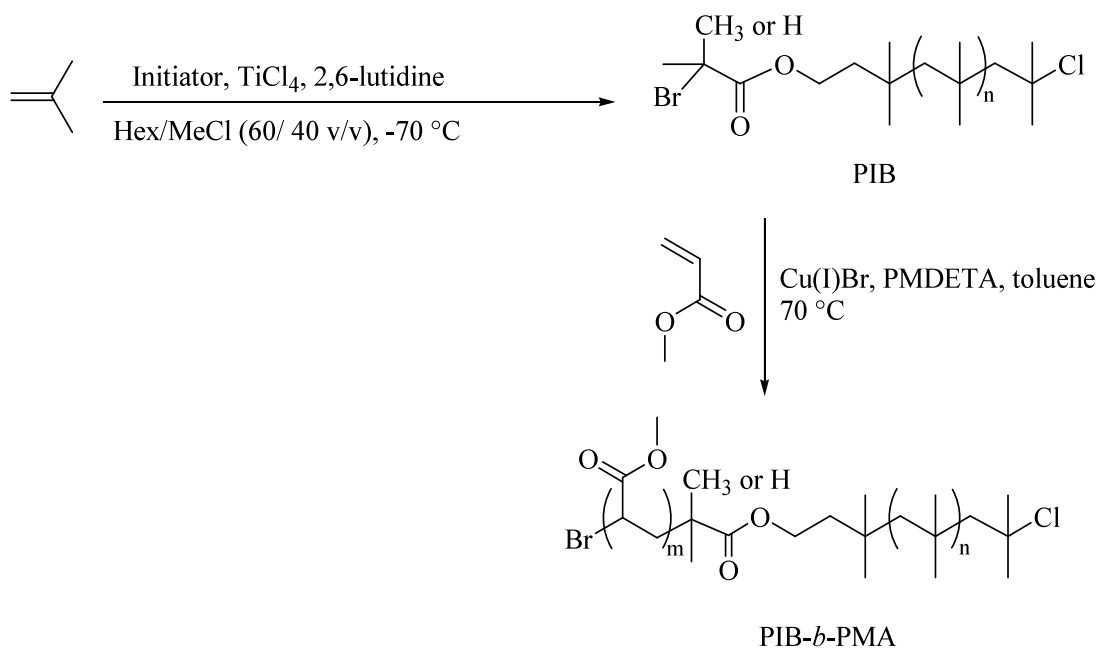
Figure 10. Synthesis of PIB-*b*-PMA copolymers using dual initiators via combined

LCP and ATRP.
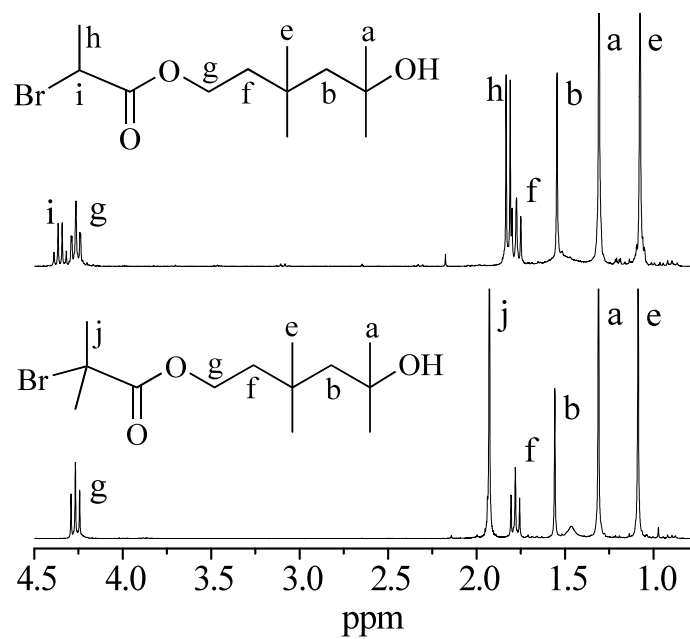
Figure 11. Proton NMR spectra of 5-hydroxy-3,3,5-trimethylhexyl 2-bromopropionate

(upper) and 5-hydroxy-3,3,5-trimethylhexyl 2-bromo-2-methylpropionate (lower).
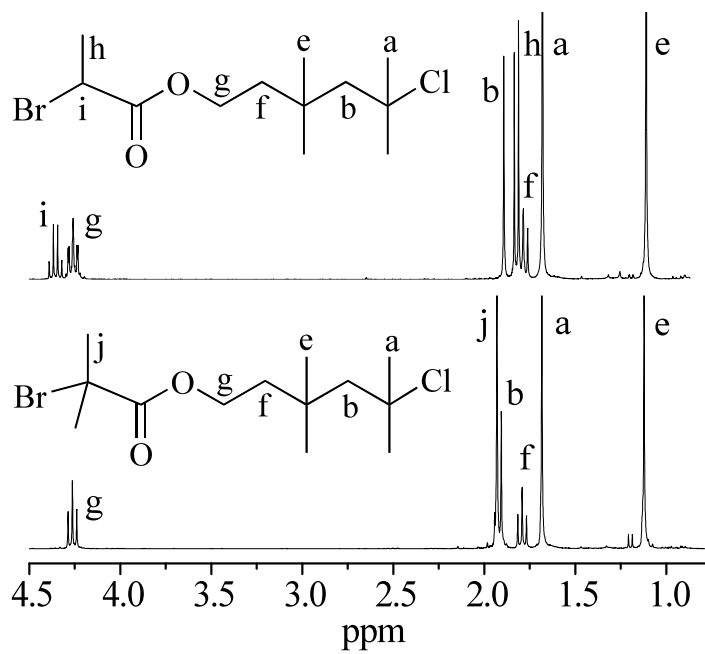
Figure 12. Proton NMR spectra of IB$_2$BP (upper) and IB$_2$BMP (lower).
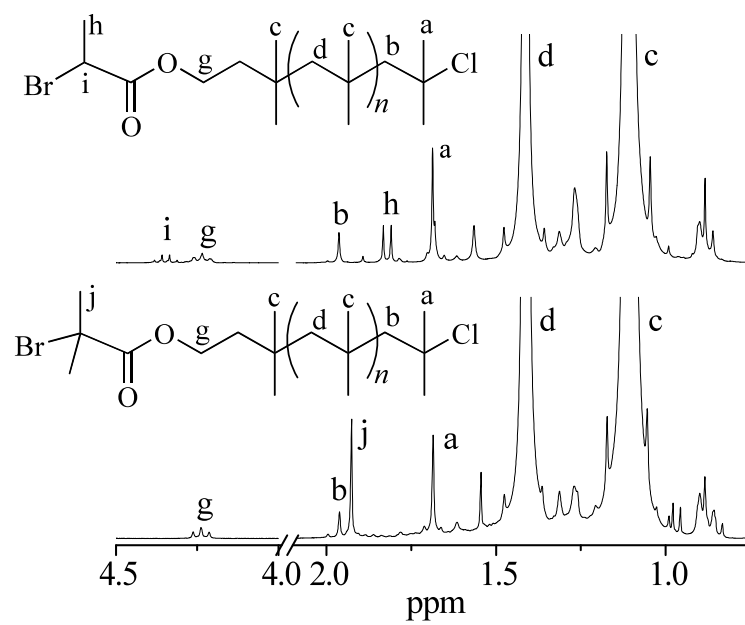
Figure 13. Proton NMR spectra of BP-PIB (Run 15, upper) and BMP-PIB (Run 2, lower).
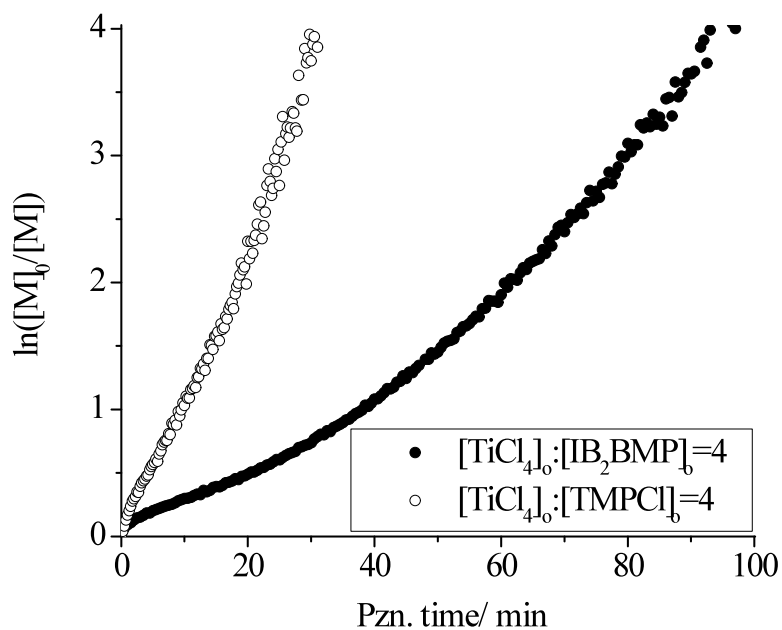
Figure 14. First-order kinetic plots for IB polymerizations initiated by IB$_2$BMP and

TMPCl. Conditions were as follows: 60/40 Hex/MeCl cosolvents (v/v); -70 °C; [IB]$_0$ =

1.00 M; [I]$_0$ = 12.2 mM; [TiCl$_4$]$_0$ = 48.8 mM; [2,6-lutidine]$_0$ = 4.00 mM.
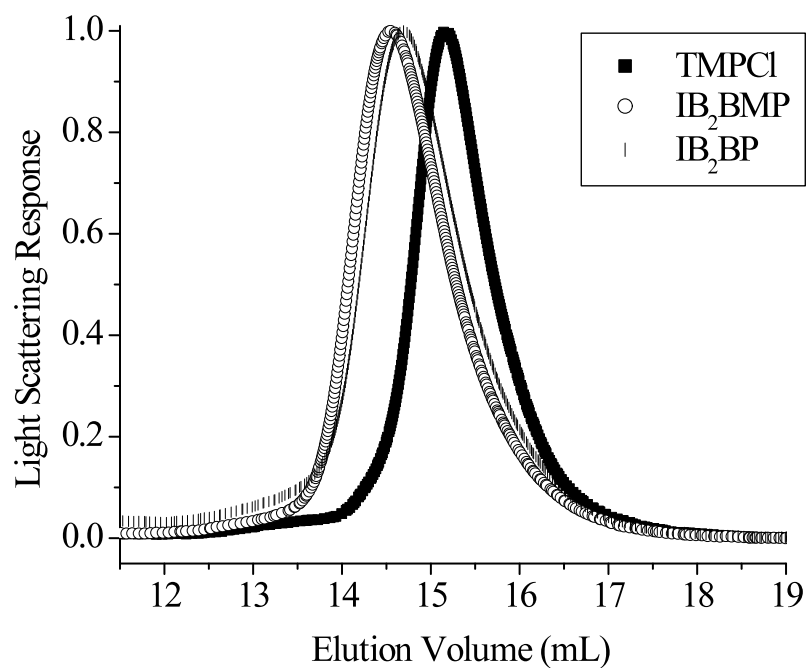
Figure 15. The SEC elution curves for IB polymerizations initiated by TMPCl, IB$_2$BMP, and IB$_2$BP. Conditions were as follows: 60/40 Hex/MeCl cosolvents (v/v); -70 °C; $[IB]_0 = 1.00$ M; $[I]_0 = 12.2$ mM; $[TiCl_4]_0 = 48.8$ mM; $[2,6\text{-lutidine}]_0 = 4.00$ mM.
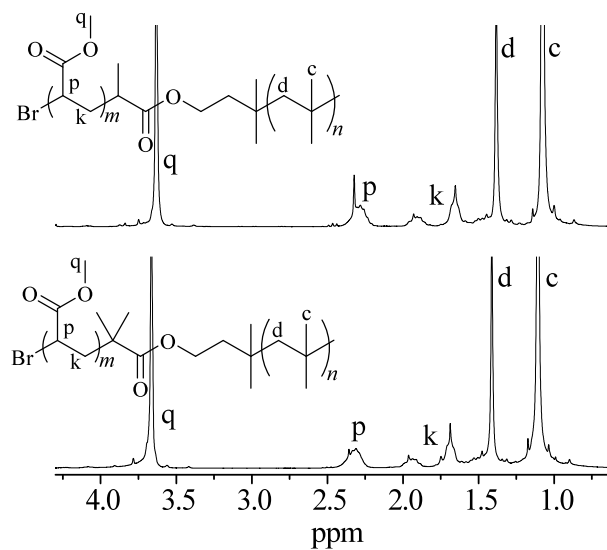
Figure 16. Proton and NMR spectra of BP-PIB-*b*-PMA$_{60}$ (upper) and BMP-PIB-*b*-PMA$_{60}$ (lower).
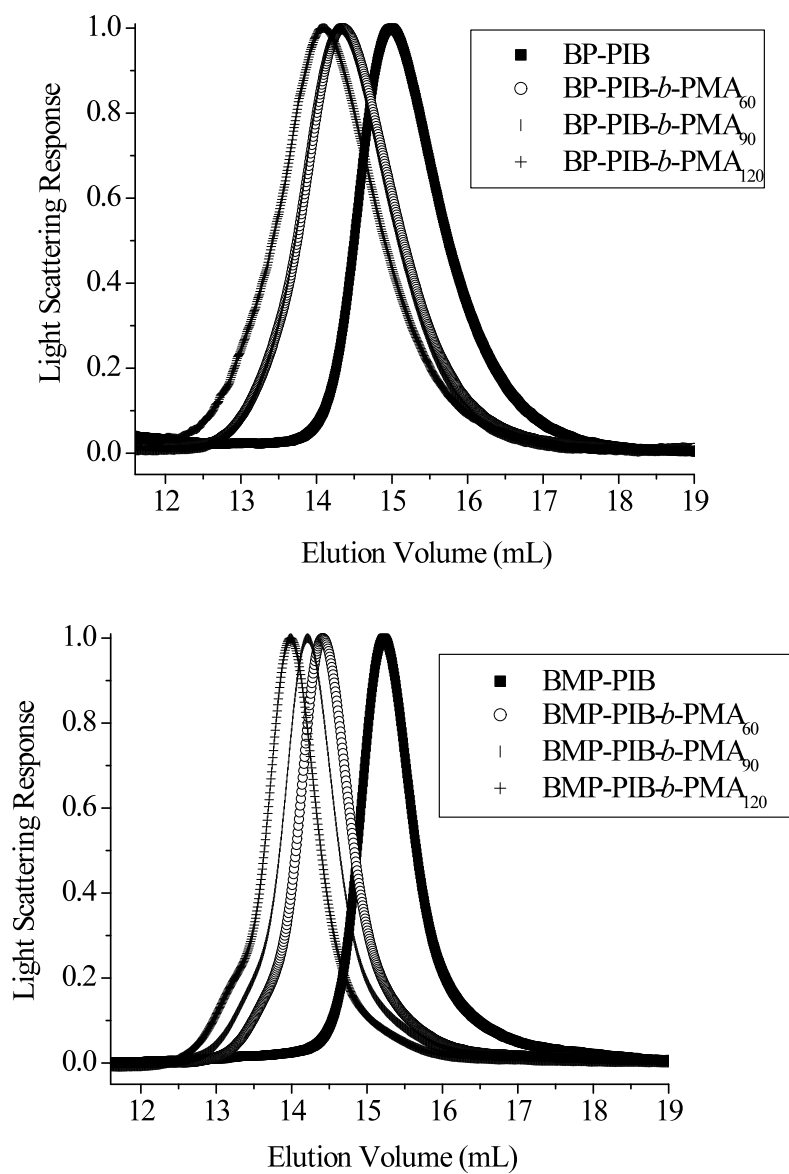
Figure 17. The SEC elution curves (crude samples prior to precipitation) of BP-PIB-*b*-PMA (upper) and BMP-PIB-*b*-PMA (lower) with different length of PMA block.

CHAPTER III

MODIFICATION OF MONO-CATIONIC MONO-RADICAL DUAL INITIATORS

TO TARGET QUANTITATIVE INITIATION EFFICIENCY

Objective

As discussed in earlier chapters, dual initiators, 3,3,5-trimethyl-5-chlorohexyl 2-bromo-2-methylpropionate (IB$_2$BMP) and 3,3,5-trimethyl-5-chlorohexyl 2-bromopropionate (IB$_2$BP) (Figure 9) possessing initiating sites for both living carbocationic polymerization (LCP) and atom transfer radical polymerization (ATRP) were developed to imporove upon an earilier initiator, 3,3,5-trimethyl-5-chlorohexyl acetate (TMCHA), which required intermediate chemical reactions to be fitted with an ATRP initiating site. It was expected that IB$_2$BP and IB$_2$BMP would also improve or eliminate the low initiation efficiency (I_{eff}) displayed by TMCHA.[182] We demonstrated that IB$_2$BMP and IB$_2$BP show equal ability to initiate LCP of isobutylene (IB), and that the α-bromoester head groups are unaffected by the cationic polymerization and remains intact for subsequent ATRP initiation of, for example, an acrylate monomer methyl acrylate (MA). However, at low temperature (-70 °C) and relatively low monomer/initiator ratio (48-82), these initiators also displayed low cationic initiation efficiencies, in the range 0.50 - 0.80 depending on polymerization time, catalyst concentration, and solvent polarity. Higher cationic initiation efficiencies (0.80 < I_{eff} < 0.90) were observed when temperature was increased to -50 °C and/or the monomer/initiator ratio was increased.

Low I_{eff} of IB$_2$BMP, IB$_2$BP, and similar initiators such as TMCHA has been attributed to complexation between the Lewis acid catalyst, TiCl$_4$, and the carbonyl

oxygen of the ester group.[249,245,182] Complexation between Lewis acids and carbonyl

groups is well known[250,251,252] and nearly always characterized by a 1:1 stoichiometry.[251]

In the IB_2BMP, IB_2BP, and TMCHA systems, complexation is revealed by a lower

polymerization rate caused by a lower effective concentration of $TiCl_4$, $[TiCl_4]_{eff}$.[182] The

effect on rate can be offset by compensating the amount of $TiCl_4$. However, we have

observed that I_{eff} of IB_2BMP is unaffected by changes in $TiCl_4$ concentration.[249]

By studying the structure of IB_2BMP, we now hypothesize that low I_{eff} is not

caused by complexation or the presence of the ester carbonyl within the molecule, *per se*,

but rather proximity of the $TiCl_4$:carbonyl complex to the initiating center (*tert*-chloride

group). In IB_2BMP, the $TiCl_4$:carbonyl complex and the *tert*-chloride group interact

readily via an entropically favored cycle conformer. This interaction may substantially

diminish the rate of ionization of the *tert*-chloride group, thereby reducing I_{eff}.

To test this hypothesis, we designed a new initiator 1,5-dichloro-3,3,5-

trimethylhexane (TMHDCl) (Figure 18), which shares the same 5-chloro-3,3,5-

trimethylhexyl cationic initiating structure with IB_2BMP. Instead of an ATRP-ready

initiating site, it is functionalized with a primary chloride, which is inert under LCP

conditions. Therefore, there is no concern of the initiator-$TiCl_4$ complexation issue, and

TMHDCl is expected to be able to initiate cationic polymerization of IB quantitatively.

Moreover, we synthesized a new dual initiator, 3,3,5,5,7-pentamethyl-7-

chlorooctyl 2-bromo-2-methylpropionate (IB_3BMP) (Figure 19), which preserves the

same α-bromoester and *tert*-chloride functional groups as in IB_2BMP, but separates

them by one additional IB repeating unit. With this structure, cyclic conformers that

bring the $TiCl_4$:carbonyl complex and *tert*-chloride group into proximity are not likely

and interactions between them should be disrupted. Therefore, if the hypothesis is

correct, IB$_3$BMP should exhibit excellent initiation efficiency.

<div align="center">Experimental</div>

Materials

2-Methallyltrimethylsilane (MATMS) (>95%) was used as received from Gelest

Inc. Thionyl chloride (SOCl$_2$) (≥99%) was used as received from Sigma-Aldrich, Inc.

Ammonium hydroxide (NH$_4$OH) (28.0-30.0%) was used as received from Fisher

Scientific. 2,4,4,6,6-Pentamethyl-1-heptene (PM1H) was generously provided by

Chevron Oronite Company, LLC, and was vacuum distilled prior to use. The sources

and purity of all other reagents were the same as reported in the previous chapter.

Instrumentation

Absolute molecular weights and polydispersity index of polyisobutylene (PIB)

and poly(isobutylene-*b*-methyl acrylate) copolymer (PIB-*b*-PMA) were determined

using size exclusion chromatography (SEC) (35 °C, THF) with interferometric

refractometer and multi-angle laser light scattering (MALLS) detectors. The dn/dc

value used for PIB homopolymer was calculated from the following equation:[241] dn/dc =

0.116(1-108/$\overline{M}_n$) ($\overline{M}_n$ = number average molecular weight); the dn/dc value for PIB-*b*-

PMA was calculated from the interferometric refractometer detector response and

assuming 100% mass recovery from the columns. Solution ^{1}H and ^{13}C nuclear magnetic

resonance (NMR) spectra were obtained at 22 °C using CDCl$_3$ as the solvent and

tetramethylsilane as internal reference. Progress of IB polymerizations was monitored

using real-time, remote-probe (light conduit type) attenuated total reflectance Fourier

Transform infrared spectroscopy (FTIR) (ReactIR™ 4000). Detailed descriptions of the

SEC, NMR, and FTIR instrumentation and corresponding procedures have been included in Chapter II.

Synthesis of 1,5-Dichloro-3,3,5-trimethylhexane (TMHDCl)

The synthesis of the starting material, DTHMH was synthesized as previously described in Chapter II according to the synthetic route shown in Figure 9. The tertiary hydroxyl group was chlorinated by reaction with excess HCl (g) in CH_2Cl_2 following the same procedure as described in Chapter II. After removal excess gaseous HCl in the solution using sodium bicarbonate, the solution was dried over $MgSO_4$ and 5-chloro-3,3,5-trimethylhexanol was isolated by vacuum stripping of the solvent.

The hydroxyl group of 5-chloro-3,3,5-trimethylhexanol was converted to chloride by reaction with $SOCl_2$ as follows: Into a 100 mL round-bottom flask equipped with magnetic stirrer were charged 5-chloro-3,3,5-trimethylhexanol (4.0 g, 0.022 mol) and 50 mL triethylamine. $SOCl_2$ (2.0 mL, 0.027 mol) was added dropwise into this solution over a period of 30 min. The reaction was allowed to proceed for another additional 7 h. Then diethyl ether was added to extract the product, and the solution was washed thrice with de-ionized water (DI H_2O) to remove triethylamine. The organic phase was dried over magnesium sulfate. The crude liquid product was then distilled to obtain pure TMHDCl as a light yellow oil in 10% yield (0.44 g). ^{1}H NMR ($CDCl_3$): δ = 1.08 (s, 6H, 3-Me), 1.68 (s, 6H, CH_3CCl), 1.86 (s, 2H, 4-H), 1.92 (t, 2H, 2-H), 3.57 (t, 2H, 1-H) ppm. ^{13}C NMR: δ = 28.64 (3-Me), 34.95 (5-Me), 35.25 (C3), 41.11 (C2), 46.38 (C4), 55.41 (C1), 70.69 (C5) ppm.

Synthesis of 3,3,5,5,7-Pentamethyl-7-chlorooctyl 2-bromo-2-methylpropionate (IB₃BMP)

The starting material, IB$_2$BMP, was prepared as described in Chapter II, with the synthetic route shown in Figure 9. As illustrated in Figure 19, IB$_3$BMP was synthesized from IB$_2$BMP by reaction with 2-methallyltrimethylsilane (MATMS) at -94 °C with TiCl$_4$ as the catalyst, followed by hydrochlorination with anhydrous HCl (g). The procedure was analogous to that of Mayr et al.[253]

In a 250 mL round-bottom flask, MATMS (4.12 g, 3.21×10^{-2} mol) in 180 mL CH$_2$Cl$_2$ was cooled to about -94 °C using an external acetone/liquid N$_2$ bath. TiCl$_4$ (1.60 mL, 1.46×10^{-2} mol) was slowly added, and the color of the reaction mixture turned to dark red. Next, a solution of IB$_2$BMP (2.63 g, 8.03×10^{-3} mol) and MATMS (2.36 g, 1.84×10^{-2} mol) in about 10 mL CH$_2$Cl$_2$ was dropped into the mixture during 30 min. The solution was stirred for 2 h at low temperature, and then the reaction was terminated by addition of 20 mL NH$_4$OH aqueous solution. A fine, solid precipitate appeared, and the solution turned from dark orange to white. The reaction mixture was filtered, and the organic and aqueous layers were separated. The aqueous layer was extracted with CH$_2$Cl$_2$, and the combined organic fractions were dried with MgSO$_4$. The solution was filtered and vacuum stripped to yield 2.54 g (91.1%) of the crude olefin, 3,3,5,5,7-pentamethyl-7-octenyl 2-bromo-2-methylpropionate. After vacuum distillation, the pure olefin was isolated as a colorless oil in 45.3% yield (1.26 g). ^{1}H NMR (CDCl$_3$): $\delta =$ 1.03 (s, 6H, 5-Me), 1.05 (s, 6H, 3-Me), 1.34 (s, 2H, 3-H), 1.69 (t, 2H, 2-H), 1.78 (s, 3H, 7-Me), 1.93 (s, 6H, CH$_3$CBr), 2.00 (s, 2H, 6-H), 4.24 (t, 2H, 1-H), 4.64 (m, 1H, olefin), 4.86 (m, 1H, olefin) ppm. ^{13}C NMR: $\delta = 25.70$ (7-Me), 28.97 (5-Me), 29.28 (3-Me), 30.73 (CH$_3$CBr), 34.26 (C3), 35.82 (C5), 42.41 (C2), 53.12 (C6), 53.59 (C4), 55.85 (CBr), 63.61 (C1), 114.53 (C8), 143.45 (C7), 171.61 (CO) ppm.

The olefin was hydrochlorinated with dry, gaseous HCl using a procedure analogous to that used for IB$_2$BMP as reported in Chapter II, and the final product, 3,3,5,5,7-pentamethyl-7-chlorooctyl 2-bromo-2-methylpropionate (IB$_3$BMP) was obtained in 93.5% yield (1.38 g). ^{1}H NMR (CDCl$_3$): δ = 1.07 (s, 6H, 3-Me), 1.18 (s, 6H, 5-Me), 1.45 (s, 2H, 4-H), 1.68 (s, 6H, CH$_3$CCl), 1.70 (t, 2H, 2-H), 1.93 (s, 6H, CH$_3$CBr), 1.95 (s, 2H, 6-H), 4.25 (t, 2H, 1-H) ppm. ^{13}C NMR: δ = 29.32 (3-Me), 29.96 (5-Me), 30.73 (CH$_3$CBr), 34.41 (C3), 35.18 (C8), 37.28 (C5), 42.68 (C2), 54.91 (C4), 55.85 (CBr), 58.44 (C6), 71.51 (C7), 171.61 (CO) ppm.

Synthesis of 2-Chloro-2,4,4,6,6-pentamethylheptane (PMHCl)

PMHCl was synthesized from 2,4,4,6,6-pentamethyl-1-heptene (PM1H) by hydrochlorination with dry, gaseous HCl using a procedure analogous to that used for IB$_2$BMP as reported in Chapter II. ^{1}H NMR (CDCl$_3$): δ = 1.00 (s, 9H, *t*-Bu), 1.15 (s, 6H, 4-Me), 1.39 (s, 2H, 5-H), 1.68 (s, 6H, CH$_3$CCl), 1.96 (s, 2H, 3-Me) ppm. ^{13}C NMR: δ = 29.90 (4-Me), 32.29 (6-Me), 32.48 (C6), 35.17 (CH$_3$CCl), 37.28 (C4), 57.07 (C5), 58.31 (C3), 71.82 (C2) ppm.

Polymerizations

LCPs of IB were carried out using either IB$_2$BMP, IB$_3$BMP, TMHDCl, 2-chloro-2,4,4-trimethylpentane (TMPCl), or PMHCl as initiator, TiCl$_4$ as catalyst, and 2,6-lutidine as proton trap/common ion salt precursor, in 60/40 (v/v) hexane/MeCl cosolvents at -70 °C as described in Chapter II. All polymerizations were conducted within an inert atmosphere drybox equipped with a hexane/heptane cold bath using FTIR (ReactIR™ 4000) to monitor isobutylene conversion by observing the olefinic =CH$_2$ wag (887 cm^{-1}) of IB.

ATRP of methyl acrylate (MA) was carried out in toluene at 70 °C using IB$_3$BMP-initiated PIB (BMP-PIB) as macroinitiator, Cu(I)Br as catalyst, and 1,1,4,7,7-pentamethyldiethylenetriamine (PMDETA), as solvating ligand for Cu(I), in a molar ratio of 1:1:1, as described in Chapter II. The concentration of BMP-PIB was 0.05 M. $\overline{M}_n$ of BMP-PIB by SEC was 4,650 g/mol; the PDI was 1.02, and $\overline{X}_n$ = 77 by NMR.

Results and Discussion

Synthesis of initiators

TMHDCl was prepared by chlorinating both primary and tertiary hydroxyl groups in 1,5-dihydroxy-3,3,5-trimethylhexane (DTHMH). The reactivity of those hydroxyl are not the same, therefore we first performed electrophilic chlorination using gaseous HCl, which selectively converts the tertiary one. The resulting compound was then reacted with thionyl chloride under basic conditions, thereby converting the primary hydroxyl to chlorine.

Since the final product has a low boiling point and the second step is an exothermic reaction, it is important to add thionyl chloride slowly to maintain a slow reaction rate, and thereby maintaining a low reaction temperature. If the reaction is under well control, light yellow liquid should be produced instead of charcoal-like solid.

^{1}H and ^{13}C NMR spectra of the diol starting material (upper) and TMHDCl (lower) are shown in Figures 20 and 21. After reaction with HCl, the methyl and methylene protons next to the *tert*-OH, which appear at 1.3 ppm (peak k) and 1.6 ppm (peak l) shifted to 1.7 ppm and 1.9 ppm, respectively (Figure 20). When the primary hydroxyl was reacted with thionyl chloride, the protons of the C1 methylene, adjacent to the OH group, shifted upfield from 3.7 ppm to 3.6 ppm (peak g); while the signal of the

C2 methylene shifted in the opposition direction to 1.9 ppm (peak f). The C3 methyl protons shifted to 1.1 ppm (peak e) after the 2-step preparation. Integrated areas of all peaks were consistent with the structure of TMHDCl.

In the carbon spectrum (Figure 21), the hydroxyl functionalized quaternary carbon (C5) shifted from 72.3 ppm (peak k) to 70.4 ppm. The 5-methyl and C4 methylene carbons next to the *tert*-OH, which appears at 32.3 ppm (peak b) and 52.5 ppm (peak i), shifted to 34.9 ppm and 40.9 ppm, respectively. Upon conversion of the primary hydroxyl group, the 3-methyl and C3 carbon (peaks c and e) shifted to 28.6 ppm and 35.3 ppm, respectively; while two methylene carbons, C1 and C2 (peaks k and g) shifted downfield to 55.4 ppm and 41.1 ppm, respectively. At the same time, the hydroxyl functionalized quaternary carbon (C5) shifted downfield to 70.7 ppm (peak k). The 5-methyl and C4 methylene carbons next to the *tert*-OH shifted to 35.0 ppm (peak b) and 46.4 ppm (peak i), respectively.

IB$_3$BMP cannot be prepared by reacting IB$_2$BMP with IB, since the desired 1:1 addition product reacts rapidly with additional IB to form polymer.[254] Instead, IB$_2$BMP was first reacted with MATMS in the presence of TiCl$_4$ at low temperature to yield the intermediate olefin, 3,3,5,5,7-pentamethyl-7-octenyl 2-bromo-2-methylpropionate. Then, after vacuum distillation, the olefin was hydrochlorinated to produce the final product.

Figures 22 and 23 show ^{1}H and ^{13}C NMR spectra, respectively, of the intermediate olefin (upper) and IB$_3$BMP (lower). The olefinic protons of the intermediate appear at 4.6 (peak m) and 4.9 ppm (peak n), and the methyl and methylene protons adjacent to the double bond are observed at 1.7 (peak a) and 2.0 ppm (peak b),

respectively (Figure 22, upper). Upon hydrochlorination of the intermediate, the olefinic protons (peaks m and n) disappear. Peaks k, e, and l shift downfield; while peaks a and b shift slightly upfield. Integrated peak areas are consistent with the targeted structures. Similarly, in the carbon spectra (Figure 23) the peaks for the olefinic carbons of the intermediate (peaks l and m) disappear upon hydrochlorination. The new quaternary carbon bonded to chlorine shows a resonance at 72 ppm (peak m). Moreover, peaks h, i, and a move downfield after hydrochlorination.

The initiator PMHCl was prepared by simple hydrochlorination of 2,4,4,6,6-pentamethyl-1-heptene (PM1H). Figures 24 and 25 show the NMR characterization of both the starting material, 2,4,4,6,6-pentamethyl-1-heptene (PM1H) (upper) and PMHCl (lower). After hydrochlorination, the double bond proton peaks (peaks m and n) disappear (Figure 24). Peaks k, e, and l shift downfield, and peaks a and b shifted slightly upfield, exactly the same pattern observed with IB₃BMP. In addition, integrated peak areas are consistent with the targeted structures. In the carbon NMR spectrum, the double bond cartons (peaks m and l) moved from the olefinic region above 100 ppm to the region below 80 ppm (Figure 25), similarly to the change observed for IB₃BMP.

IB Polymerizations

To test the initiation performance of TMHDCl, living carbocationic polymerizations of IB were conducted with $TiCl_4$ as the catalyst and 2,6-lutidine as the proton trap targeting molecular weights of 5,000 (5k) g/mol. Results presented in Chapter II have shown that $[TiCl_4]_0$ does not influence $I_{eff.}$[249] In the cationic polymerizaiton of IB initiated by TMHDCl, the concentration of $TiCl_4$ catalyst was set at $[TiCl_4]_0 = 3.5 \times [I]_0$ in order to maintain a relatively slow polymerization rate. To

better evaluate TMHDCl, control polymerizations were conducted with IB_2BMP and the standard IB cationic polymerization initiator TMPCl, used as initiators. The latter compound contains the same cationic initiating site and thus the same degree of back strain as TMHDCl. Because TMHDCl does not contain a secondary functional group that can interact with $TiCl_4$ and thereby interfere with IB polymerization, an I_{eff} higher than IB_2BMP and similar to TMPCl is expected, provided the low initiation efficiency displayed by IB_2BMP is due to the ester-$TiCl_4$ complex.

Polymerization kinetics for the three initiators were studied employing data collected by FTIR spectroscopy; the first-order kinetic plots are shown in Figure 26. The most rapid polymerization was produced by TMPCl, the only initiator to yield a linear first-order plot. This confirms that the concentration of active species is constant throughout the course of polymerization. Thus initiation with TMPCl is rapid and complete ($I_{eff} \sim 1$). The polymerization induced by IB_2BMP yielded an upwardly concave curve with the smallest initial slope. This behavior is characteristic of slow and incomplete initiation. The upward curvature indicates that the concentration of active species is initially low, increasing over time as initiation and propagation occur simultaneously. The final, linear region is considerably lower in slope than the TMPCl plot. This is consistent not only with incomplete initiation but also a lower effective $TiCl_4$ concentration due to complexation with IB_2BMP. This analysis is supported by the observed broad polydispersity (PDI = 1.11, Table 7) for the final polymer from IB_2BMP. The behavior of TMHDCl was similar to that of IB_2BMP. It also displayed an upwardly concave first-order plot indicative of slow initiation. The fact that the overall rate of polymerization was higher for TMHDCl than for IB_2BMP suggests that

the former does not complex $TiCl_4$.

The apparent rapid monomer consumption (RMC) observed in Figure 26 (apparent y-intercept) is due to precipitation resulting from proton scavenging by 2,6-lutidine.[255] The precipitate plates onto to the ReactIR probe, thereby distorting the FTIR spectral baseline and creating the appearance of a psudo-RMC phenomenon.

Characterization results for polymers produced from TMPCl, IB_2BMP and TMHDCl are listed in Table 7. Here I_{eff} was calculated as $\overline{X}_{n\,theo}/\overline{X}_{n\,PIB}$ and $\overline{M}_{n\,theo}/\overline{M}_{n\,PIB}$ using NMR and SEC/MALLS data, respectively. The $\overline{X}_{n\,theo}$ was calculated as the molar ratio of monomer to initiator charged to the reactor. The number average molecular weight was calculated using $\overline{M}_{n\,theo} = \left(\overline{X}_{n\,theo} \times M_{IB}\right) + M_I$, where M_{IB} and M_I are the molecular weights of isobutylene and the initiator, respectively. The $\overline{X}_{n\,PIB}$ was calculated from ^{1}H NMR data using equation (1),

$$\overline{X}_{n\,PIB} = \frac{A_{Me}/6}{A_{CE}} - i \tag{1}$$

here A_{Me} is the integrated peak area of the methyl protons in the PIB repeat unit, A_{CE} is the same as defined in Chapter II, and i assumes a value of 1 for IB_2BMP and TMPCl and a value of 2 for IB_3BMP and PMHCl.

The standard initiator, TMPCl yielded a narrow-PDI polymer with an I_{eff} of almost 1 (0.98 from NMR and 0.97 from SEC results). However, polymers produced by IB_2BMP and TMHDCl possessed comparably high molecular weights and broad PDIs. Their I_{eff} value calculated from SEC data were 0.63 and 0.65, respectively. The results of SEC analysis are presented in Figure 27. TMPCl-initiated PIB has a narrow and

symmetric elution peak, whereas IB$_2$BMP-initiated PIB has a shorter retention time and an asymmetric elution peak. The SEC profile of PIB initiated by TMHDCl almost overlaps with that of IB$_2$BMP, which is consistent with the data in Table 7 and the kinetic study. It is unclear why TMHDCl displays slow initiation and in other respects behaves similarly to IB$_2$BMP, even though it apparently does not complex TiCl$_4$.

The performance of IB$_3$BMP as a cationic polymerization initiator was evaluated by conducting TiCl$_4$-co-initiated IB polymerizations at -70 °C. The targeted molecular weights were 3,000 (3k), 5,000 (5k), and 10,000 (10k) g/mol. Low target molecular weights were chosen to better judge the performance of the initiators. If IB$_3$BMP displays good initiation efficiency for preparing low molecular weight PIBs, its efficiency will be the same or higher at greater monomer/initiator ratios. The direct comparison of IB$_3$BMP directly with three control initiators, IB$_2$BMP and the two monofunctional initiators TMPCl and PMHCl (hydrochlorinated IB dimer and trimer, respectively) was done. Faust and Mayr et al.[256] reported that, compared to the PIB *tert*-chloride chain end, TMPCl is approximately 2.5 times more slowly ionizing and PMHCl is approximately 1.4 times more slowly ionizing due to lower degrees of back strain.

Table 8 lists the characterization results of PIB polymers produced from the four initiators. Standard initiators TMPCl and PMHCl exhibited high initiation efficiencies (~1) in all cases with near-monodisperse PIBs having targeted molecular weights obtained. Polymers initiated by IB$_2$BMP were relatively polydisperse, with I_{eff} around 0.5 for a 3k molecular weight target, 0.6 for 5k, and 0.8 for 10k. Although I_{eff} increased with higher target molecular weight, it remained less than quantitative. In contrast, IB$_3$BMP was an excellent ATRP-ready cationic initiator. It consistently performed well

in preparing both low and high molecular weight PIBs. The NMR and SEC data

showed that the resulting PIBs achieved the target molecular weights with narrow PDIs.

The SEC elution curves of representative PIB-3k samples are shown in Figure 28.

These curves clearly demonstrate the difference between IB_2BMP and IB_3BMP. The

elution curve for IB_3BMP is nearly identical to those of PMHCl and TMPCl; all are very

narrow and symmetrical. In contrast, the curve for IB_2BMP is much broader and

displays a low molecular weight tail, characteristic of slow initiation.

Polyisobutylenes produced from IB_3BMP possess the desired 2-bromo-2-

methylpropionate head group. Figure 29 shows the ^{1}H NMR spectrum of a

representative PIB-3k produced from IB_3BMP. The methylene unit adjacent to the ester

linkage was observed as a triplet centered at 4.2 ppm. The integrated area of this peak

was approximately one-third that for the methyl groups (peak a) adjacent to the *tert*-

chloride end group, indicating that the α-bromoester functionality was quantitatively

maintained during the LCP of IB. This dual initiator therefore produces ATRP-ready

polymers.

Because of complex formation between Lewis acid and carbonyl oxygen,

IB_3BMP requires a higher $TiCl_4$ concentration, compared to standard initiators TMPCl

or PMHCl, to achieve a given rate of polymerization. Figure 30 shows first-order

kinetic plots as determined by *in situ* FTIR (ReactIR™ 4000) for IB polymerizations

initiated from IB_3BMP and PMHCl. The slight deviations from linearity observed in the

plots reflect shifts in the equilibrium between dormant and active chain ends, due to the

rise and fall of the reaction temperature caused by the initial exotherm of polymerization.

This effect has been explained in detail previously.[242] The two polymerizations depicted

in Figure 30 were formulated identically except for the identity of the initiator, and the fact that one additional equivalent of $TiCl_4$ (relative to the initiator) was used for the case of IB_3BMP. The kinetic plots are identical within experimental error, indicating that $[TiCl_4]_{eff}$ was the same in the two reactions. This demonstrates the existence of complexation and shows that it is approximately 1:1.

The results in Table 8 and Figure 28 clearly show that IB_2BMP is a relatively inefficient cationic initiator as compared with the standard oligoisobutylene hydrochlorides PMHCl and TMPCl, and IB_3BMP. Disappointing results have also been reported for other ester initiators derived from 5-chloro-3,3,5-trimethylhexanol, such as 3,3,5-trimethyl-5-chlorohexyl 2-bromopropionate (IB_2BP),[249] 3,3,5-trimethyl-5-chlorohexyl acetate $(TMCHA)$,[182] 3,3,5-trimethyl-5-chlorohexyl methacrylate,[245,257] and 3,3,5-trimethyl-5-chlorohexyl isobutyrate.[257] These authors concluded the poor initiating performance is caused by complexation between Lewis acid and carbonyl oxygen of the ester group. However, this explanation cannot be correct based on the essentially ideal initiating performance displayed by IB_3BMP. The latter ester is composed of the same carboxylic acid component as IB_2BMP, and the two molecules have essentially identical structure in the immediate environment of the ester group. Furthermore, polymerization kinetics show that IB_3BMP and IB_2BMP tend to produce the same $[TiCl_4]_{eff}$ within the reactor, suggesting a similar degree of complexation.

The results in Table 7 and Figure 26 and 27 also show the poor initiation performance of IB_2BMP. The new cationic initiator, TMHDCl, which does not contain bromoester functionality, was predicted to have initiation performance similar to the standard cationic initiator, TMPCl. However, TMHDCl-initiated polymerizations were

actually slower than those initiated by TMPCl. In addition, the first-order plots of

TMHDCl and IB$_2$BMP are similar in shape. The fact that the rate of polymerization was

higher with TMHDCl than with IB$_2$BMP indicates that [TiCl$_4$]$_{eff}$ was decreased in the

latter system through complexation with the ester. Furthermore, TMHDCl displayed

slow initiation and low I_{eff} to almost the same degree as IB$_2$BMP.

The results obtained with TMHDCl are consistent with the explanation that in

IB$_2$BMP and similar initiators, the TiCl$_4$:carbonyl complex and the *tert*-chloride group

interact via an entropically favorable cyclic conformer. This interaction diminishes the

rate of ionization of the *tert*-chloride group, thereby reducing I_{eff}. In IB$_3$BMP, the

increased separation between the two sites eliminates this interaction. The TMHDCl

results show that this through-space interaction is not limited to initiators with ester

functionality. Because it shares the same 5-chloro-3,3,5-trimethylhexyl backbone

structure with IB$_2$BMP, TMHDCl is capable of forming similar cyclic conformers. The

only difference is that the interacting group is a chloride instead of a TiCl$_4$:ester

complex. Based on these results, we theorize that this interaction and its negative effect

on initiation performance can be expanded to include other interfering functionalities,

provided the basic initiator backbone structure is the same. Further study is needed to

substantiate this hypothesis.

ATRP Polymerization

We have demonstrated successful ATRP of MA from PIB macroinitiators

produced from IB$_2$BMP in the previous chapter. Because PIB macroinitiators prepared

from IB$_2$BMP and IB$_3$BMP are identical, their behavior in subsequent ATRP initiation

should also be the same. To confirm this expectation, the ATRP of MA was initiated

using a representative BMP-PIB macroinitiator; the results are summarized in Table 9.

The observed polymerization degree of the PMA block, $\overline{X}_{n\,PMA}$, was very close to the

targeted value (40); SEC and NMR analysis indicated quantitative initiation efficiency.

Figure 31 and 32 show SEC elution curves of BMP-PIB macroinitiator and resulting

BMP-PIB-*b*-PMA$_{40}$ block copolymer, and the ^{1}H NMR spectrum of BMP-PIB-*b*-PMA$_{40}$

block copolymer, respectively.

Conclusions

IB$_3$BMP, a dual initiator possessing the same radical and cationic initiating sites

as the dual initiator IB$_2$BMP described in Chapter II, but with an additional IB repeating

unit between the ester and *tert*-Cl functional groups, was shown to be an excellent

cationic initiator. Structure of the new initiator was characterized using ^{1}H and ^{13}C

NMR spectroscopy. Its initiation efficiency in the LCP of IB was quantitative ($I_{\text{eff}} \sim 1$)

under all polymerization conditions studied, including low temperature (-70 ºC) and low

monomer/initiator ratios. NMR and SEC analysis showed IB$_3$BMP-initiated PIBs have

the same molecular weights and PDIs as those obtained from the standard initiators

TMPCl and PMHCl. Since its radical initiating site is identical to that of IB$_2$BMP, PIB

macroinitiators produced from IB$_3$BMP perform equally well in ATRP.

We also synthesized a new cationic initiator, TMHDCl, by chlorinating both the

primary and tertiary hydroxyl groups of DTHMH. This compound does not have an

ester function, preventing complexation with the TiCl$_4$ catalyst. It contains the same

cationic initiating site as TMPCl and it is expected to have the same initiation efficiency.

However, TMHDCl performed poorly in IB polymerization. Kinetic studies utilizing

FTIR and NMR spectroscopy as well as SEC characterization showed that this initiator

performed similarly as IB_2BMP.

Therefore, we conclude that the poor initiation efficiency of IB_2BMP, TMCHA, and other initiators derived from 3,3,5-trimethyl-5-chlorohexanol is not simply caused by complexation. Instead, it is the interaction between the interfering functionality on C1 and the *tert*-chloride group, via an entropically favorable cyclic conformer. This explains why differences in the carboxylic acid component of the ester, i.e., acetyl group in TMCHA, 2-bromo-2-methylpropionoyl group in IB_2BMP, etc., that to introduce different steric and/or inductive properties to the carbonyl group, do not result in any improvement in I_{eff}. However, when *tert*-chloride and ester groups are further separated, as in IB_3BMP, the interfering interaction disappears and I_{eff} approaches 100%. Moreover, this interaction is not limited to initiators containing ester groups, but is also applicable to other interfering functionalities such as primary chloride, as evidenced by the slow initiation of TMHDCl.

Table 7. Charaterization of Living Carbocationic Polymerizations (LCP) of isobutylene (IB) Induced by IB_2BMP, TMHDCl and TMPCl

| | NMR | | | SEC | | | |
	$\overline{X}_{n\ PIB}$	$\overline{X}_{n\ theo}$	I_{eff}	$\overline{M}_{n\ PIB}$ (g/mol)	$\overline{M}_{n\ theo}$ (g/mol)	I_{eff}	PDI
IB_2BMP-5k	111	82	0.74	7860	4930	0.63	1.11
TMHDCl-5k	107	82	0.77	7390	4800	0.65	1.08
TMPCl-5k	84	82	0.98	4920	4750	0.97	1.02

Note. 60/40 Hex/MeCl cosolvents (v/v); -70 °C; $[IB]_0 = 1.00$ M; $[I]_0 = 12.2$ mM; $[TiCl_4]_0 = 4.27$ mM; $[2,6\text{-lutidine}]_0 = 4.00$ mM

Table 8. Characterization Results for PIBs Prepared from Different Initiators: IB_2BMP,

IB_3BMP, TMPCl and PMHCl

	NMR			SEC			
	$\overline{X}_{n\,PIE}$	$\overline{X}_{n\,the}$	I_{eff}	$\overline{M}_{n\,PIB}$ (g/mol)	$\overline{M}_{n\,theo}$ (g/mol)	I_{eff}	PDI
TMPCl-3k	52	48	0.92	3090	2840	0.92	1.02
IB_2BMP-3k	94	48	0.51	5630	3020	0.53	1.10
IB_3BMP-3k	49	48	0.98	3180	3080	0.97	1.07
PMHCl-3k	49	48	0.98	2900	2900	1.00	1.01
TMPCl-5k	87	82	0.94	4920	4750	0.96	1.01
IB_2BMP-5k	120	82	0.64	8410	4930	0.59	1.05
IB_3BMP-5k	86	82	0.95	5070	4990	0.98	1.03
PMHCl-5k	85	82	0.97	4800	4810	1.00	1.01
TMPCl-10k	161	164	1.02	9050	9350	1.03	1.05
IB_2BMP-10k	201	164	0.82	11370	9530	0.84	1.06
IB_3BMP-10k	170	164	0.96	9580	9590	1.00	1.06
PMHCl-10k	165	164	0.99	9340	9410	1.01	1.06

Note. 60/40 Hex/MeCl cosolvents (v/v); -70ºC; $[IB]_0 = 1.00$ M; $[2,6\text{-lutidine}]_0 = 4.00$ mM

$[I]_0 = 20.8$ mM; $[TiCl_4]_0 = 62.5$ mM for 3k samples

$[I]_0 = 12.2$ mM; $[TiCl_4]_0 = 48.8$ mM for 5k samples

$[I]_0 = 6.1$ mM; $[TiCl_4]_0 = 48.8$ mM for 10k samples

Table 9. ATRP[a] of methyl acylate(MA) Initiated from a PIB Macroinitiator[b] Prepared from IB$_3$BMP

	NMR		SEC		
	$\overline{X}_{n\text{ PMA}}$	wt% PMA	$\overline{M}_{n\text{ PMA}}$ (g/mol)	PDI	wt% PMA
BMP-PIB-*b*-PMA$_{40}$	38	41.0	3600	1.03	43.6

Note. [a][BMP-PIB]$_0$:[CuBr]$_0$:[PMDETA]$_0$ = 1:1:1 ([BMP-PIB]$_0$ = 0.05 M) in toluene at 70 °C; 0.60[MA]$_0$/[MacroI]$_0$ = 40; conversion of MA limited to 60%

[b]BMP-PIB: $\overline{M}_n$ = 4,650 g/mol and PDI = 1.02 (SEC); $\overline{X}_n$ = 77 (NMR)
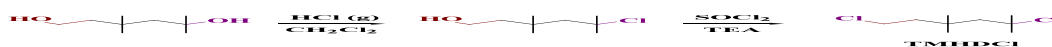
Figure 18. Synthesis of 3,3,5-trimethyl-1,5-dichlorohexane (TMHDCl) from 1,5-dihydroxy-3,3,5-trimethylhexane (DTHMH).
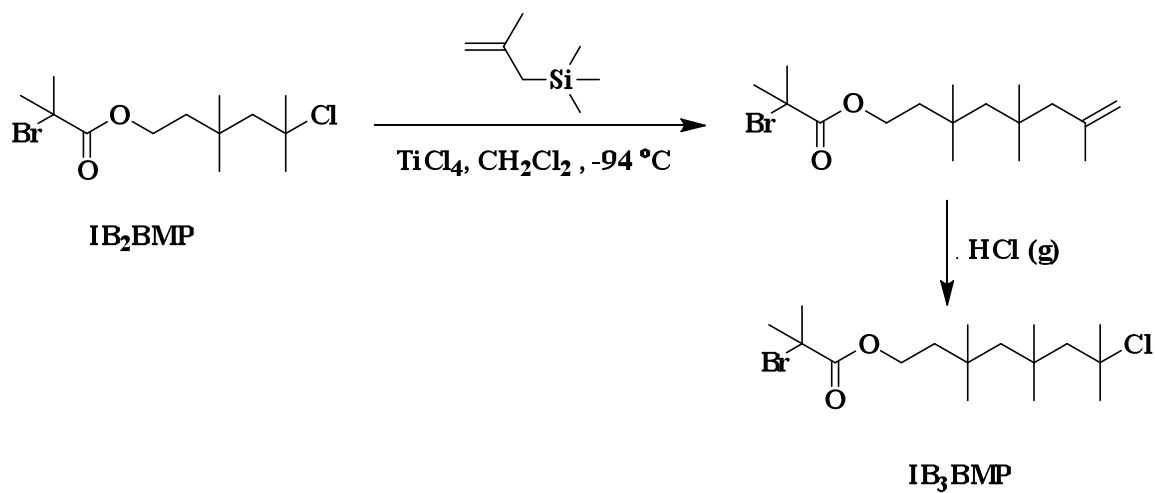
Figure 19. Previously reported dual initiator 3,3,5-trimethyl-5-chlorohexyl 2-bromo-2-methylpropionate (IB$_2$BMP) and synthesis of 3,3,5,5,7-pentamethyl-7-chlorooctyl 2-bromo-2-methylpropionate (IB$_3$BMP) therefrom.
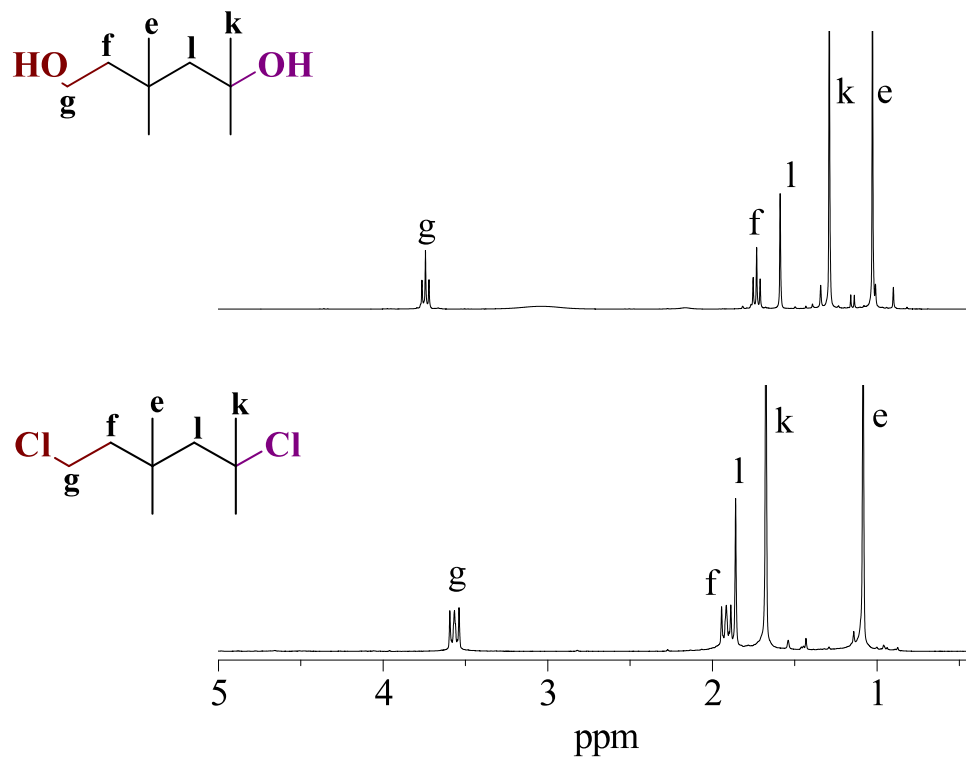
Figure 20. Proton NMR spectra of 1,5-dihydroxy-3,3,5-trimethylhexane (DTHMH)

(upper) and 1,5-dichloro-3,3,5-trimethylhexane (TMHDCl) (lower).
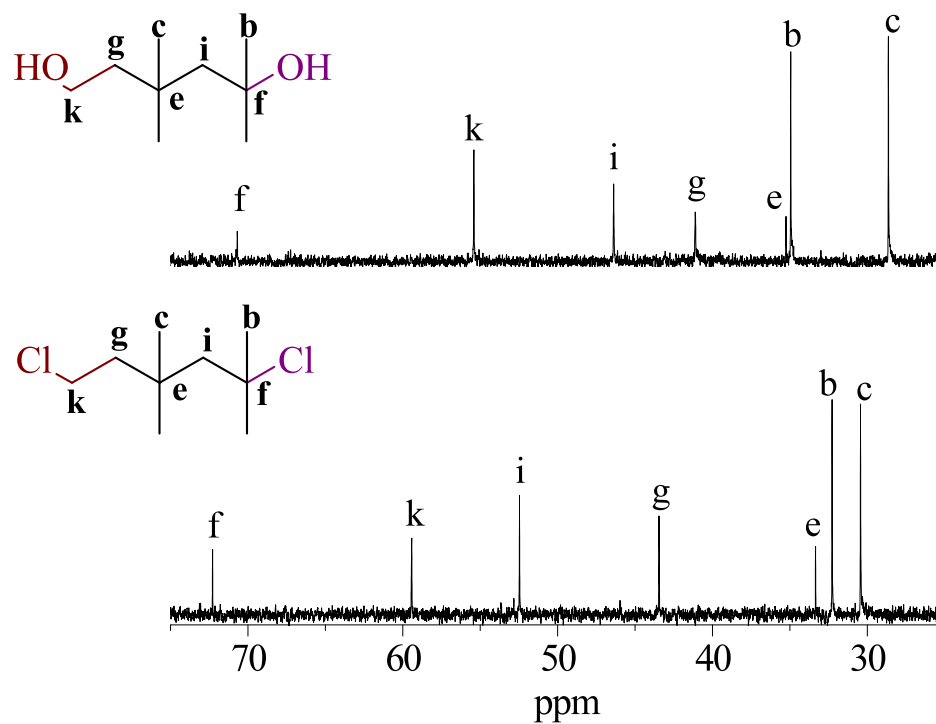
Figure 21. Carbon NMR spectra of 1,5-dihydroxy-3,3,5-trimethylhexane (DTHMH) (upper) and 1,5-dichloro-3,3,5-trimethylhexane (TMHDCl) (lower).
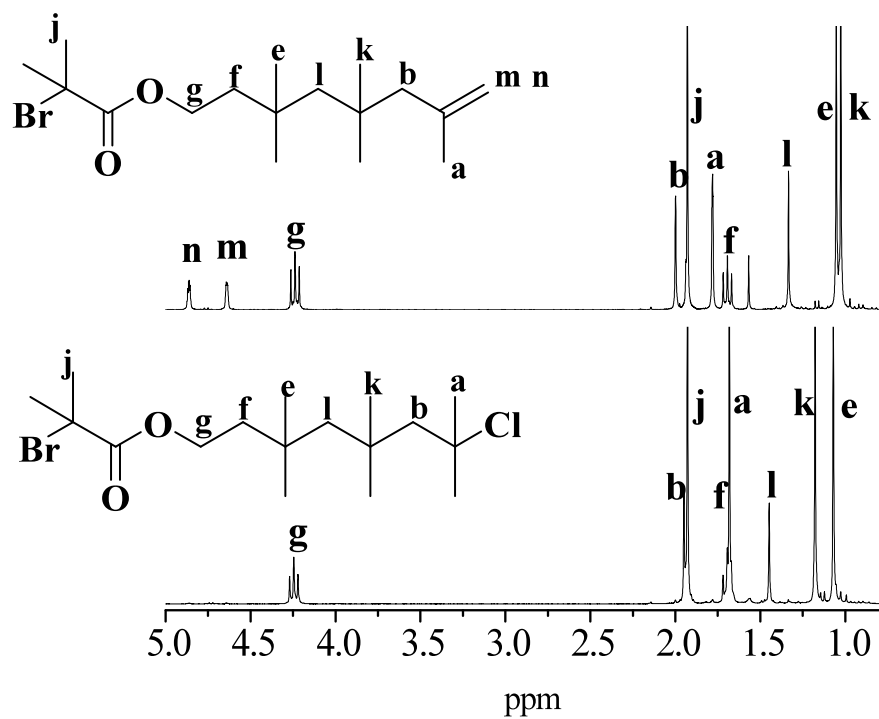
Figure 22. Proton NMR spectra of 3,3,5,5,7-pentamethyl-7-octenyl 2-bromo-2-methylpropionate (upper) and 3,3,5,5,7-pentamethyl-7-chlorooctyl 2-bromo-2-methylpropionate (IB$_3$BMP) (lower).
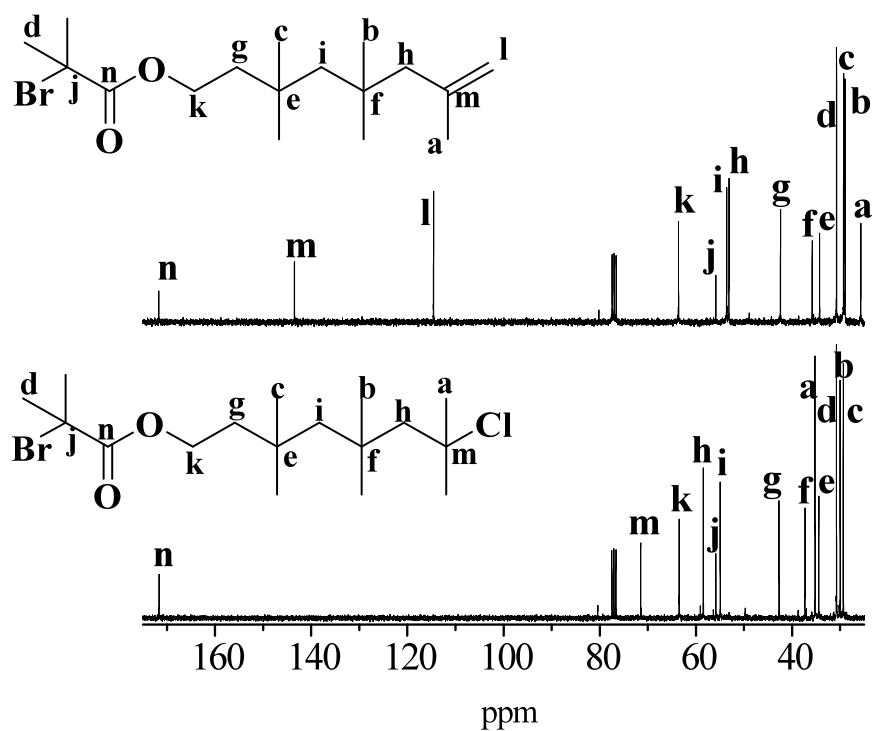
Figure 23. Carbon NMR spectra of 3,3,5,5,7-pentamethyl-7-octenyl 2-bromo-2-methylpropionate (upper) and 3,3,5,5,7-pentamethyl-7-chlorooctyl 2-bromo-2-methylpropionate (IB₃BMP) (lower).
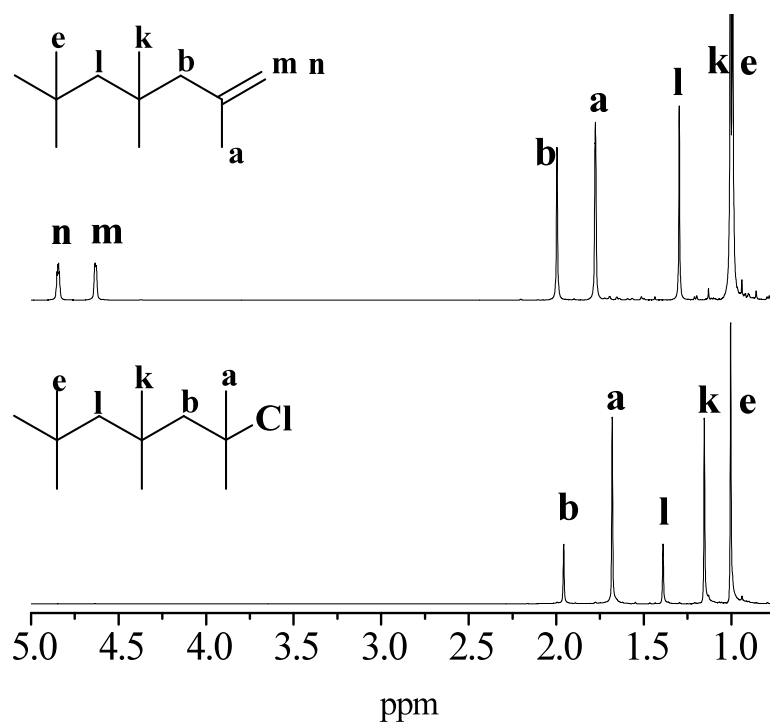
Figure 24. Proton NMR spectra of 2,4,4,6,6-pentamethyl-1-heptene (PM1H) (upper) and 2-chloro-2,4,4,6,6-pentamethylheptane (PMHCl) (lower).
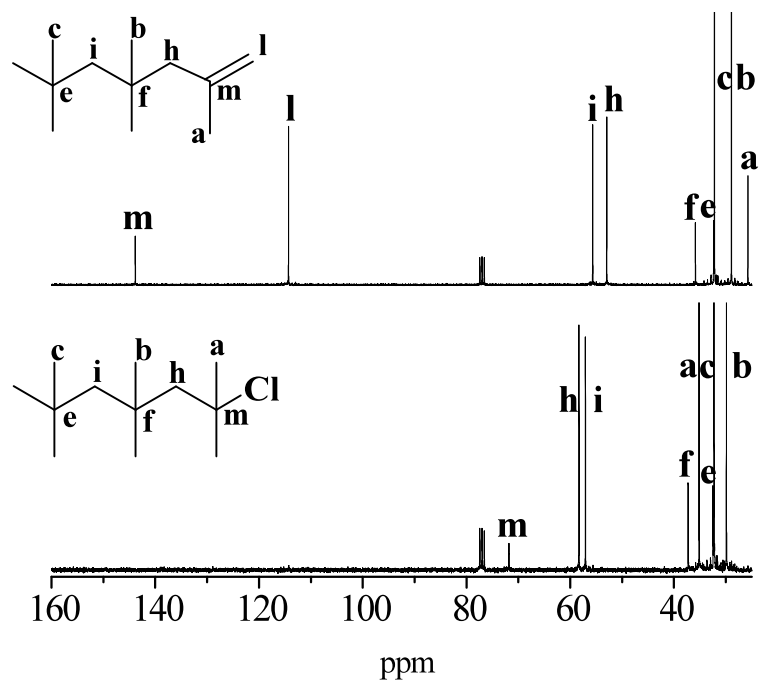
Figure 25. Carbon NMR spectra of 2,4,4,6,6-pentamethyl-1-heptene (PM1H) (upper) and 2-chloro-2,4,4,6,6-pentamethylheptane (PMHCl) (lower).
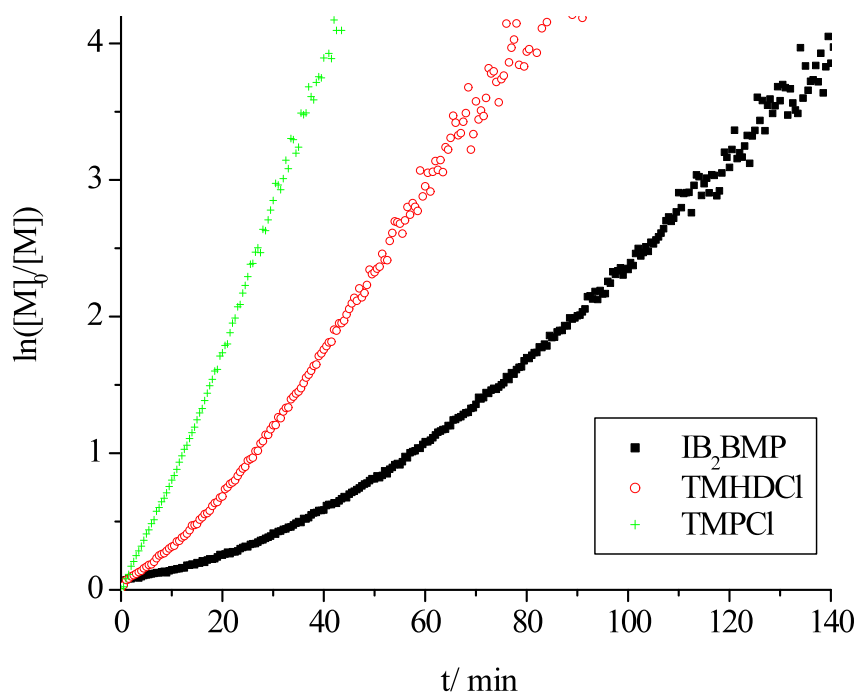
Figure 26. First-order kinetic plots for IB polymerizations at -70 °C using IB_2BMP,

TMHDCl, and TMPCl as the intiator. Conditions were as follows: 60/40 Hex/MeCl

cosolvents (v/v); $[IB]_0 = 1.00$ M; $[2,6\text{-lutidine}]_0 = 4.00$ mM. $[I]_0 = 12.2$ mM; $[TiCl_4]_0 =$
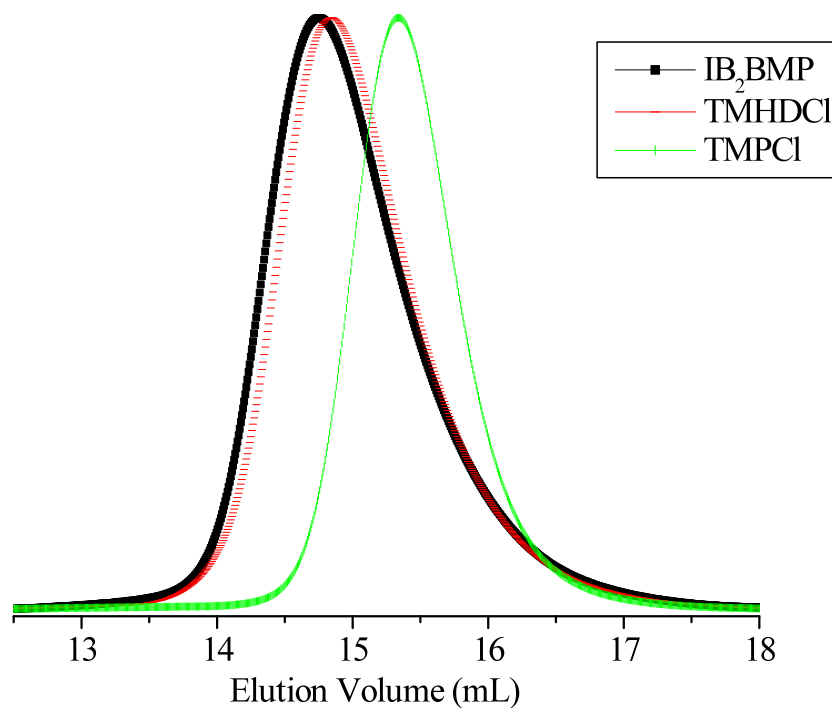
42.7 mM.

Figure 27. The SEC elution curves of PIB-5k samples initiated by IB_2BMP, TMHDCl, and TMPCl. Conditions were as follows: 60/40 Hex/MeCl cosolvents (v/v); $[IB]_0 = 1.00$ M; $[2,6\text{-lutidine}]_0 = 4.00$ mM. $[I]_0 = 12.2$ mM; $[TiCl_4]_0 = 42.7$ mM.
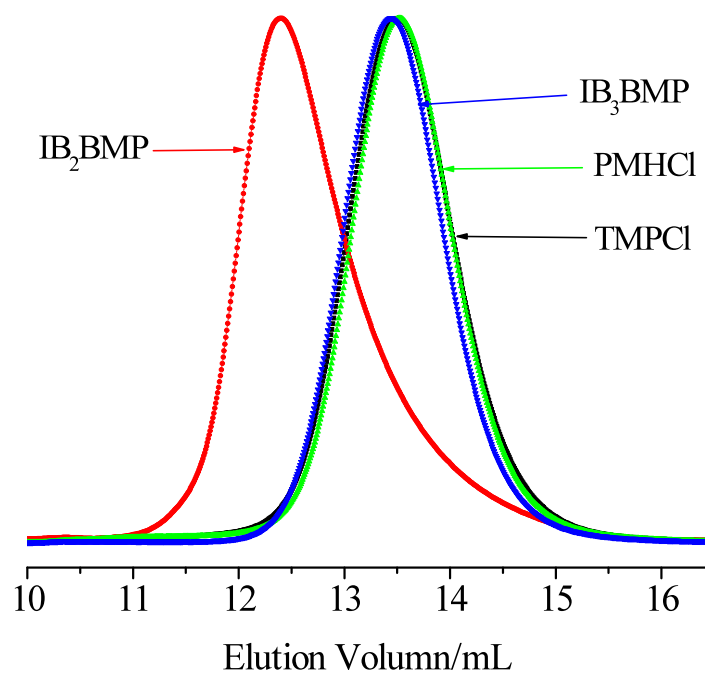
Figure 28. The SEC elution curves of PIB-3k samples initiated by four different

initiators: IB_2BMP, IB_3BMP, TMPCl and PMHCl. Conditions were as follows: 60/40

Hex/MeCl cosolvents (v/v); $[IB]_0 = 1.00$ M; $[2,6\text{-lutidine}]_0 = 4.00$ mM. $[I]_0 = 20.8$ mM;

$[TiCl_4]_0 = 62.5$ mM
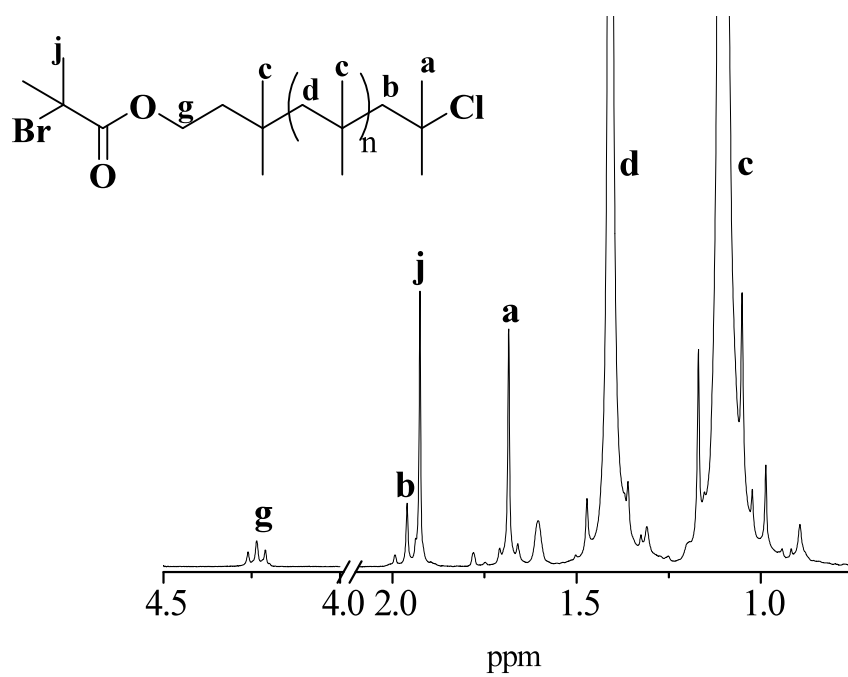
Figure 29. Proton NMR spectrum of a representative PIB (IB$_3$BMP-3k).
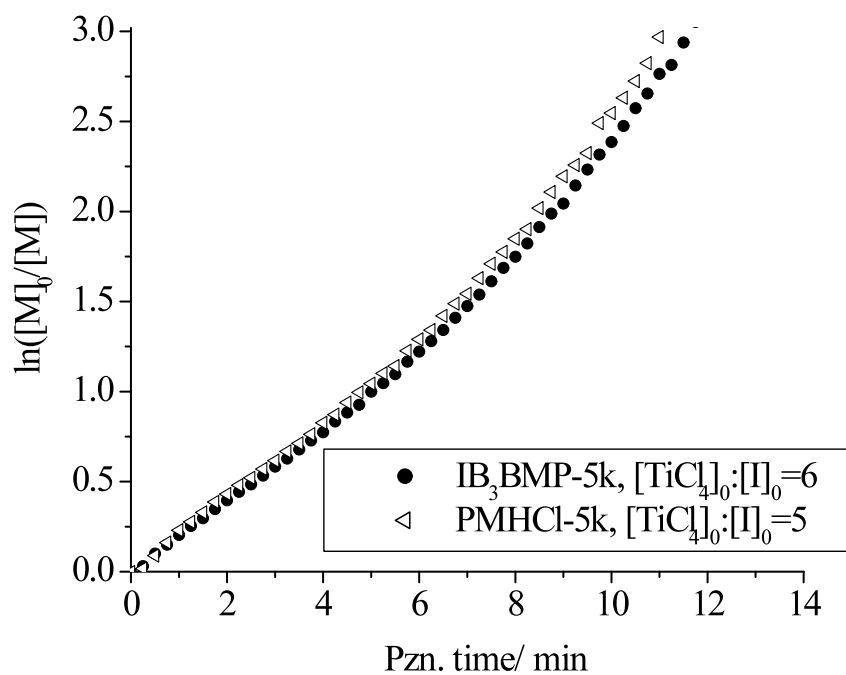
Figure 30. First-order kinetic plots for IB polymerizations at -70 °C using IB_3BMP or PMHCl as the intiator. Conditions were as follows: 60/40 Hex/MeCl cosolvents (v/v); $[IB]_0 = 1.00$ M; $[2,6\text{-lutidine}]_0 = 4.00$ mM; $[I]_0 = 12.2$ mM; $[TiCl_4]_0 = 6\times[I]_0$ for IB_3BMP; $[TiCl_4]_0 = 5\times[I]_0$ for PMHCl.
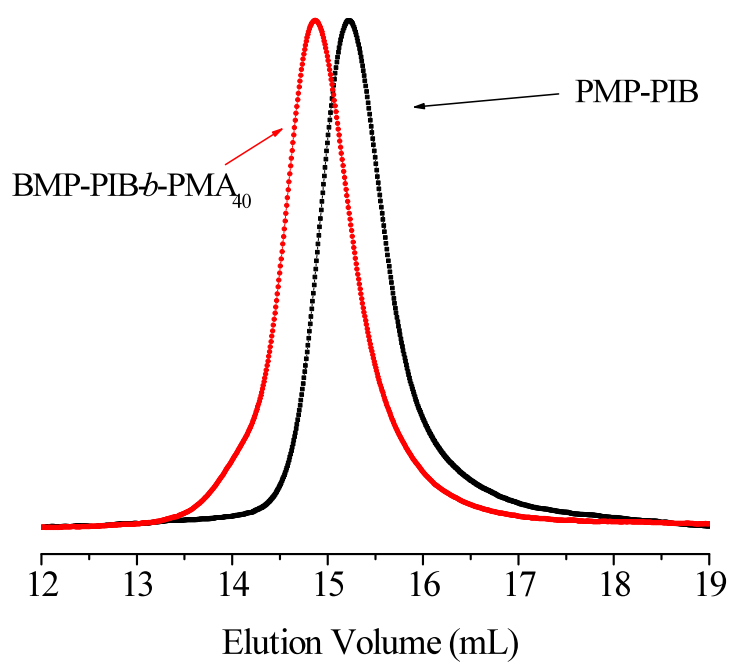
Figure 31. The SEC elution curves for BMP-PIB macroinitiator prepared from IB$_3$BMP and resulting BMP-PIB-*b*-PMA$_{40}$ block copolymer prepared by the ATRP of methyl acrylate (MA).
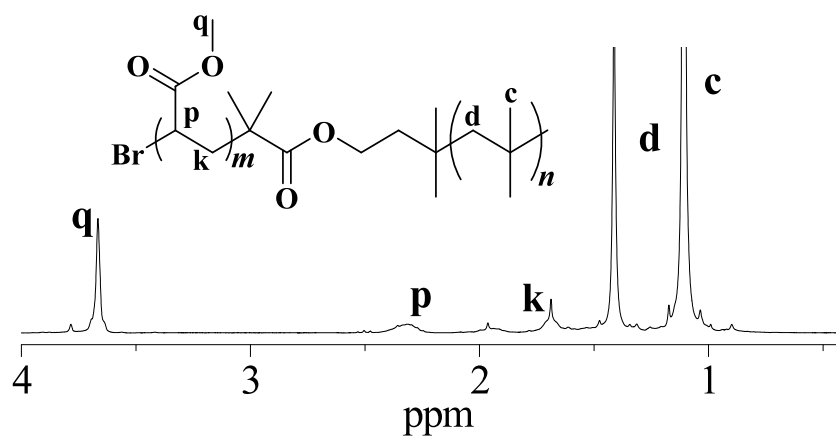
Figure 32. Proton NMR spectrum of BMP-PIB-*b*-PMA$_{40}$ block copolymer prepared by the ATRP of methyl acrylate (MA).

CHAPTER IV

DESIGN AND SYNTHESIS OF DI-CATIONIC MONO-RADICAL DUAL

INITIATOR FOR POLYISOBUTYLENE-BASED MIKTOARM STAR POLYMERS

Objective

As introduced in Chapter I, Storey et al. in 2005[110] prepared P*t*BA-PS-PIB-PS-P*t*BA pentablock terpolymers as potential permselective barrier elastomers with enhanced moisture transmission capabilities. The synthesis employed LCP to first produce PS-PIB-PS, followed by site transformation to ATRP to create the poly(*tert*-butyl acrylate) (P*t*BA) outer blocks. Acid-catalyzed[110,209] or thermal cleavage[258] of the *tert*-butyl ester side groups yielded PAA-PS-PIB-PS-PAA, with water transmitting poly(acrylic acid) (PAA) block segments. Transmission electron microscopy (TEM) revealed a PIB continuous phase, and concentric PS (outer) and PAA (inner) cylinders. At a composition of 50:25:25 PIB:PS:PAA (wt%), the membranes were elastomeric and relatively water permeable (10^{-5}–10^{-4} $g^{-1}h^{-1}mmHg^{-1}$); below 25 wt% PAA, the PAA domains were discontinuous within the PS cylinders and water permeation decreased by an order of magnitude.[110] However, polymers prepared via site transformation from PS-PIB-PS are limited to structures in which the third block (e.g. PAA) is covalently attached to the PS block. This precludes morphologies possessing an interface between PIB and the third block, causing the PAA domains to be constrained within the rigid PS cylinders and potentially limiting water swelling and permeation. To address this issue, we have targeted a new miktoarm star-branched configuration whereby the third block is covalently attached to the PIB block (Figure 33, right). This structure retains the PS-PIB-PS configuration, provideing elastic recovery and strength by physically

constraining the PIB segments at their ends. In addition, phase-separated morphologies possessing an interface between PIB and the third block are possible.

The architecture shown in Figure 33 requires a di-cationic initiator with an initiation site for another polymerization process such as ATRP. In this chapter, we will describe the synthesis of such an initiator, 3-[3,5-bis(1-chloro-1-methylethyl)phenyl]-3-methylbutyl 2-bromo-2-methylpropionate (DCCBMP) via two different synthetic routes. As shown in Figure 34, the intermediate 3-(3,5-diisopropylphenyl)-3-methylbutyl 2-bromo-2-methylpropionate (DIPBMP) is either selectively brominated with *N*-bromosuccinimide (NBS) or oxidized using *N*-hydroxyphthalimide (NHPI)/Co(OAc)$_2$•4H$_2$O catalyzed aerobic oxidation.

The proper use of DCCBMP requires that the carbocationic polymerization be carried out first, followed by ATRP. The LCP of styrene naturally results in *sec*-benzylic chloride PS chain ends, which are known to initiate ATRP.[110] Therefore, PS-PIB-PS polymers synthesized from DCCBMP require a procedure that will remove these groups and leave only the desired bromoester function. Ivan *et al.* found that poly(vinyl chloride) readily and quantitatively dehydrochlorinates upon heating to 180-200 °C.[259] Here the PS-PIB-PS macroinitiator is processed in the same way to deactivate the PS chain ends and produce the miktoarm star, poly(styrene-*b*-isobutylene)$_2$-*s*-poly(*tert*-butyl acrylate) [(PS-PIB)$_2$-*s*-P*t*BA] after ATRP of *tert*-butyl acrylate (*t*BA). The *tert*-butyl ester side groups are then cleaved using the simple thermal treatment described by Kopchick *et al.*[258] to convert P*t*BA to PAA and yield the desired amphiphilic poly(styrene-*b*-isobutylene)$_2$-*s*-poly(acrylic acid) [(PS-PIB)$_2$-*s*-PAA] miktoarm star terpolymer (Figure 35, right).

The original PS-PIB-PS macroinitiator can also be used to initiate *t*BA in three directions to produce poly(*tert*-butyl acrylate-*b*-styrene-*b*-isobutylene)$_2$-*s*-poly(*tert*-butyl acrylate) [(P*t*BA-PS-PIB)$_2$-*s*-P*t*BA] miktoarm star terpolymer. Tis can be further converted into poly(acrylic acid-*b*-styrene-*b*-isobutylene)$_2$-*s*-poly(acrylic acid) [(PAA-PS-PIB)$_2$-*s*-PAA] through the thermal treatment as described above. As mentioned in Chapter I, architecturally asymmetric ABCA tetrablock terpolymers are able to form interesting bilayer vesicles[238] and platelets[239] when placed in a selective solvent for the A block, as reported by Bates and Balsara, respectively. We anticipate similar morphological behavior will be observed for our (ABC)$_2$A star polymers.

Experimental

Materials

3-Methyl-3-buten-1-ol ($\geq$ 97%), 2-bromo-2-methylpropionyl bromide (98%), 1,3-diisopropylbenzene (96%), *N*-hydroxyphthalimide (NHPI) (97%), Co(OAc)$_2$•4H$_2$O ($\geq$ 98.0%), acetonitrile (anhydrous, 99.8%), methylcyclohexane (MCHex) (anhydrous, $\geq$ 99%), CCl$_4$ (99.9%), azobisisobutyronitrile (AIBN) (98%), *N*-bromosuccinimide (NBS) (99%), triethylamine (TEA) (99.5%), 1,1,4,7,7-pentamethyldiethylenetriamine (PMDETA) (99%), hexane (anhydrous, 99%), 2,6-lutidine (99+%), TiCl$_4$ (99.9%), Cu(I)Br (99.999%), AlCl$_3$ (99.99%), toluene (99.8%), CDCl$_3$, and balloons with wall thickness of 15 mil were used as received from Sigma-Aldrich, Inc. Compressed oxygen was used as received from Praxair, Inc. Petroleum ether, CH$_2$Cl$_2$, K$_2$CO$_3$, tetrahydrofuran (THF), MgSO$_4$, and NaHCO$_3$ were used as received from Fisher Chemical Co. Dowex HCR-W2 ion-exchange resin (strong cationic type) was used as received from Dow Chemical, Germany. Isobutylene (IB) (99.5%, BOC Gases) and

MeCl (99.5%, Alexander Chemical Co.) were dried through columns packed with CaSO$_4$ and CaSO$_4$/4 Å molecular sieves, respectively. Methyl acrylate (MA) (99%) and *tert*-butyl acrylate (*t*BA) (99%) were passed through a K$_2$CO$_3$ and Al$_2$O$_3$ column to remove inhibitor.

Instrumentation

Absolute molecular weights and polydispersity index (PDI) of polymers were determined using size exclusion chromatography (SEC) (35 °C, THF) with interferometric refractometer and multi-angle laser light scattering (MALLS) detectors. The dn/dc value used for PIB homopolymer was calculated from the following equation:[241] dn/dc = 0.116(1-108/$\overline{M}_n$) ($\overline{M}_n$ = number average molecular weight); the dn/dc values for block and miktoarm star copolymers were calculated from the interferometric refractometer detector response and assuming 100% mass recovery from the columns. Solution ^{1}H and ^{13}C nuclear magnetic resonance (NMR) spectra were obtained at 22°C using CDCl$_3$ as the solvent and tetramethylsilane as internal reference. Progress of IB polymerizations was monitored using real-time, remote-probe (light conduit type) attenuated total reflectance Fourier Transform infrared spectroscopy (FTIR) (ReactIR™ 4000). Detailed descriptions of the SEC, NMR, and FTIR instrumentation and corresponding procedures have been included in Chapter II.

The melting point of 3-[3,5-bis(1-hydroxy-1-methylethyl)phenyl]-3-methylbutyl 2-bromo-2-methylpropionate (DCOHBMP) was measured using a Q200 (TA Instruments) differential scanning calorimeter. The furnace atmosphere was purged with a 50 mL/min nitrogen stream. Standard capped aluminum crucibles were loaded

with ~5 mg of DCOHBMP solid, and the sample was subjected to a temperature ramp of 1 °C/min from 35 °C to 100 °C.

Synthesis of 3-(3,5-diisopropylphenyl)-3-methylbutyl 2-bromo-2-methylpropionate (DIPBMP)

3-Methyl-3-butenyl 2-bromo-2-methylpropionate, **3**, was produced by reacting 3-methyl-3-buten-1-ol (**2**) with 2-bromo-2-methylpropionyl bromide (**1**) using a variation of a previously reported procedure (Figure 34).[182] The intermediate DIPBMP was then synthesized by the Friedel-Crafts alkylation of 1,3-diisopropylbenzene by **3**, using a modification of the procedure of Cheon and Yamamoto,[260] as follows: within an inert atmosphere glove box equipped with a hexane/heptane cold bath, a 250 mL two-necked, round-bottom flask, equipped with mechanical stirrer, was charged with 1,3-diisopropylbenzene (85.7 g, 0.528 mol) and $AlCl_3$ (26.5 g, 0.200 mol). This mixture was chilled to -20°C and stirred vigorously. Then, **3** (40.6 g, 0.173 mol) was slowly added, and the mixture was stirred vigorously for another 25 h. The solution was added to ice-cold water (500 mL), and this mixture stirred vigorously for 2 h. The organic phase was separated, and the water layer was extracted with CH_2Cl_2. The combined organic solutions were washed with brine and then DI H_2O and dried over anhydrous $MgSO_4$. After filtration, CH_2Cl_2 was removed by vacuum stripping, and the desired compound, 3-(3,5-diisopropylphenyl)-3-methylbutyl 2-bromo-2-methylpropionate, was obtained as a light yellow oil (34.0 g, 49.5% yield) after purification by vacuum distillation. ^{1}H NMR ($CDCl_3$): δ = 1.25 (d, 12H, $PhCH(C\underline{H}_3)_2$), 1.38 (s, 6H, 3-Me), 1.86 (s, 6H, $(CH_3)_2CBr$), 2.02 (t, 2H, 2-H), 2.88 (m, 2H, $PhC\underline{H}(CH_3)_2$), 4.03 (t, 2H, 1-H), 6.92 (m, 1H, 4-PhH), 7.02 (m, 2H, 2,6-PhH) ppm. ^{13}C NMR: δ = 24.1 ($PhCH(\underline{C}H_3)_2$),

29.2 (3-Me), 30.7 ((C̲H$_3$)$_2$CBr), 34.3 (PhC̲H(CH$_3$)$_2$), 36.7 (C3), 42.1 (C2), 55.9

((CH$_3$)$_2$C̲Br), 63.9 (C1), 121.3 (2,6-PhC), 121.8 (4-PhC), 147.8 (1-PhC), 148.5 (3,5-

PhC), 171.5 (CO) ppm.

Synthesis of 3-(3,5-diisopropenylphenyl)-3-methylbutyl 2-bromo-2-methylpropionate

(DMVBMP) via AIBN-induced bromination

Into a 100 mL round-bottom flask, equipped with magnetic stirrer and

condenser, were charged DIPBMP (4.0 g, 0.010 mol), *N*-bromosuccinimide (NBS) (3.9

g, 0.022 mol), azobisisobutyronitrile (AIBN) (0.62 g, 3.8×10^{-3} mol), and 40 mL CCl$_4$.

The mixture was heated at reflux for 1.5 h. After the flask cooled down to room

temperature, the reaction mixture was filtered to remove precipitated succinimide, and

50 mL of water and 10 mL of 0.1 mol/L NaHCO$_3$ were added. The brominated product

3-[3,5-bis(1-bromo-1-methylethyl)phenyl]-3-methylbutyl 2-bromo-2-methylpropionate

(DCBBMP) was then extracted with CH$_2$Cl$_2$ (3×25 mL) and then dried over MgSO$_4$.

The crude product was purified using column chromatography (SiO$_2$, petroleum

ether/ethyl acetate (v/v) = 35:1 cosolvents as the eluent), which lead to the loss of HBr

at the benzylic 1-bromo-1-methylethyl functionalities, yielding a diolefin product,

DMVBMP as a light yellow liquid in (1.07 g, 27.2% yield).

Synthesis of 3-[3,5-bis(1-hydroxy-1-methylethyl)phenyl]-3-methylbutyl 2-bromo-2-

methylpropionate (DCOHBMP) via aerobic oxidation

The title compound was prepared via aerobic oxidation of DIPBMP (Figure 34,

right) using the *N*-hydroxyphthalimide (NHPI)/Co(OAc)$_2$•4H$_2$O catalyst system.[261] Into

a 250 mL Erlenmeyer flask equipped with a magnetic stirrer and a balloon filled with

pure oxygen, DIPBMP (7.30 g, 18.4 mmol), NHPI (1.303 g, 8 mmol), Co(OAc)$_2$•4H$_2$O

(0.101 g, 0.41 mmol), and 25 mL MeCN were added. Because $Co(OAc)_2 \cdot 4H_2O$ and

NHPI are sparingly soluble in MeCN, an orange heterogeneous mixture was obtained.

The reaction was stirred vigorously at 23°C for 72 h. The solvent was vacuum stripped,

and the solid was washed with CH_2Cl_2 (3 × 25 mL). A clear, light-yellow liquid was

obtained after drying over $MgSO_4$. The oxidized dihydroxy product, 3-[3,5-bis(1-

hydroxy-1-methylethyl)phenyl]-3-methylbutyl 2-bromo-2-methylpropionate

(DCOHBMP) (2.61 g, 6.05 mmol, 33.1% yield) was obtained as a white solid after

removing the dihydroperoxy, diolefin, mono-hydroxy mono-hydroperoxy by-products,

as well as the substituted acetophenone side product by column chromatography (SiO_2,

hexane/THF (v/v) = 2:1 cosolvents as the eluent). The crude product was dissolved to

saturation in toluene at 60°C. Upon cooling to -10°C for several hours, white crystals

formed, which were collected by filtration. Melting point = 90-92 °C by DSC. [1]H

NMR ($CDCl_3$): δ = 1.40 (s, 6H, 3-Me), 1.60 (s, 12H, PhCOH(C$\underline{H}_3$)$_2$), 1.86 (s, 6H,

$(CH_3)_2CBr$), 2.06 (t, 2H, 2-H), 2.31 (s, 2H, PhCO$\underline{H}(CH_3)_2$), 4.01 (t, 2H, 1-H), 7.40 (m,

2H, 2,6-PhH), 7.43 (m, 1H, 4-PhH) ppm. ^{13}C NMR: δ = 29.4 (3-Me), 30.7 (($\underline{C}H_3)_2CBr$),

31.9 (PhCOH($\underline{C}H_3)_2$), 37.0 (C3), 41.9 (C2), 55.9 (($CH_3)_2\underline{C}Br$), 63.8 (C1), 72.8

(Ph$\underline{C}OH(CH_3)_2$), 118.1 (4-PhC), 120.1 (2,6-PhC), 148.0 (1-PhC), 149.0 (3,5-PhC),

171.6 (CO) ppm. High-resolution mass spectrometry (HRMS) (EI): $C_{21}H_{33}O_4{}^{79}Br$ [M][+],

calcd. 428.1562, found 428.1575; $C_{21}H_{33}O_4{}^{81}Br$ [M][+], calcd. 430.1542, found 430.1553.

Figures 46 and 47, show ^{1}H and ^{13}C NMR spectra of dihydroperoxy by-product

3-[3,5-bis(1-hydroperoxy-1-methylethyl)phenyl]-3-methylbutyl 2-bromo-2-

methylpropionate (DCOOHBMP), and mono-hydroxy mono-hydroperoxy by-product 3-

[(3-hydroperoxy-1-methylethyl-5-hydroxy-1-methylethyl)phenyl]-3-methylbutyl 2-

bromo-2-methylpropionate, respectively. Upon hydrochlorination following the same

procedure as reported in Chapter II, these by-products are able to yield the same final

product DCCBMP.

Synthesis of 3-[3,5-bis(1-chloro-1-methylethyl)phenyl]-3-methylbutyl 2-bromo-2-

methylpropionate (DCCBMP)

The final product, DCCBMP, was obtained as a yellow-brown liquid (2.63 g,

93.2% yield) by chlorination of DCOHBMP using anhydrous HCl, as previously

reported. [249] ^{1}H NMR (CDCl$_3$): δ = 1.41 (s, 6H, 3-Me), 1.86 (s, 6H, (CH$_3$)$_2$CBr), 2.01

(s, 12H, PhCCl(C$\underline{H}$$_3$)$_2$), 2.06 (t, 2H, 2-H), 4.04 (t, 2H, 1-H), 7.50 (m, 2H, 2,6-PhH), 7.62

(m, 1H, 4-PhH) ppm. ^{13}C NMR: δ = 29.2 (3-Me), 30.6 ((C$\underline{H}$$_3$)$_2$CBr), 34.4

(PhCCl(C$\underline{H}$$_3$)$_2$), 37.0 (C3), 41.8 (C2), 55.8 ((CH$_3$)$_2$$\underline{C}$Br), 63.5 (C1), 69.9 (Ph$\underline{C}$Cl(CH$_3$)$_2$),

120.2 (4-PhC), 122.1 (2,6-PhC), 146.0 (1-PhC), 148.0 (3,5-PhC), 171.5 (CO) ppm.

Initiation performance test (isobutylene homopolymerization)

The LCPs of IB were carried out within an inert atmosphere glove box equipped

with a hexane/heptane cold bath, following the previously reported procedure.[249]

Polymerizations were performed at -70°C using DCCBMP or 5-*tert*-butyl-1,3-(1-chloro-

1-methylethyl)benzene (*t*-Bu-*m*-DCC) as the initiator. TiCl$_4$ served as the catalyst, and

2,6-lutidine as the Lewis base in 60/40 (v/v) MCHex/MeCl cosolvents.

PS-PIB-PS synthesis

PS-PIB-PS triblock copolymers were produced via LCP and sequential monomer

addition within a drybox at -70 °C, using DCCBMP as the initiator, TiCl$_4$ as the catalyst,

and 2,6-lutidine as the Lewis base in 60/40 (v/v) MCHex/MeCl cosolvents. FTIR

(ReactIR 4000) was used to monitor isobutylene and styrene conversions by observing

the olefinic $=CH_2$ wag of IB (887 cm^{-1}) and styrene (907 cm^{-1}).[242] The DiComp probe

was inserted into a 250 mL 4-necked round bottom flask equipped with a temperature

probe and a stirring shaft with a Teflon paddle. The reactor was placed into the cold

bath and allowed to equilibrate to -70 °C. Into the flask were charged 57.9 mL

prechilled MCHex, 38.6 mL prechilled MeCl, 2,6-lutidine (0.0489 mL, 4.23×10^{-4} mol),

and DCCBMP (0.3005 g, 6.45×10^{-4} mol). The mixture was allowed to stir for 10 min to

reach thermal equilibrium before a background spectrum was collected. Prechilled IB

(8.50 mL, 0.106 mol) was added to the flask; about 15 spectra were aquired to establish

the average intensity of the 887 cm^{-1} peak, A_0, corresponding to the initial monomer

concentration. At this point, TiCl$_4$ (0.707 mL, 6.44×10^{-3} mol) was injected into the

flask. The molar concentrations of reagents were [IB]$_0$ = 1.0 M, [DCCBMP]$_0$ = 6.1

mM, [2,6-lutidine]$_0$ = 4.0 mM, and [TiCl$_4$]$_0$ = 61.0 mM, and the total volume was 105.7

mL. Once the IB monomer was fully consumed (>99% conversion), indicated by the

887 cm^{-1} absorbance approaching an asymptotic value (A_r), a mixture of prechilled 25.7

mL MCHex, 17.1 mL MeCl, and 7.1 g styrene was added. These amounts were

designed to achieve [styrene]$_0$ = 0.4 M, assuming no volume loss when IB monomer

was converted into polymer, while maintaining a 60/40 (v/v) MCHex/MeCl cosolvents

system. The FTIR instrument was reset to monitor the disappearance of the styrene

band at 907 cm^{-1}. Once the styrene conversion reached ~50%, 20 mL prechilled

CH$_3$OH was added to quench the polymerization. After warming to room temperature

and loss of MeCl, the MCHex solvent and any remaining styrene monomer were

vacuum stripped, and sufficient tetrahydrofuran (THF) was added to completely dissolve

the polymer. The PIB-PS-PIB sample was precipitated into a 5-10X volume excess of MeOH and dried under vacuum to yield a white solid product.

Star polymers synthesis

Miktoarm star terpolymers based on (P*t*BA-PS-PIB)$_2$-*s*-P*t*BA were prepared by initiating *t*BA directly from unmodified PS-PIB-PS, which inherently carries *sec*-benzylic chloride PS chain ends as well as the bromoester functionality at the initiator moiety. However, to produce (PS-PIB)$_2$-*s*-P*t*BA, the *sec*-benzylic chloride chain ends had to be deactivated; this was achieved by heating PS-PIB-PS to 180-200°C at 30 mmHg of vacuum overnight.

ATRP of *t*BA was performed using CuBr as the catalyst, PMDETA as the ligand, and PS-PIB-PS as the macroinitiator (MacroI) following the same procedure as previously reported for ATRP of methyl acrylate.[249] Polymerizations were performed using a molar ratio [MacroI]$_0$:[CuBr]$_0$:[PMDETA]$_0$ = 1:1:1 in toluene at 70 °C , with [MacroI]$_0$ = 0.01 M and with [*t*BA]$_0$ set at various levels to achieve different molecular weights. Conversion of *t*BA monomer was limited to ~60% to avoid coupling. After polymerization, the solution was passed through a column packed with ion-change resin and neutral Al$_2$O$_3$ to remove copper salt. Then THF was added to completely dissolve the polymer, and the resulting solution was passed through a 0.2 μm filter to remove any remaining Al$_2$O$_3$. The solution was precipitated into a 5-10X volume excess of MeOH, and white (PS-PIB)$_2$-*s*-P*t*BA was collected by vacuum filtration and dried under vacuum at room temperature.

To convert P*t*BA into PAA, the star polymers were exposed to 150°C at 30 mmHg of vacuum overnight to yield amphiphilic (PAA-PS-PIB)$_2$-*s*-PAA and (PS-PIB)$_2$-*s*-PAA miktoarm star polymers.

Results and Discussion

Synthesis of DIPBMP

The key intermediate for DCCBMP, 3-(3,5-diisopropylphenyl)-3-methylbutyl 2-bromo-2-methylpropionate (DIPBMP), was produced by Friedel-Crafts alkylation of diisopropylbenzene by 3-methyl-3-butenyl 2-bromo-2-methylpropionate, **3**, at -20 °C in the drybox. AlCl$_3$ was added at approximately an equal molar ratio to **3**, forming a thick, deep red slurry. Low temperature was employed to prevent unwanted substitution reactions at other carbons on the 1,3-diisopropylbenzene.

Proton and carbon NMR spectra of DIPBMP are shown in Figure 36. Upon alkylation, the olefinic protons in **3** disappeared, and the new methyl protons of the tether unit appeared at 1.4 ppm (peak a). The triplet at 4.0 ppm (peak e) was assigned to the methylene protons of the tether unit adjacent to the bromoester (1-H). The methylene protons further from the ester (2-H) are observed as a triplet at 2.0 ppm (peak d). The methyl groups of the 2-bromo-2-methylpropionate moiety (ATRP initiating site) exhibit a peak at 1.9 ppm (peak b). The splitting pattern of the aromatic proton peaks changed upon substitution at 1-Ph, yielding two main peaks at 6.92 ppm (peak g) and 7.0 ppm (peak f). Peak integration values were consistent with the proposed chemical structure. Carbon NMR data provided better resolved peaks for analysis. After **3** was attached to 1,3-diisopropylbenzene, the olefinic carbon peaks disappeared, and corresponding new peaks a and d appeared at 29.3 ppm and 36.7 ppm, respectively.

Peak l (1-PhC) shifted downfield to 147.8 ppm. Peaks i and j shifted upfield to 121.8 and 121.3 ppm, respectively. Only four peaks were observed in the aromatic carbon region, indicating that a symmetric structure was obtained and that substitution occurred only at the 1-Ph carbon.

Synthesis of DMVBMP

Selective benzylic bromination of DIPBMP with NBS using AIBN as a free radical source was carried out following a previously reported procedure.[262] By checking the crude product with NMR, we found that the benzylic isopropyl protons disappeared and a new singlet appeared with the expected chemical shift. However, olefinic proton peaks were also observed above 5 ppm, indicating that the reaction produced a mixture of substitution and elimination products, namely 3-[3,5-bis(1-bromo-1-methylethyl)phenyl]-3-methylbutyl 2-bromo-2-methylpropionate (DCBBMP) and 3-(3,5-diisopropenylphenyl)-3-methylbutyl 2-bromo-2-methylpropionate (DMVBMP). In addition, other unwanted peaks appeared in the region above 7 ppm and between 4 and 4.5 ppm, representing the production of side products. Upon column chromatography, HBr was removed from DCBBMP through the interaction with silica gel substrate. Therefore, the fully dehydrohalogenated diolefin product DMVBMP was obtained as a light yellow liquid; although a significant amount of product was retained on the column causing a low yield (27.2%).

The proton and carbon NMR spectra of DMVBMP are illustrated in Figure 37. The multiplet at 2.8 ppm (peak j, Figure 36) associated with the benzylic isopropyl proton of DIPBMP disappeared. New olefinic proton peaks appeared at 5.1 and 5.3 ppm (peaks k), and the protons of the newly formed isopropenyl methyl group appeared

at 2.2 ppm. Aromatic protons appeared as a singlet at 7.4 ppm; while the bromoester tether signals remained the same. The integrated areas of olefinic protons and protons of methylene next to the ester were found to be in a ratio of approximately 1:1, as predicted based upon the structure of DMVBMP. The carbon spectrum also presented two new olefinic carbon peaks at 112.6 ppm (peak s) and 141.2 ppm (peak h). Peak c shifted upfield to 21.9 ppm upon conversion of isopropyl to isopropenyl. The number of peaks visible in the spectrum corresponds to the number of carbons in DMVBMP, indicating the desired structure was obtained.

Synthesis of DCOHBMP

Due to the difficult purification and low yield of DMVBMP, we sought a different route to the final DCCBMP dual initiator. In addition to the olefin, the *tert*-hydroxyl was the obvious alternative intermediate starting from DIPBMP. We found that NHPI/Co(OAc)$_2$•4H$_2$O catalyzed free radical aerobic oxidation (Figure 34, right) works efficiently to convert DIPBMP into the di-*tert*-hydroxyl intermediate, DCOHBMP.

Minisci et al. showed that aerobic oxidation of cumene using this catalyst system usually produces a methyl aryl ketone side product (i.e., acetophenone in the case of cumene);[261] however, selectivity toward the desired cumyl alcohol could be increased by using low reaction temperature and a non-polar solvent medium. Solvents recommended by these authors, such as chlorobenzene and acetonitrile, as well as the non-polar aliphatic solvent hexane, were tested as reaction solvents for the room temperature oxidation of DIPBMP. No reaction was observed for hexane. Very low conversion was obtained with chlorobenzene. We next conducted a series of reactions

in acetonitrile at various temperatures (40 °C, 23 °C and 0 °C); we found that more

methyl aryl ketone was obtained at 40 °C, while 0 °C led to insufficient conversion after

a reasonably long reaction time. Moreover, elevated temperature reaction was found to

produce stable hydroperoxy by-products (di- and mono-substituted), as well as some

methyl aryl ketone, in addition to the desired DCOHBMP. The best combination for

this reaction is to use acetonitrile as the solvent at room temperature, despite the

relatively long reaction time required.

Regarding product isolation, the original purification strategy involved the use of

column chromatography, which, although effective at removal of the methyl aryl ketone

impurity, led to unacceptably high losses of DCOHBMP product, either by retention on

the column or conversion to the diolefin, 3-(3,5-diisopropylphenyl)-3-methylbutyl 2-

bromo-2-methylpropionate (DMVBMP). The resulting mixture of *tert*-benzilic alcohol

and olefin was a eutectic liquid that was carried forward to the hydrochlorination

reaction without further attempts at purification. With greater experience, we

discovered that pure DCOHBMP is a solid. This was a significant breakthrough, since it

enabled purification by recrystallization in toluene. The resulting pure DCOHBMP was

obtained as a stable, white solid.

Figure 38 shows the NMR characterization results for DCOHBMP. In the

proton spectrum, the multiplet at 2.9 ppm (peak j, Figure 36) associated with the

benzylic protons of DIPBMP was absent. The doublet representing the methyl protons

of the isopropyl groups, formerly at 1.2 ppm (peak c, Figure 36), was converted into a

singlet at 1.6 ppm (peak c) upon aerobic oxidation. A new peak representing the

hydroxy proton appeared at 2.3 ppm (peak h). Peaks f and g shifted downfield to 7.4

ppm and 7.5 ppm. In the carbon spectrum, the oxidized carbon and adjacent methyl carbons shifted downfield to 72.7 ppm (peak h) and 31.6 ppm (peak c), respectively, and peak i shifted upfield. The other three aromatic carbon peaks, as well as all carbon signals for the bromoester tail, were observed at the same chemical shift in reactant and product.

High-resolution mass spectrometry (HRMS) analysis of the recrystallized product revealed two molecular ions, corresponding to the presence of either [79]Br and [81]Br, thus confirming the structure of DCOHBMP. Differential scanning calorimetry (DSC) revealed the m.p. to be 91.3 °C.

Synthesis of DCCBMP

Intermediate DMVBMP, synthesized via NBS bromination and purified by column chromatography, was not obtained in a very pure form as indicated by extraneous small peaks in the ^{1}H NMR spectrum (Figure 37). DCCBMP obtained from hydrochlorination of DMVBMP showed the same unwanted proton peaks, indicating that this initiator was not very pure.

Pure DCCBMP was prepared by chlorination of DCOHBMP. Figure 39 shows the ^{1}H and ^{13}C NMR spectra of DCCBMP prepared in this way. Methyl protons of the tether shifted downfield to 2.01 ppm (peak c) after chlorination. Peaks associated with the aromatic protons shifted slightly downfield to 7.5 (peak f) and 7.6 (peak g) ppm. The carbon attached to chloride and the adjacent methyl groups shifted to 69.9 and 34.4 ppm, respectively. Moreover, the ^{13}C NMR spectrum consisted of exactly 13 signals, which were unambiguously assigned to the 13 carbons in DCCBMP, providing further evidence that the targeted structure was obtained.

Initiation Performance Test

Performance of DCCBMPs prepared by NBS bromination plus column chromatography, as shown in Figure 34, was tested by using this initiator for the synthesis of PIB-5k and PIB-10k.

Molecular weight data for PIB-5k and PIB-10k are listed in Table 10. Number average degree of polymerization ($\overline{X}_{n,PIB}$) was calculated from ^{1}H NMR data using equation 1,

$$\overline{X}_{n,PIB} = \frac{A_{Me}/3}{A_{CE}} + 2 \tag{1}$$

where, A_{Me} is the integrated peak area of the methyl protons in the PIB repeat unit, and A_{CE} is the sum of the integrated peak areas of characteristic resonances representing the various polymer chain ends, defined by equation 2,

$$A_{CE} = A_{exo} + A_{endo} + A_{tert\text{-}Cl}/2 + 2A_{coupled} \tag{2}$$

In equation 2, A_{exo} is the area of the upfield *exo*-olefinic resonance at 4.64 ppm, A_{endo} is the area of the single *endo*-olefinic resonance at 5.15 ppm, and $A_{tert\text{-}Cl}$ is the area of the resonance at 1.96 ppm due to the methylene protons of the *tert*-chloride end group. $A_{coupled}$ was calculated as follows:

$$A_{coupled} = \frac{\left(A_{4.75\text{-}5.0} - A_{exo}\right)}{2} \tag{3}$$

where $A_{4.75\text{-}5.0}$ is the integrated area of the convoluted peaks from 4.75-5.0 ppm associated with the downfield *exo*-olefinic proton and the two identical protons of the coupled product. Equation 2 accounts for all likely terminal chain end types; however, the vast majority is *tert*-Cl.

Initiation efficiency of DCCBMP, I_{eff}, was calculated as $\overline{X}_{n,theo} / \overline{X}_{n,PIB}$ and

$\overline{M}_{n,theo} / \overline{M}_{n,PIB}$ from NMR and SEC/MALLS data, respectively. $\overline{X}_{n,theo}$ was calculated

as the molar ratio of monomer to initiator charged to the reactor;

$\overline{M}_{n,theo} = \left(\overline{X}_{n,theo} \times M_{IB} \right) + M_{I}$, where M_{IB} and M_{I} are the molecular weights of

isobutylene and the initiator, respectively.

As Table 10 shows, PDIs of PIB homopolymers initiated by DCCBMP prepared

by NBS bromination were < 1.2, indicating reasonable control of the IB polymerization.

However, $\overline{M}_{n,PIB}$ and $\overline{X}_{n,PIB}$ data were larger than the designed value, yielding an

apparent initiator efficiency, I_{eff} < 1. We believe that this is indicative of low purity of

this initial batch of DCCBMP, as opposed to some inherent problem with this particular

initiator structure. Thus, the actual amount of DCCBMP charged to the reactor was

lower than designed.

Three PIB samples, PIB-5k, PIB-10k and PIB-20k, were prepared in order to

study the cationic initiation performance of DCCBMP prepared via aerobic oxidation.

Table 11 lists NMR and SEC characterization data for these samples. Figure 40 shows

the proton NMR spectrum of a representative sample, PIB-5k. The PIB backbone

methyl and methylene protons appear at about 1.1 ppm (peak o) and 1.4 ppm (peak p),

respectively. Characteristic peaks for the DCCBMP initiator, b, e, f, and g, are present,

indicating that the radical initiating site remained intact after cationic polymerization.

Number average functionality with respect to the ATRP initiating site, $\overline{F}_{n,Br}$, was

quantified and found to be in the range 0.93-1 (Table 11). $\overline{F}_{n,Br}$ was calculated from [1]H

NMR data using equation 4, where A_{CH_2O} is the integrated area of the methylene protons

adjacent to the ester group (peak e) and A_{CE} is defined by equation 2.

$$\overline{F}_{n,Br} = \frac{A_{CH_2O}}{A_{CE}} \qquad (4)$$

I_{eff} of DCCBMP characterized by NMR spectroscopy was 0.93-0.95. SEC eulograms of

all three PIBs were symmetrical, and PDIs were all less than 1.02. I_{eff} calculated from

SEC data were in the range 0.89-0.98.

Control experiments were conducted under the same conditions using the

standard difunctional cationic initiator, 5-*tert*-butyl-1,3-di(1-chloro-1-

methylethyl)benzene (*t*-Bu-*m*-DCC). PDIs of the resulting PIBs were the same as those

obtained from DCCBMP, i.e., less than 1.02 (Table 11). I_{eff}s calculated from SEC data

were ~1, comparable with those of DCCBMP. In addition, real-time ATR-FTIR

monitoring of IB polymerizations initiated from DCCBMP yielded linear 1st order

kinetic plots, similar to those obtained with *t*-Bu-*m*-DCC, as illustrated in Figure 41.

These results show that the presence of the ATRP initiating site on DCCBMP does not

interfere with or present any special problems in LCP and that pure DCCBMP prepared

via the aerobic oxidation route enables precise control over molecular weight,

polydispersity, and functionality of the resulting polymers.

PS-PIB-PS Synthesis

PS-PIB-PS triblock copolymers with bromoester functionality in the center of

PIB block were prepared via sequential LCP of IB and then styrene, using DCCBMP as

the initiator. Results of SEC analysis of these copolymers are given in Table 12 and

Figure 42. As listed in Table 12, PS-PIB-PS macroinitiators were prepared with very

narrow PDIs (1.06 for PS-PIB-PS-1, 1.02 for PS-PIB-PS-2). The targeted molecular weight of the PIB block in PS-PIB-PS-1 was 9670 g/mol; the experimental molecular weight was 11380 g/mol, yielding I_{eff} = 0.85. For PS-PIB-PS-2, the experimental $\overline{M}_{n\,PIB}$ (20020 g/mol) was almost the same as $\overline{M}_{n\,theo}$ (19540 g/mol), yielding I_{eff} =0.98. Conversion of styrene (0.88 for PS-PIB-PS-1, 0.82 for PS-PIB-PS-2) was higher than targeted (0.50), yielding PS-PIB-PS polymers composed of more PS volume than the designed value.

Figure 42 shows the progression of SEC elution curves during synthesis of PS-PIB-PS-1, which is representative. PIB initiated by DCCBMP (black) was characterized by a narrow and symmetrical peak. Elution profile of the triblock copolymer (red) was still symmetrical but shifted to lower elution volumes, indicating that LCP of the second monomer, styrene, occurred to form the targeted triblock copolymer.

Figure 43 (upper) shows the ^{1}H NMR spectrum of a representative sample, PS-PIB-PS-2. The styrene backbone methylene and methine protons were observed at 1.4 ppm (peak q) and 1.8 ppm (peak r). The broad peaks at 6.4-7.2 ppm (collectively denoted s) were assigned to the aromatic protons both of the PS block and DCCBMP initiator. The methylene protons next to the bromoester group were observed as a well-defined triplet at 4.0 ppm (peak e). The characteristic broad absorbance due to the ultimate CH of the PS block (*sec*-benzyl chloride proton, peak t) was observed at 4.3-4.4 ppm.

Star polymers Synthesis

As illustrated in Figure 35, quenching LCP of styrene with MeOH produces *sec*-benzylic chloride end groups, which are known to be active radical initiation

centers.[110,114,263] To selectively grow *t*BA only from the designated bromoesters, PS-PIB-PS macroinitiators were thermolyzed to eliminate HCl and thus deactivate the PS chain ends. After thermolysis, the broad peak associated with CH of *sec*-benzyl chloride at 4.3-4.4 ppm disappeared, as shown in the lower spectrum in Figure 43. Small peaks appeared at 3.1 ppm and 6.1 ppm, which were attributed to the newly formed olefinic chain ends. PS-PIB-PS macroinitiators were re-analyzed by SEC after thermolysis, and as expected, the molecular weights of the treated and untreated PS-PIB-PS were about the same. As shown in Figure 42, elution curve of the thermolyzed PS-PIB-PS-1 (green) overlaps with PS-PIB-PS-1 (red), indicating the difference between treated and untreated macroinitiators concerns only PS chain ends.

The ATRP of *t*BA was next used to produce (P*t*BA-PS-PIB)$_2$-*s*-P*t*BA and (PS-PIB)$_2$-*s*-P*t*BA miktoarm terpolymers from PS-PIB-PS and thermolyzed PS-PIB-PS macroinitiators, respectively. SEC characterization results for these star polymers are given in Table 13. PS-PIB-PS macroinitiators, either in their original state or after thermal deactivation of the PS chain ends, worked well in ATRP. The resulting miktoarm stars possessed molecular weights of the P*t*BA very close to the targeted values, and the overall PDIs were narrow (< 1.1). Only four sets (two for each macroinitiator) of ATRP results were demonstrated in Table 13.

Figure 42 illustrates the SEC elution profiles of (PS-PIB)$_2$-*s*-P*t*BA star polymers, ATRP-1 (cyan) and ATRP-2 (blue), initiated by thermolyzed PS-PIB-PS-1. Both star polymers possessed narrow PDIs (<1.1), and the elution profiles were symmetrical with no apparent shoulders, indicating very high blocking efficiency from the macroinitiator and negligible radical-radical coupling during ATRP. High blocking efficiency

confirms that the ATRP initiating site of the DCCBMP initiator survives LCP and thermolysis at 180-200°C.

Figure 44 (upper) shows the ^{1}H NMR spectrum of (PtBA-PS-PIB)$_2$-s-PtBA star polymer (ATRP-3). Addition of the PtBA blocks introduced new peaks at 1.5 (peak u) and 2.2 ppm (peak v), corresponding to the methylene and methine backbone protons, respectively, of PtBA. As expected, (PS-PIB)$_2$-s-PtBA prepared from deactivated PS-PIB-PS showed the same characteristic proton signals.

Thermolysis has been reported to eliminate isobutylene molecules from PtBA via beta-type scission and thus produce PAA hydrophilic blocks.[258] This technique proved to also work very well for the present systems. Figure 44 (lower) shows the ^{1}H NMR spectrum of (PAA-PS-PIB)$_2$-s-PAA polymer obtained after thermolysis. The integrated area for the combined PIB backbone methylene and PtBA *tert*-butyl protons (peak p and t) decreased. ^{13}C NMR gave better evidence for removal of the *tert*-butyl groups. Figure 45 shows ^{13}C NMR spectra of ATRP-3 before (upper) and after thermolysis (lower). The methyl and quaternary carbons of the *tert*-butyl groups of PtBA, which appear at 81 ppm (peak y) and 29 ppm (peak t) in the upper spectrum, as reported,[258,264] completely disappear after thermolysis.

Conclusions

The dual initiator DCCBMP containing two *sec*-benzylic chloride groups for cationic initiation and one bromoester for radical initiation was synthesized in four steps. Instead of brominating the DIPBMP intermediate radically, a new aerobic oxidation using NHPI and Co(OAc)$_2$•4H$_2$O catalyst system was employed to convert DIPBMP into DCOHBMP, a new compound easily purified by recrystallization. The chemical

structure of this crystalline solid was confirmed by proton and carbon NMR spectroscopy and HRMS. The melting point was determined by DSC to be 91.3 °C. Chlorination of DCOHBMP yielded the final product, DCCBMP, as a light yellow liquid. The chemical structure of DCCBMP was confirmed by NMR spectroscopy. Compared with AIBN bromination, this mild aerobic oxidation reaction can easily convert benzylic $CH(CH_3)_2$ into $COH(CH_3)_2$ without destroying other functional groups. Although a small amount of side products were observed, the technique provids a better synthetic route and can be applied in other organic syntheses.

The initiation performance of DCCBMP was investigated by conducting $TiCl_4$-catalyzed IB polymerizations at -70 °C. FTIR spectroscopy demonstrated a linear first-order kinetic plot that passes through the origin, indicating fast initiation and a constant concentration of active chain ends during polymerization. SEC results showed that high initiation efficiency (I_{eff} = 0.89-0.98) and near-monodisperse polymers (PDI ≤ 1.02) were obtained when DCCBMP was used to polymerize isobutylene, targeting molecular weights of 5k, 10k and 20k g/mol. The cationic initiation performance of DCCBMP was essentially identical to the standard aromatic difunctional cationic initiator, t-Bu-m-DCC, which was utilized as a control (Table 11). The bromoester functionality, which is designed for the subsequent ATRP, was observed in the proton NMR spectrum of the resulting PIB. The number average functionality, $\overline{F}_{n\,Br}$ was calculated to be 0.93~1.00, indicating that radical initiating group was intact during IB polymerization.

DCCBMP was utilized to prepare a series of amphiphilic $(PAA-PS-PIB)_2$-s-PAA and $(PS-PIB)_2$-s-PAA miktoarm star polymers using a combination of LCP, sequential monomer addition, and ATRP techniques. PS-PIB-PS triblock copolymers were

produced by living carbocationic polymerization of IB followed by sequential addition of styrene. After quenching with MeOH, the polymers thus obtained carried *sec*-benzylic chlorides at the PS chain ends, which are able to induce radical polymerization. Thus, as obtained, these polymers possessed three ATRP initiating sites and were used to produce (P*t*BA-PS-PIB)$_2$-*s*-P*t*BA miktoarm star polymers.

The PS terminal functionality could alternatively be selectively deactivated by heating the polymers to 180-200 °C in a vacuum oven. Proton NMR spectra showed that only *sec*-benzylic chlorides were removed with no change observed for the bromoester group. SEC characterization of PS-PIB-PS macroinitiators before and after thermolysis generated identical polymer elution profiles, indicating that there were no backbone structure changes. Deactivated PS-PIB-PS macroinitiators enabled P*t*BA growth only from the bromoester group, yielding (PS-PIB)$_2$-*s*-P*t*BA star polymers under the same ATRP conditions.

Both types of miktoarm stars were prepared with designed composition and narrow PDIs (<1.1) as confirmed by NMR and SEC analysis. Upon thermolyzing these star polymers, P*t*BA was completely converted to PAA, yielding amphiphilic PIB-based star polymers (PAA-PS-PIB)$_2$-*s*-PAA and (PS-PIB)$_2$-*s*-PAA, in which the third block can share an interface with the PIB block. Their intriguing self-assembly behavior in aqueous solution as well as phase separation morphology in solid state will be examined.

Table 10. Molecular Weight Data for PIB-5k, PIB-10k Prepared from Di-cationic

Mono-radical Dual Initiator DCCBMP[a] via LCP[b]

	NMR			SEC			
	$\overline{X}_{n,PIB}$	$\overline{X}_{n,theo}$	I_{eff}	$\overline{M}_{n,PIB}$ (g/mol)	$\overline{M}_{n,theo}$ (g/mol)	I_{eff}	PDI
PIB-5k	105	82	78.2%	5910	5060	85.6%	1.14
PIB-10k	217	164	75.6%	12470	9670	77.5%	1.18

Note. [a]This DCCBMP was prepared DMVBMP, synthesized via NBS bromination and column chromatography

[b]-70°C; 60/40 MCHex/MeCl cosolvents (v/v); $[IB]_0 = 1.00$ M; $[2,6\text{-lutidine}]_0 = 4.00$ mM

$[I]_0 = 12.2$ mM; $[TiCl_4]_0 = 48.8$ mM for 5k samples

$[I]_0 = 6.10$ mM; $[TiCl_4]_0 = 48.8$ mM for 10k samples

Table 11. Characterization Results of PIBs Prepared from Di-cationic Mono-radical Dual Initiator DCCBMP[a] and Difunctional Cationic Initiator, *t*-Bu-*m*-DCC via LCP[b]

	NMR				SEC				
	$\overline{X}_{n,PIB}$	$\overline{X}_{n,theo}$	$\overline{F}_{n,Br}$	I_{eff}	$\overline{M}_{n,PIB}$ (g/mol)	$\overline{M}_{n,theo}$ (g/mol)	I_{eff}	PDI	$I_{eff,}$ *t*-Bu-*m*-DCC
PIB-5k	88	82	0.97	0.93	5700	5070	0.89	1.02	0.97
PIB-10k	174	164	0.93	0.94	10170	9670	0.95	1.01	1.00
PIB-20k	357	340	1.00	0.95	20020	19540	0.98	1.01	0.99

Note. [a]This DCCBMP was synthesized DCOHBMP, which was obtained via NHPI induced aerobic oxidaton

[b]-70°C; 60/40 MCHex/MeCl cosolvents (v/v); $[IB]_0 = 1.00$ M; $[2,6\text{-lutidine}]_0 = 4.00$ mM

$[I]_0 = 12.2$ mM; $[TiCl_4]_0 = 48.8$ mM for 5k samples

$[I]_0 = 6.10$ mM; $[TiCl_4]_0 = 48.8$ mM for 10k samples

$[I]_0 = 3.05$ mM; $[TiCl_4]_0 = 91.5$ mM for 20k samples

Table 12. Molecular weight data for PS-PIB-PS macroinitiators prepared from DCCBMP via LCP and Sequential Monomer Addtion[a]

	$\overline{M}_{n,PIB}$ (g/mol)	$\overline{M}_{n,PIB-PS-PIB}$ (g/mol)	PDI
PS-PIB-PS-1[b]	11380	20150	1.06
PS-PIB-PS-2[c]	20020	32060	1.02

Note. [a]-70°C; 60/40 MCHex/MeCl cosolvents (v/v); $[IB]_0 = 1.00$ M; $[2,6\text{-lutidine}]_0 = 4.00$ mM; $[St]_0 = 0.4$ M

[b]$[DCCBMP]_0 = 6.1$ mM; $[TiCl_4]_0 = 61.0$ mM; $[St]_0/[DCCBMP]_0 = 96$; conv.(styrene) = 0.88 calculated based on SEC result

[c]$[DCCBMP]_0 = 2.94$ mM; $[TiCl_4]_0 = 88.2$ mM; $[St]_0/[DCCBMP]_0 = 160$; conv.(styrene) = 0.72 calculated based on SEC result

Table 13. Molecular weight data for (PS-PIB)$_2$-s-PtBA and (PtBA-PS-PIB)$_2$-s-PtBA star polymers Prepared via ATRP[a]

	$\overline{M}_{n,star}$ (g/mol)	$\overline{M}_{n,PtBA}$ (g/mol)	$\overline{M}_{n\ theo}$ (g/mol)	PDI
ATRP-1 [b]	26120	5970	7690	1.08
ATRP-2 [b]	36350	16200	15380	1.07
ATRP-3 [c]	40250	8190	7690	1.02
ATRP-4 [c]	77450	45390	45140	1.03

Note. [a]70°C; toluene; [MacroI]$_0$ = 0.01 M; [MacroI]$_0$:[CuBr]$_0$:[PMDETA]$_0$ = 1:1:1; quenched at 60% tBA conversion

[tBA]$_0$/[MacroI]$_0$ = 100 for ATRP-1 and ATRP-3

[tBA]$_0$/[MacroI]$_0$ = 200 for ATRP-2

[tBA $_0$/[MacroI]$_0$ = 580 for ATRP-4

[b]using thermolyzed PS-PIB-PS-1 as macroinitiator, producing (PS-PIB)$_2$-s-PtBA star polymers

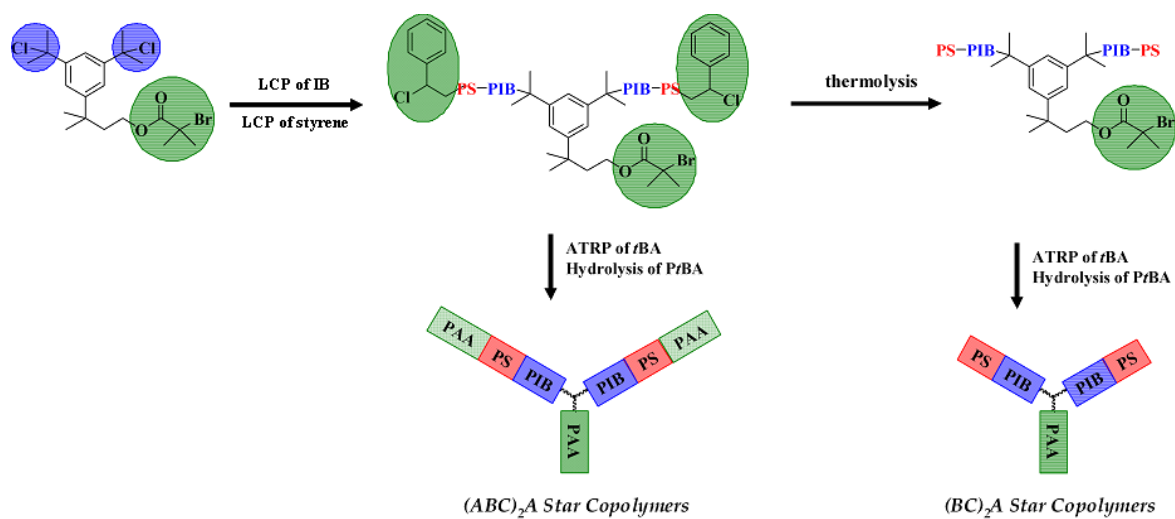[c]using PS-PIB-PS-2 as macroinitiator, producing (PtBA-PS-PIB)$_2$-s-PtBA star polymers

Figure 33. Schematic synthesis route of amphiphilic poly(acrylic acid-*b*-styrene-*b*-isobutylene)$_2$-*s*-poly(acrylic acid) [(PAA-PS-PIB)$_2$-*s*-PAA] and poly(styrene-*b*-isobutylene)$_2$-*s*-poly(acrylic acid) [(PS-PIB)$_2$-*s*-PAA] miktoarm star terpolymers from dual initiator 3-[3,5-bis(1-chloro-1-methylethyl)phenyl]-3-methylbutyl 2-bromo-2-methylpropionate (DCCBMP) using the combination of living carbocationic polymerization (LCP) and atom transfer radical polymerization (ATRP).
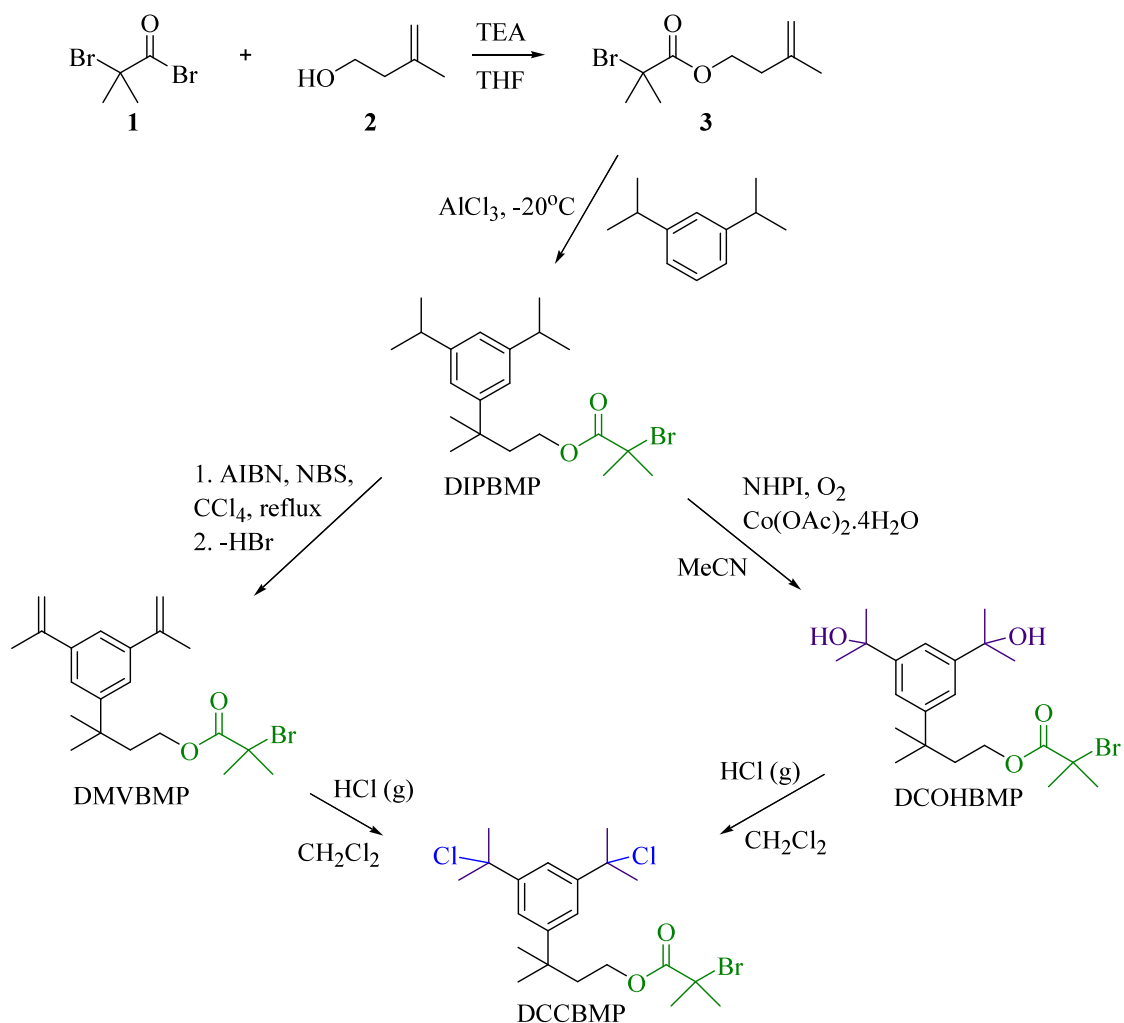
Figure 34. Synthesis routes to DCCBMP via 3-(3,5-diisopropylphenyl)-3-methylbutyl

2-bromo-2-methylpropionate (DIPBMP): radical bromination and aerobic oxidation.
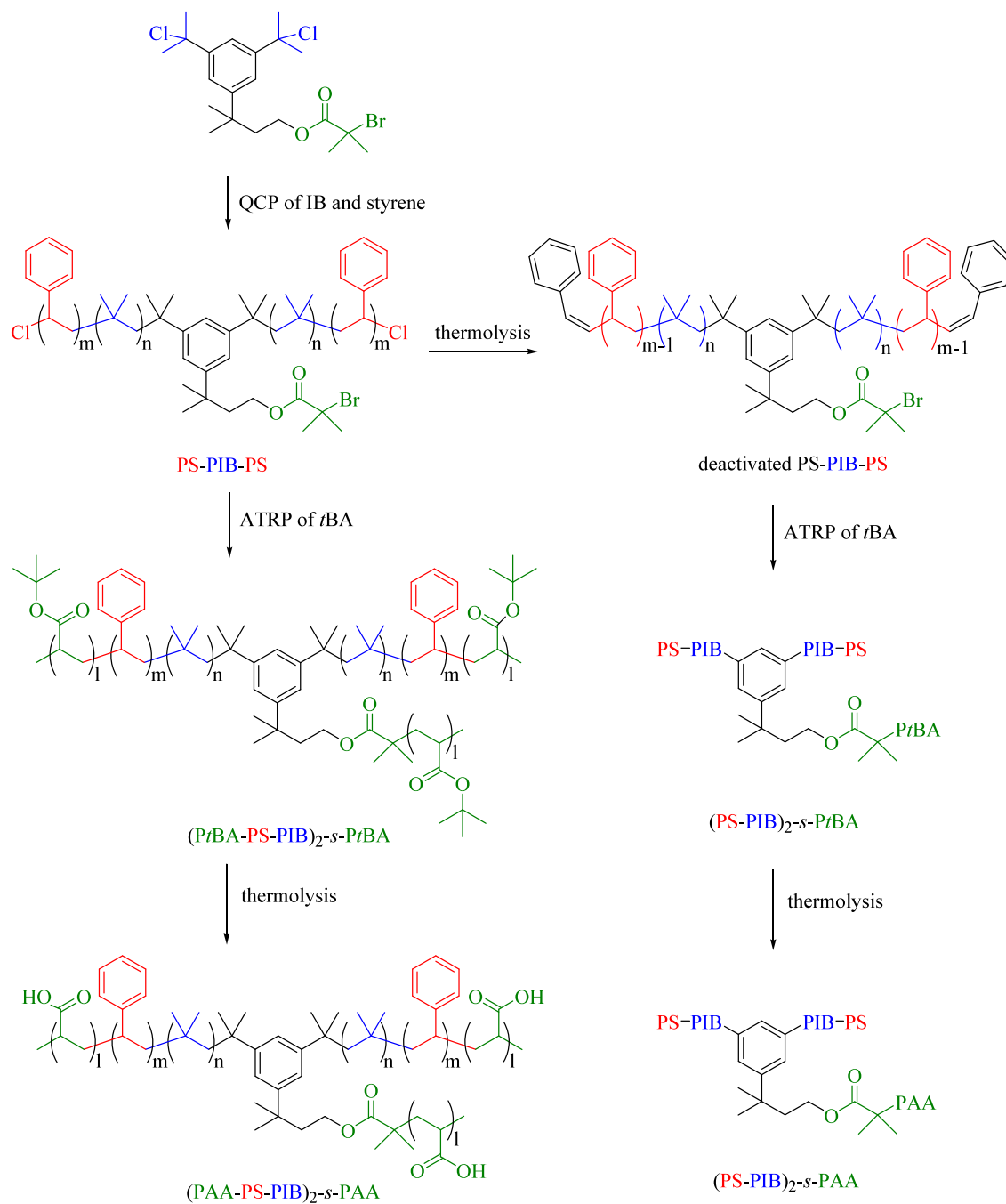
Figure 35. Synthesis of (PAA-PS-PIB)₂-*s*-PAA and (PS-PIB)₂-*s*-PAA miktoarm star polymers.
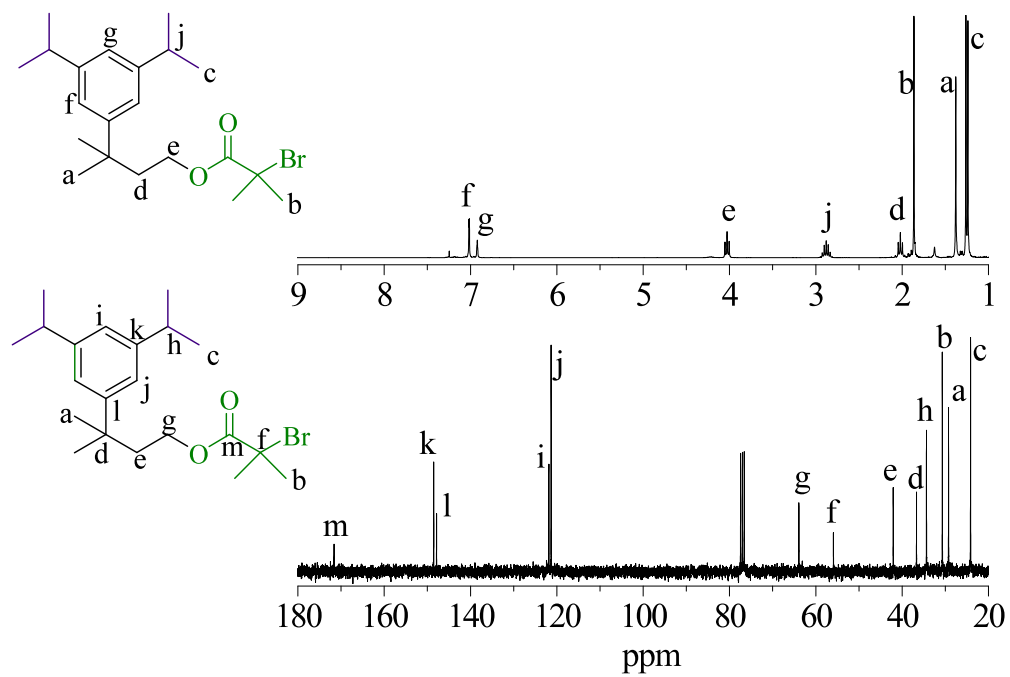
Figure 36. Proton and carbon NMR spectra of 3-(3,5-diisopropylphenyl)-3-methylbutyl

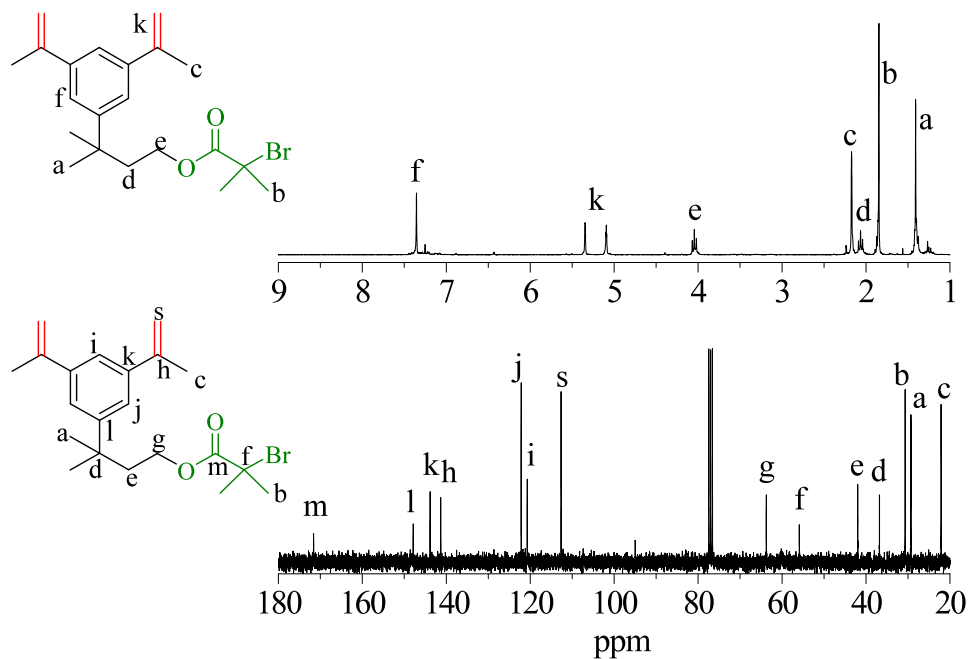2-bromo-2-methylpropionate (DIPBMP).

Figure 37. Proton and carbon NMR spectra of 3-(3,5-diisopropenylphenyl)-3-

methylbutyl 2-bromo-2-methylpropionate (DMVBMP) obtained after NBS bromination

of DIPBMP and column chromatography.

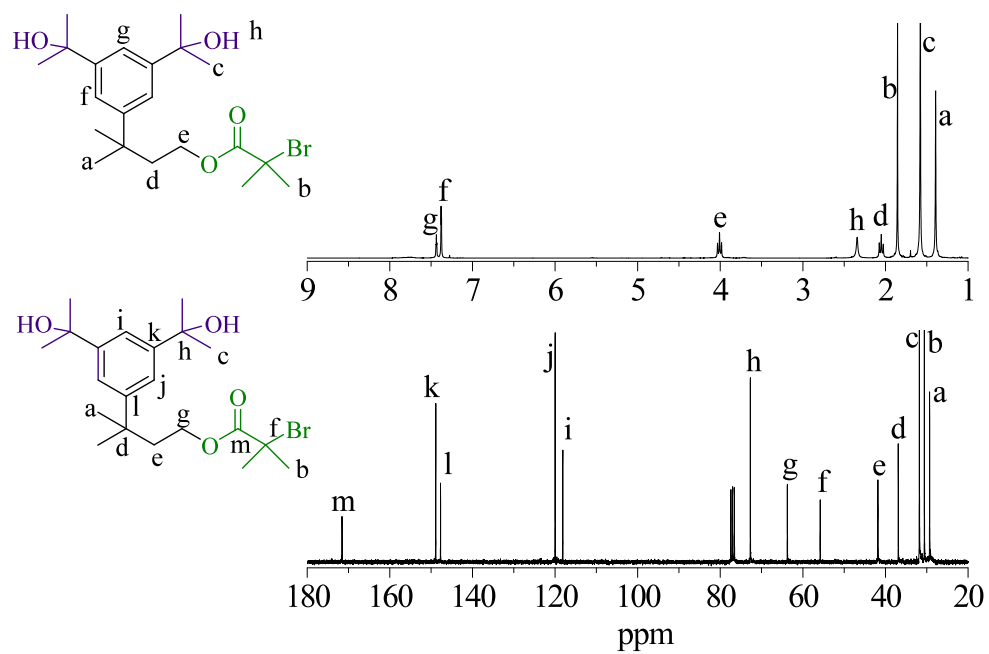*Figure 38.* Proton and carbon NMR spectra of 3-[3,5-bis(1-hydroxy-1-methylethyl)phenyl]-3-methylbutyl 2-bromo-2-methylpropionate (DCOHBMP) obtained by aerobic oxidation of DIPBMP.
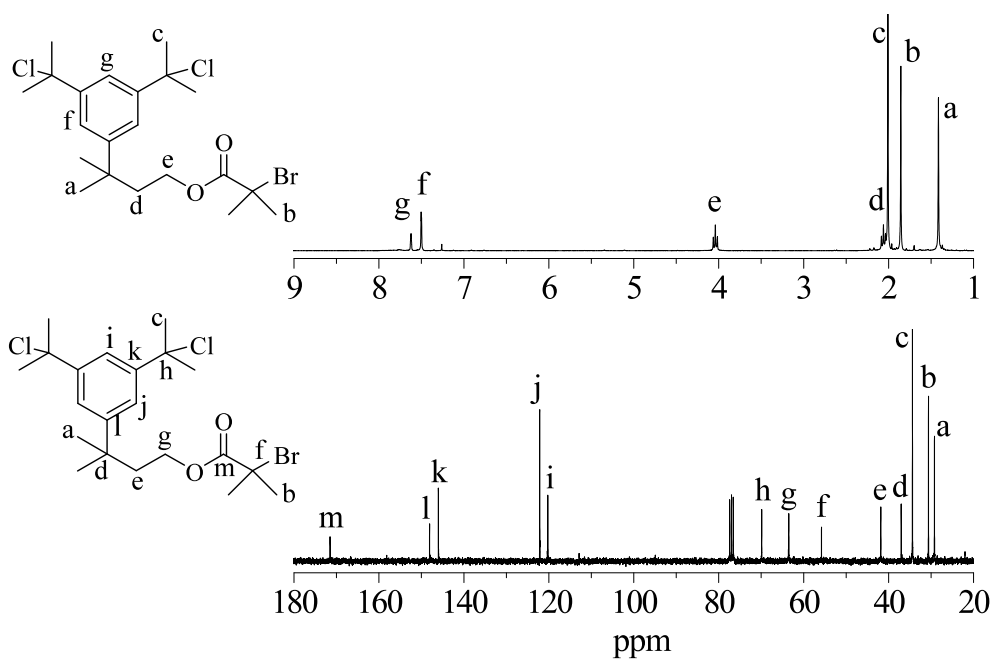
Figure 39. Proton and carbon NMR spectra of di-cationic mono-radical dual initiator 3-[3,5-bis(1-chloro-1-methylethyl)phenyl]-3-methylbutyl 2-bromo-2-methylpropionate (DCCBMP).
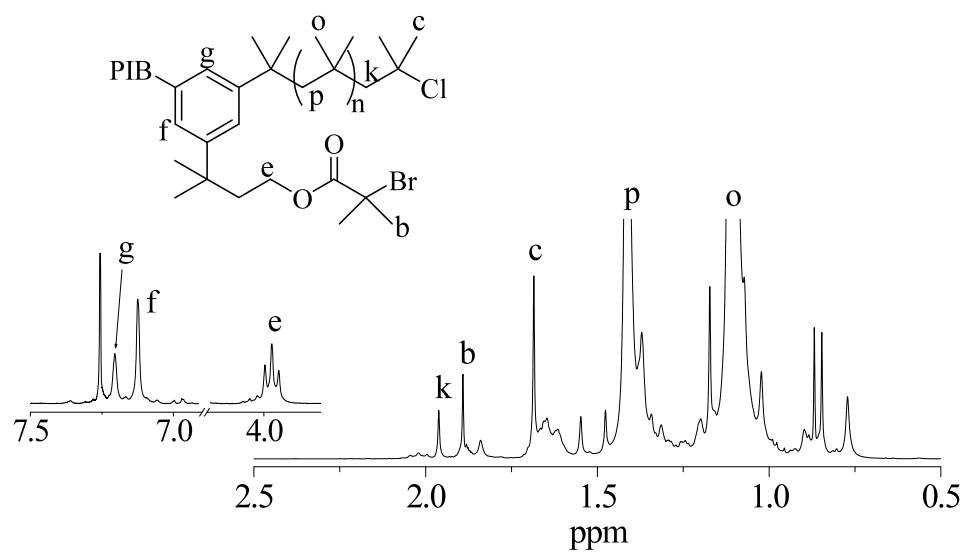
Figure 40. Proton NMR spectrum of PIB-5k initiated by DCCBMP.
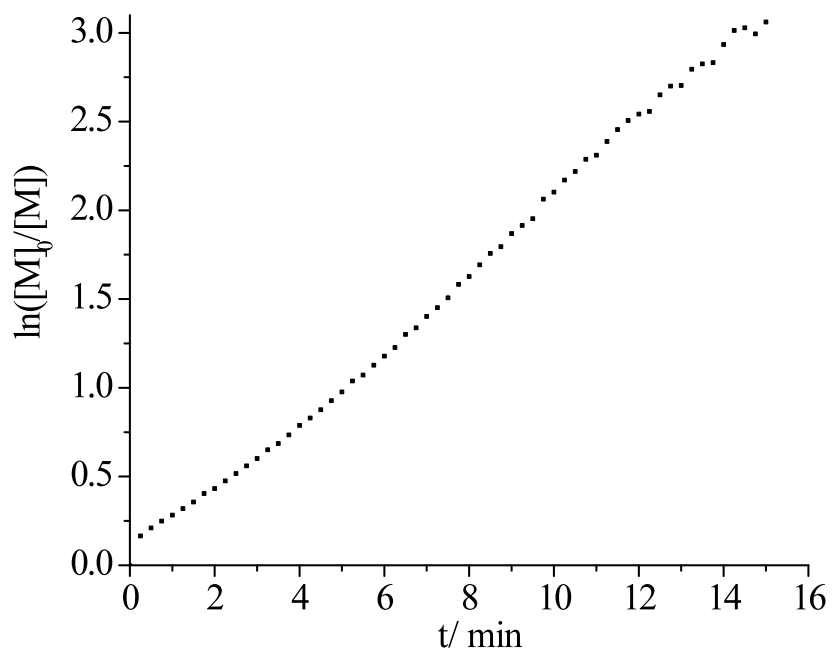
Figure 41. First-order kinetic plots for IB polymerizations at -70 °C. Conditions were

as follows: 60/40 Hex/MeCl cosolvents (v/v); $[IB]_0 = 1.00$ M; $[2,6\text{-lutidine}]_0 = 4.00$

mM; $[DCCBMP]_0 = 12.2$ mM; $[TiCl_4]_0 = 48.8$ mM targeting 5k.
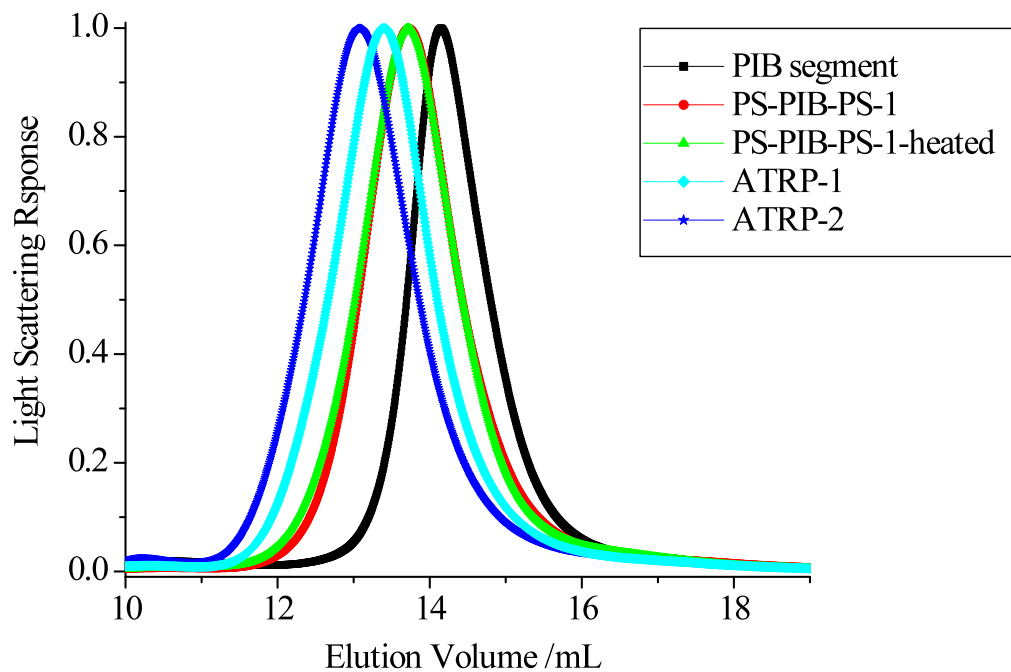
Figure 42. The SEC curves of PIB segment in PS-PIB-PS-1 (black), PS-PIB-PS-1 (red),

PS-PIB-PS-1 after thermolysis (green) which overlaps with PS-PIB-PS-1, and (PS-

PIB)₂-*s*-P*t*BA star polymers, ATRP-1 (cyan) and ATRP-2 (blue).
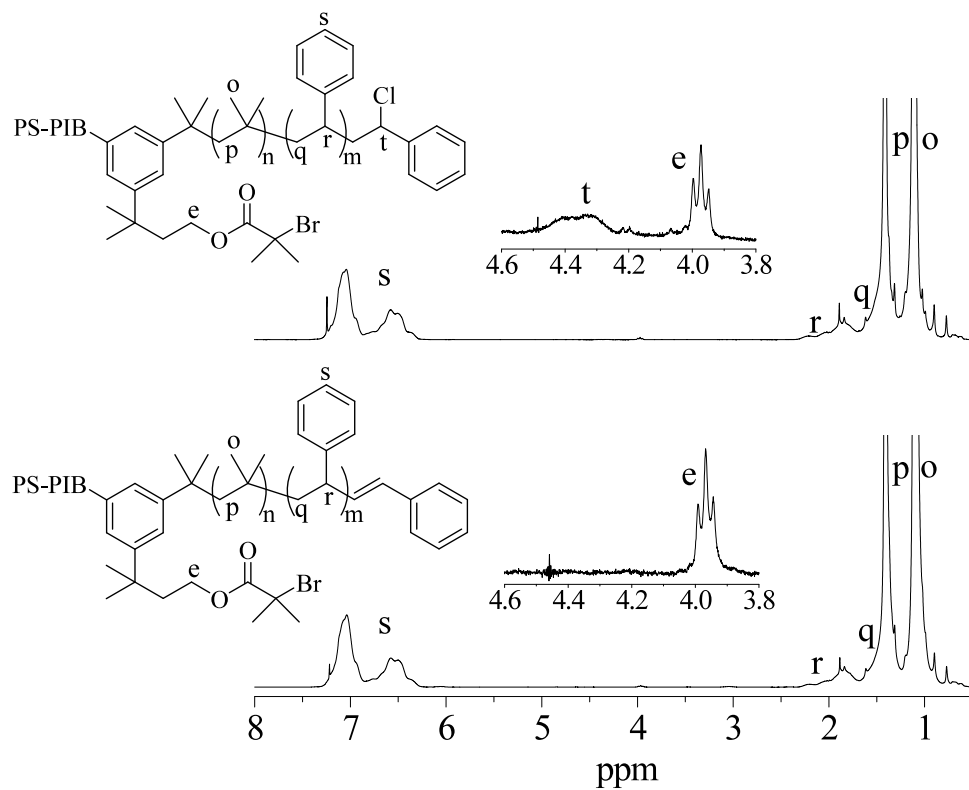
Figure 43. Proton NMR spectra of PS-PIB-PS-2 before (upper) and after thermolysis (lower).
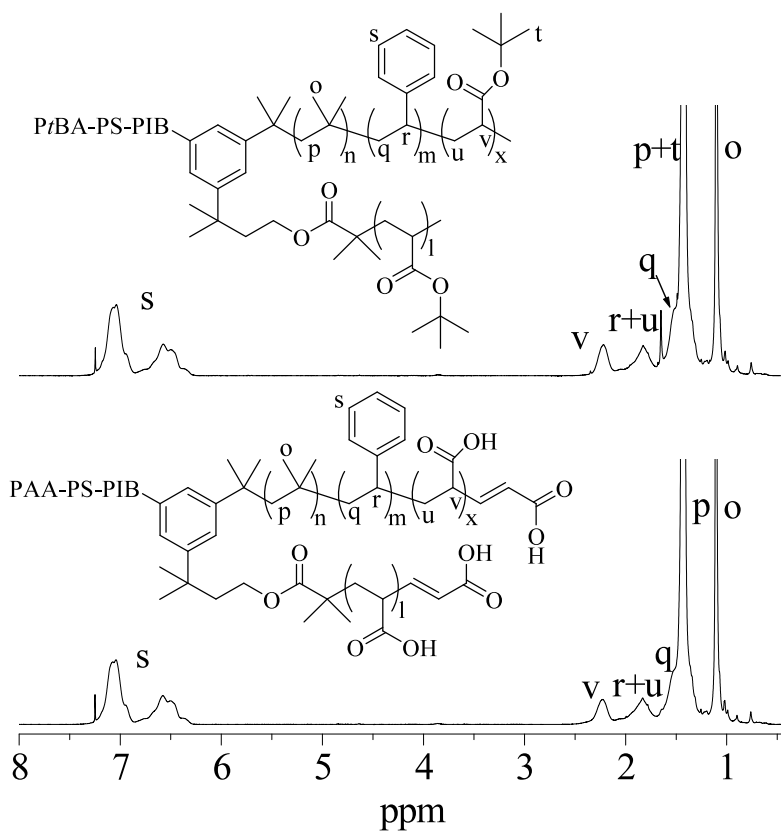
Figure 44. Proton NMR spectra of (P*t*BA-PS-PIB)₂-*s*-P*t*BA (ATRP-3) miktoarm star polymer (upper), and (PAA-PS-PIB)₂-*s*-PAA prepared upon thermolysis (lower).
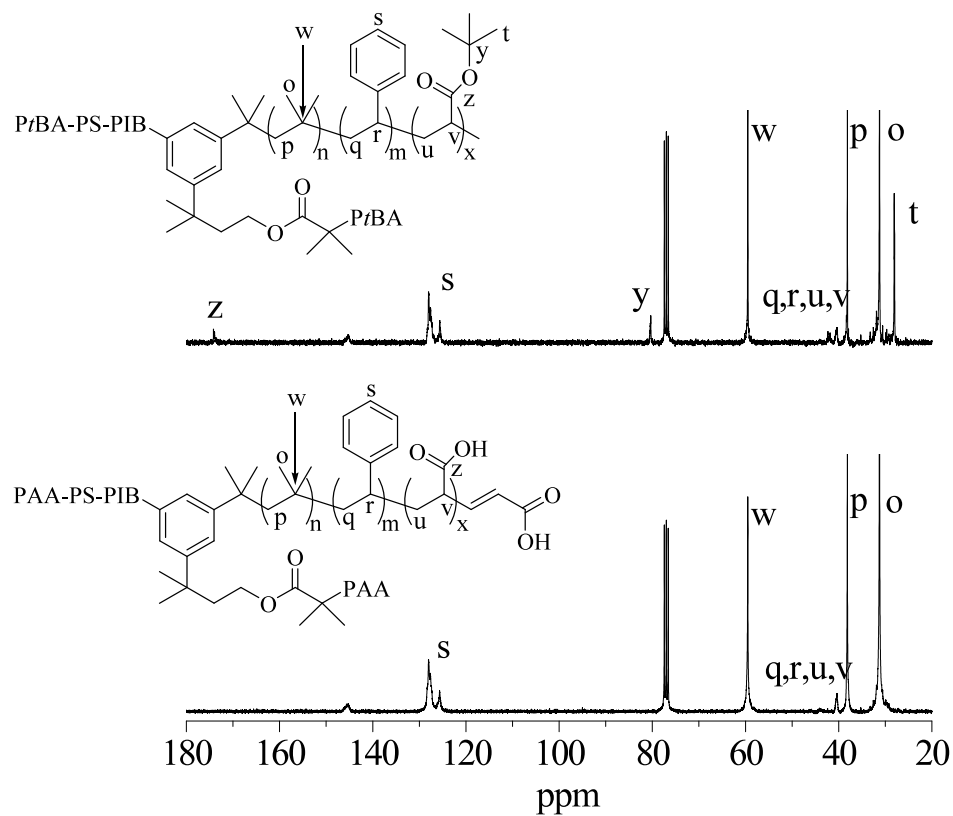
Figure 45. Carbon NMR spectra of (P*t*BA-PS-PIB)$_2$-*s*-P*t*BA (ATRP-3) and the

corresponding (PAA-PS-PIB)$_2$-*s*-PAA obtained by thermolysis.
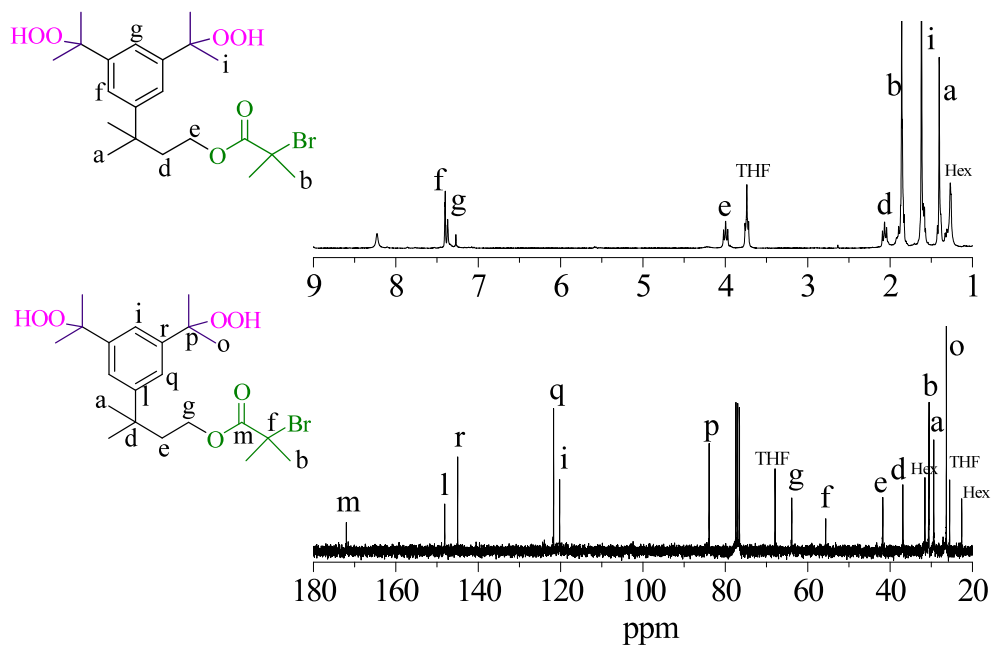
Figure 46. Proton and carbon NMR spectra of di-hydroperoxy product upon aerobic oxidation of 3-(3,5-diisopropylphenyl)-3-methylbutyl 2-bromo-2-methylpropionate.
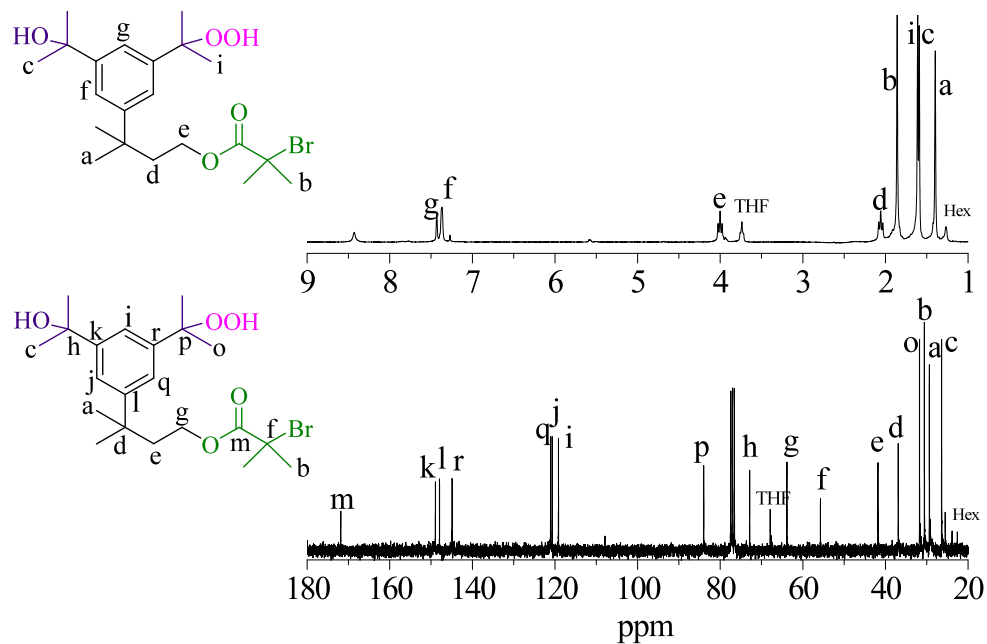
Figure 47. Proton and carbon NMR spectra of mono-hydroxy mono-hydroperoxy product upon aerobic oxidation of 3-(3,5-diisopropylphenyl)-3-methylbutyl 2-bromo-2-methylpropionate.

REFERENCES

1. Mach, H.; Rath, P. *Lubr. Sci.* **1999**, *11*, 175-186.

2. Bahadur, M.; Suzuki, T.; Toth, S. U.S. Patent 6,258,878 B1, 2001.

3. Odian, G. *Principles of Polymerization*, 4th ed.; John Wiley & Sons: Hoboken, NJ, 2004.

4. Puskas, J. E.; Chen, Y. *Biomacromolecules* **2004**, *5*, 1141-1154.

5. Szwarc, M.; Levy, M.; Milkovich, R. *J. Am. Chem. Soc.* **1956**, *78*, 2656-2657.

6. Miyamoto, M.; Sawamoto, M.; Higashimura, T. *Macromolecules* **1984**, *17*, 265-268.

7. Miyamoto, M.; Sawamoto, M.; Higashimura, T. *Macromolecules* **1984**, *17*, 2228-2230.

8. Faust, R.; Kennedy, J. P. *J. Polym. Sci., Part A: Polym. Chem.* **1987**, *25*, 1847-1869.

9. Puskas, J.; Kaszas, G.; Kennedy, J.P.; Kelen, T.; Tudos, F. *J. Macromol. Sci.-Pure Appl.Chem.* **1982**, *A18*, 1229-1244.

10. Faust, R.; Kennedy, J. P. *J. Macromol. Sci.-Pure Appl.Chem.* **1990**, *A27*, 649-667.

11. Kaszas, G.; Puskas, J.; Kennedy, J. P. *Polym. Bull. (Berlin)* **1987**, *18*, 123-130.

12. Kennedy, J. P.; Chang, V. S. C.; Smith, R. A.; Ivan, B. *Polym. Bull.* **1979**, *1*, 575-580.

13. Nielsen, L. V.; Nielsen, R. P.; Gao, B.; Kops, J.; Ivan, B. *Polymer* **1997**, *38*, 2529-2534.

14. Harrison, J. J.; Mijares, C. M.; Cheng, M. T.; Hudson, J. *Macromolecules* **2002**, 35, 2494-2500.

15. Keki, S.; Nagy, M.; Deak, G.; Levai, A.; Zsuga, M. *J. Polym. Sci., Part A: Polym. Chem.* **2002**, *40*, 3974-3986.

16.. Ivan, B.; Kennedy, J. P. *J. Polym. Sci., Part A: Polym. Chem.* **1990**, *28*, 89-104.

17. Ivan, B.; Kennedy, J. P.; Chang, V. S. C. *J. Polym. Sci., Part A: Polym. Chem.* **1980**, *18*, 3177-3191.

18. Kennedy, J. P.; Guhaniyogi, S. C.; Percec, V. *Polym. Bull.* **1982**, *8*, 563-570.

19. Kennedy, J. P.; Guhaniyogi, S. C.; Percec, V. *Polym. Bull.* **1982**, *8*, 571-578.

20. Kennedy, J. P.; Storey, R. F. *ACS Org. Coat. Plast. Chem.* **1982**, *46*, 182-185.

21. Nemes, S.; Peng, K. L.; Wilczek, L.; Kennedy, J. P. *Polym. Bull.* **1990**, *24*, 187-194.

22. Storey, R. F.; Donnalley, A. B. *Polym. Prepr. (Am. Chem. Soc. Div. Polym. Chem.)* **1997**, *38*, 174-175.

23. Storey, R. F.; Donnalley, A. B. *Polym. Prepr. (Am. Chem. Soc. Div. Polym. Chem.)* **1997**, *38*, 283-284.

24. Nagy, M.; Keki, S.; Orosz, L.; Deak, G.; Herczegh, P.; Levai, A.; Zsuga, M. *Macromolecules* **2005**, *38*, 4043-4046.

25. Lange, A.; Mach, H.; Rath, H. P.; Karl, U.; Ivan, B.; Groh, P. W.; Nagy, Z. T.; Palfi, V. U.S. Patent 0276,588 A1, 2006 (German Patent 10322164.6, 2004).

26. Kwon, Y.; Faust, R.; Chen, C. X.; Thomas, E. L. *Macromolecules* **2002**, *35*, 3348-3357.

27. Kemp, L. K.; Donnalley, A. B.; Storey, R. F. *J. Polym. Sci., Part A: Polym. Chem.* **2008**, *46*, 3229-3240.

28. Wilczek, L.; Kennedy, J. P. *J. Polym. Sci., Part A: Polym. Chem.* **1987**, *25*, 3255-3265.

29. Roth, M.; Mayr, H. *Macromolecules* **1996**, *29*, 6104-6109.

30. Hadjikyriacou, S.; Faust, R. *Polym. Bull.* **1999**, *43*, 121-128.

31. Simison, K. L.; Stokes, C. D.; Harrison, J. J.; Storey, R. F. *Macromolecules* **2006**, *39*, 2481-2487.

32. Morgan, D. L.; Harrison, J. J.; Stokes, C. D.; Storey, R. F. *Macromolecules* **2011**, *44*, 2438-2443.

33. De, P.; Faust, R. *Polym. Bull.* **2006**, *56*, 27-35.

34. Morgan, D. L.; Stokes, C. D.; Meierhoefer, M. A.; Storey, R. F. *Macromolecules* **2009**, *42*, 2344-2352.

35. Ummadisetty, S.; Morgan, D.L.; Stokes, C.D. ; Storey, R.F. *Macromolecules* **2011**,

44, 7901-7910.

36. Storey, R. F.; Kemp, L. L.; U.S. Patent Application Publication, 2009/0318624 A1, Dec. 24, 2009.

37. Hadjikyriacou, S.; Faust, R. *Macromolecules* **1999**, *32*, 6393-6399.

38. Hadjikyriacou, S.; Faust, R. *J. Macromol. Sci.-Pure Appl.Chem.* **2000**, *A37*, 1333-1352.

39. Martinez-Castro, N.; Lanzendorfer, M. G.; Muller, A. H. E.; Cho, J. C.; Acar, M. H.; Faust, R. *Macromolecules* **2003**, *36*, 6985-6994.

40. Morgan, D. L.; Martinez-Castro, N.; Storey, R. F. *Macromolecules*, **2010**, *43*, 8724-8740.

41. Storey, R. F.; Stokes, C. D.; Harrison, J. J. *Macromolecules* **2005**, *38*, 4618-4624.

42. Martinez-Castro, N.; Morgan, D. L.; Storey, R. F. *Macromolecules* **2009**, *42*, 4963-4971.

43. Morgan, D. L.; Storey, R. F. *Macromolecules* **2010**, *43*, 1329-1340.

44. De, P.; Faust, R. *Macromolecules* **2006**, *39*, 6861-6870.

45. De, P.; Faust, R. *Macromolecules* **2006**, *39*, 7527-7533.

46. Ojiha, U.; Rajkhowa, R.; Agnihotra, S. R.; Faust, R. *Macromolecules* **2008**, *41*, 3832-3841.

47. Jakubowski, W.; Tsarevsky, N. V.; Higashihara, T.; Faust, R.; Matyjaszewski, K. *Macromolecules* **2008**, *41*, 2318-2323.

48. Kaszas, G.; Puskas, J. E.; Kennedy, J. P.; Hager, W. G. *J. Polym. Sci., Part A: Polym. Chem.* **1991**, *29*, 421-426.

49. Kaszas, G.; Puskas, J. E.; Kennedy, J. P.; Hager, W. G. *J. Polym. Sci., Part A: Polym. Chem.* **1991**, *29*, 427-435.

50. Kennedy, J. P.; Puskas, J. E.; Kaszas, G.; Hager, W. G. U.S. Patent 4,946,899, 1990.

51. Storey, R. F.; Chisholm, B. J.; Lee Y. *Polymer* **1993**, *34*, 4330-4335.

52. Storey, R. F.; Chisholm, B. J.; Masse, M.A. *Polymer* **1996**, *37*, 2925-2938.

53. Storey, R. F.; Baugh, D. W., III *Polymer* **2000**, *41*, 3205-3211.

54. Storey, R. F.; Baugh, D. W., III *Polymer* **2001**, *42*, 2321-2330.

55. U.S. FDA TAXUS Express2TM Paclitaxel-eluting coronary stent system (monorail and over the wire), 2004; PO30025.

56. Ranade, S. V.; Miller, K. M.; Richard, R. E.;Chan, A. K.; Allen, M. J.; Helmus, M. N. *J. Biomed. Mater. Res.* **2004**, *71A*, 625-634.

57. Tsunogae, Y.; Kennedy, J. P. *J. Polym. Sci., Part A: Polym. Chem.* **1994**, *32*, 403-412.

58. Li, D.; Faust, R. *Macromolecules* **1995**, *28*, 1383-1389.

59. Kwon, Y.; Cao, X.; Faust, R. *Macromolecules* **1999**, *32*, 6963-6968.

60. Puskas, J. E.; Kaszas, G.; Kennedy, J. P.; Hager, W. G. *J. Polym. Sci., Part A: Polym. Chem.* **1992**, *30*, 41-48.

61. Fodor, Z.; Faust, R. *J. Macromol. Sci.-Pure Appl.Chem.* **1994**, *A31*, 1985-2000.

62. Kennedy, J. P.; Kurian, J. *J. Polym. Sci., Part A: Polym. Chem.* **1990**, *28*, 3725-3738.

63. Sipos, L.; Som, A.; Faust, R.; Richard, R.; Scharz, M.; Ranade, S.; Boden, M.; Chan, K. *Biomacromolecules* **2005**, *6*, 2570-2582.

64. Hadjikyriacou, S.; Faust, R. *Macromolecules* **1995**, *28*, 7893-7900.

65. Zhou, Y.; Faust, R.; Chen, S.; Gido, S. P. *Macromolecules* **2004**, *37*, 6716-6725.

66. Zhou, Y.; Faust, R. *Polym. Bull.* **2004**, *52*, 421-428.

67. Hadjikyriacou, S.; Faust, R. *Macromolecules* **1996**, *29*, 5261-5267.

68. Hadjikyriacou, S.; Fodor, Z.; Faust, R. *J. Macromol. Sci.-Pure Appl.Chem.* **1995**, *A32*, 1137-1153.

69. Schlaad, H.; Erentova, K.; Faust, R.; Charleux, B.; Moreau, M.; Vairon, J. P.; Mayr, H. *Macromolecules* **1998**, *31*, 8058-8062.

70. Yun, J.; Hadjikyriacou, S.; Faust, R. *Polym. Prepr. (Am. Chem. Soc., Div. Polym. Chem.)* **1999**, *40*, 1041-1042.

71. Cao, X.; Sipos, L.; Faust, R. *Polym. Bull.* **2000**, *45*, 121-128.

72. Bae, Y. C.; Fodor, Z.; Faust, R. *Macromolecules* **1997**, *30*, 198-202.

73. Bae, Y. C.; Faust, R. *Macromolecules* **1998**, *31*, 2480-2487.

74. Hadjikyriacou, S.; Faust, R. *Macromolecules* **2000**, *33*, 730-733.

75. Coca, S.; Faust, R. *Macromolecules* **1997**, *30*, 649-651.

76. Marsalkó, T. M.; Majoros, I.; Kennedy, J. P. *J. Macromol. Sci.-Pure Appl.Chem.* **1997**, *A34*, 775-792.

77. Kennedy, J. P.; Ross, L. R.; Nuyken, O. *Polym. Bull*. **1981**, *5*, 5-10.

78. Mishra, M. K.; Wang, B.; Kennedy, J. P. *Polym. Bull.* **1987**, *17*, 307-314.

79. Storey, R. F.; Lee, Y. *J. Macromol. Sci.-Pure Appl.Chem.* **1992**, *A29*, 1017-1030.

80. Shohi, H.; Sawamoto, M.; Higashimura, T. *Macromolecules***1991**, *24*, 4926-4931.

81. Huang, K. J.; Zsuga, M.; Kennedy, J. P. *Polym. Bull.* **1988**, *19*, 43-50.

82. Jacob, S.; Majoros, I.; Kennedy, J. P. *Macromolecules* **1996**, *29*, 8631-8641.

83. Jacob, S.; Kennedy, J. P. *Adv. Polym. Sci.* **1999**, *146*, 1-38.

84. Shim, J. S.; Asthana, S.; Omura, N.; Kennedy, J. P. *J. Polym. Sci., Part A: Polym. Chem.* **1998**, *36*, 2997-3012.

85. Jacob, S.; Kennedy, J. P. *Polym. Bull.* **1998**, *41*, 167-174.

86. Shim, J. S.; Kennedy, J. P. *J. Polym. Sci., Part A: Polym. Chem.* **1999**, *37*, 815-824.

87. Shim, J. S.; Kennedy, J. P. *J. Polym. Sci., Part A: Polym. Chem.* **2000**, *38*, 279-290.

88. Storey, R. F.; Shoemake, K. A. *J. Polym. Sci., Part A: Polym. Chem.* **1998**, *36*, 471-483.

89. Asthana, S.; Kennedy, J. P. *J. Polym. Sci.: Part A: Polym. Chem.* **1999**, *37*, 2235-2243.

90. Fernyhough, C. M.; Young, R. N.; Tack, R. D. *Macromolecules* **1999**, *32*, 5760-5764.

91. Yun, J.; Faust, R. *Macromolecules* **2002,** *35,* 7860-7862.

92. Hadjichristidis, N. *J. Polym. Sci., Part A: Polym. Chem.* **1999**, *37*, 857-871.

93. Lazzari, M.; Liu, G.; Lecommandoux, S. Block Copolymers in Nanoscience; Wiley-VCH: Weinheim, 2007.

94. Zheng, W.; Wang, Z. G. *Macromolecules* **1995**, *28*, 7215-7223.

95. Chen, Z.; Cui, H.; Hales, K.; Li, Z.; Qi, K.; Pochan, D. J.; Wooley, K. L. *J. Am. Chem. Soc.* **2005**, *127*, 8592-8593.

96. Hadjichristidis, N.; Pispas, S.; Floudas, G. *Block Copolymers: SyntheticStrategies, Physical Properties, and Applications*; John Wiley & Sons:Hoboken, NJ, 2003.

97. Abetz, V. *Block Copolymers. Vol 1* Springer: Berlin, 2005.

98. Higashihara, T.; Feng, D.; Faust, R. *Macromolecules* **2006**, *39*, 5275-5279.

99. Higashihara, T.; Faust, R.; Inoue, K.; Hirao, A. *Macromolecules* **2008**, *41*, 5616-5625.

100. Rother, M.; Barqawi, H.; Pfefferkorn, D.; Kressler, J.; Binder, W. H. *Macromol. Chem. Phys.* **2010**, *211*, 204-214.

101. Nasrullah, M. J.; Vora, A.; Webster, D. C. *Macromol. Chem. Phys.* **2011**, *212*, 539-549.

102. Burgess, F. J.; Cunliffe, A. V.; Maccallum, J. R.; Richards, D. H. *Polymer* **1977**, *18*, 719-725; *Polymer* **1977**, *18*, 726-732; *Polymer* **1977**, *18*, 733-740.

103. Nomura, R.; Endo, T. *Macromolecules* **1995**, *28*, 1754-1757.

104. Nomura, R.; Shibasaki, Y.; Endo, T. *Polym. Bull.* **1996**, *37*, 597-601.

105. Feldthusen, J.; Ivan, B.; Muller, A. H. E. *Macromolecules* **1997**, *30*, 6989-6993.

106. Feldthusen, J.; Ivan, B.; Muller, A. H. E. *Macromolecules* **1998,** *31,* 578-585.

107. Feng, D.; Higashihara, T.; Faust, R. *Polymer* **2008**, *49*, 386-393.

108. Matyjaszewski, K. *Macromol. Symp.* **1998**, *132*, 85-101.

109. Zheng, F.; Kennedy, J. P. *J. Polym. Sci., Part A: Polym. Chem.* **2002**, *40*, 3662-3678.

110. Storey, R. F.; Scheuer, A. D.; Achord, B. C. *Polymer* **2005**, *46*, 2141-2152.

111. Storey, R. F.; Scheuer, A. D.; Achord, B. C. *J. Macromol. Sci.-Pure Appl.Chem.* **2006**, *A43*, 1493-1512.

112. Coca, S.; Matyjaszewski, K. *Macromolecules* **1997**, *30*, 2808-2810.

113. Jakubowski, W.; Tsarevsky, N. V.; Higashihara, T.; Faust, R.; Matyjaszewski, K. *Macromolecules* **2008**, *41*, 2318-2323.

114. Coca, S., Matyjaszewski, K. *J. Polym. Sci., Part A: Polym. Chem.* **1997**, *35*, 3595-3601.

115. Magenau, A. J. D.; Martinez-Castro, N.; Savin, D. A.; Storey, R. F. *Macromolecules* **2009**, *42*, 2353-2359.

116. Magenau, A. J. D.; Martinez-Castro, N.; Storey, R. F. *Macromolecules* **2009**, *42*, 8044-8051.

117. Feng, D.; Chandekar, A.; Whitten, J. E.; Faust, R. *Polym. Prepr. (Am. Chem. Soc., Div. Polym. Chem.)* **2007**, *48*, 1017-1018.

118. Martinez-Castro, N.; Zhang, M.; Pergushov, D. V.; Mueller, A. H. E. *Des. Monomers Polym.* **2006**, *9*, 63-79.

119. Kwon, Y.; Faust, R. *J. Macromol. Sci.-Pure Appl. Chem.* **2005**, *A42*, 385-401.

120. Keszler, B.; Fenyvesi, G.; Kennedy, J. P. *J. Polym. Sci., Part A: Polym. Chem.* **2000**, *38*, 706-714.

121. Toman, L.; Janata, M.; Spevacek, J.; Vlcek, P.; Latalova, P.; Masar, B.; Sikora, A. *J. Polym. Sci., Part A: Polym. Chem.* **2004**, *42*, 6098-6108.

122. Toman, L.; Janata, M.; Spevacek, J.; Vlcek, P.; Latalova, P.; Silora, A.; Masar, B. *J. Polym. Sci., Part A: Polym. Chem.* **2005**, *43*, 3823-3830.

123. Puts, R. D.; Sogah, D. Y. *Macromolecules* **1997**, *30*, 7050-7055.

124. Weimer, M. W.; Scherman, O. A.; Sogah, D. Y. *Macromolecules* **1998**, *31*, 8425-8428.

125. Hawker, C. J.; Hedrick, J. L.; Malmstrom, E. E.; Trollsas, M.;Mecerreyes, D.; Moineau, G.; Dubois, P.; Jerome, R. *Macromolecules* **1998**, *31*, 213-219.

126. Lim, N. K.; Arndtsen, B. A. *Macromolecules* **2000**, *33*, 2305-2307.

127. Klaerner, G.; Trollsas, M.; Heise, A.; Husemann, M.; Atthoff, B.; Hawker, C. J.; Hedrick, J. L.; Miller, R. D. *Macromolecules* **1999**, *32*, 8227-8229.

128. Sioula, S.; Hadjichristidis, N.; Thomas, E. L. *Macromolecules* **1998**, *31*, 8429-8432.

129. Liu, H.; Xu, J.; Jiang, J.; Yin, J.; Narain, R.; Cai, Y.; Liu, S. *J. Polym. Sci., Part B: Polym. Phys.* **2007**, *45*, 1446-1462.

130. Glaied, O.; Delaite, C.; Dumas, P. *J. Polym. Sci., Part B: Polym. Phys.* **2006**, *44*, 1796-1806.

131. Glaied, O.; Delaite, C.; Dumas, P. *J. Polym. Sci., Part B: Polym. Phys.* **2007**, *45*, 968-974.

132. Bernaerts, K. V.; Schacht, E. H.; Goethals, E. J.; Du Prez, F. E. *J. Polym. Sci., Part A: Polym. Chem.* **2003**, *41*, 3206-3217.

133. Guo, Y.; Xu, J. ; Pan, C. *J. Polym. Sci., Part B: Polym. Phys.* **2001**, *39*, 437-445.

134. de Geus, M.; Peeters, J.; Wolffs, M.; Hermans, T.; Palmans, A. R. A.; Koning, C. E.; Heise, A. *Macromolecules* **2005**, *38*, 4220-4225.

135. Kajiwara, A.; Matyjaszewski, K. *Macromolecules* **1998**, *31*, 3489-3493.

136. Mecerreyes, D.; Moineau, G.; Dubois, P.; Jerome, R.; Hedrick, J. L.; Hawker, C. J.; Malmstrom, E. E.; Trollsas, M. *Angew. Chem., Int.Ed.* **1998**, *37*, 1274-1276.

137. Bernaerts, K. V.; Willet, N.; Camp, W. V. ; Jerome, R.; Du Prez, F. E. *Macromolecules* **2006**, *39*, 3760-3769.

138. Meyer, U.; Palmans, A. R. A.; Loontjens, T.; Heise, A. *Macromolecules* **2002**, *35*, 2873-2875.

139. Merreceyes, D.; Atthoff, B.; Boduch, K. A.; Trollsas, M.; Hedrick, J. L. *Macromolecules* **1999**, *32*, 5175-5182.

140. Xu, Y.; Pan, C.; Tao, L. *J. Polym. Sci., Part A: Polym. Chem.* **2000**, *38*, 436-443.

141. Heise, A.; Trollsas, M.; Magbitang, T.; Hedrick, J. L.; Frank, C. W.; Miller, R. D. *Macromolecules* **2001,** *34,* 2798-2804.

142. Tunca, U.; Karhga, B.; Ertekin, S.; Ugur, A. L.; Sirkeciogiu, O.; Hizal, G. *Polymer* **2001**, *42*, 8489-8493.

143. Tunca, U.; Erdogan, T.; Hizal, G. *J. Polym. Sci., Part A: Polym. Chem.* **2002**, *40*, 2025-2032.

144. Tunca, U.; Ozyurek, Z.; Erdogan, T.; Hizal, G. *J. Polym. Sci., Part A: Polym. Chem.* **2004**, *42*, 4228-4236.

145. He, T.; Li, D.; Sheng, X.; Zhao, B. *Macromolecules* **2004**, *37*, 3128-3135.

146. Matyjaszewski, K.; Davis, T. P. *Handbook of Radical Polymerization*; John Wiley & Sons, Inc.: Hoboken, NJ, 2002.

147. Kato, M.; Kamigaito, M.; Sawamoto M.; Higashimura, T. *Macromolecules* **1995**, *28*, 1721-1723.

148. Wang, J. S.; Matyjaszewski, K. *J. Am. Chem. Soc.* **1995**, *117*, 5614-5615.

149. Percec, V.; Barboiu, B. *Macromolecules* **1995**, *28*, 7970-7972.

150. Wang, J. S.; Matyjaszewski, K. *Macromolecules* **1995**, *28*, 7901-7910.

151. Patten, T. E.; Xia, J. H.; Abernathy T.; Matyjaszewsk, K. *Science* **1996**, *272*, 866-868.

152. Matyjaszewski, K.; Patten, T. E.; Xia, J. H. *J. Am. Chem. Soc.* **1997**, *119*, 674-680.

153. Percec, V.; Barboiu, B.; Neumann, A.; Ronda, J. C.; Zhao, H. *Macromolecules* **1996**, *29*, 3665-3668.

154. Matyjaszewski, K.; Jo, S. M.; Paik H. J.; Gaynor, S. G. *Macromolecules* **1997**, *30*, 6398-6400.

155. Granel,C.; Dubois, P.; Jerome, R.; Teyssie, P. *Macromolecules* **1996**, *29*, 8576-8582.

156. Nishikawa, T.; Ando, T.; Kamigaito, M.; Sawamoto, M. *Macromolecules* **1997**, *30*, 2244-2248.

157. Uegaki, H.; Kotani, Y.; Kamigaito, M.; Sawamoto, M. *Macromolecules* **1997**, *30*, 2249-2253.

158. Matyjaszewski, K.; Jo, S. M.; Paik, H. J.; Shipp, D. A. *Macromolecules* **1999**, *32*, 6431-6438.

159. Grimaud, T.; Matyjaszewski, K. *Macromolecules* **1997**, *30*, 2216-2218.

160. Matyjaszewski, K.; Gaynor, S. G.; Kulfan, A.; Podwika, M. *Macromolecules* **1997**, *30*, 5192-5194.

161. Matyjaszewski, K.; Gaynor, S. G.; Muller, A. H. E. *Macromolecules* **1997**, *30*, 7034-7041.

162. Matyjaszewski, K. Gaynor, S. G. *Macromolecules* **1997**, *30*, 7042-7049.

163. Gaynor, S. G.; Edelman, S.; Matyjaszewski, K. *Macromolecules* **1996**, *29*, 1079-

1081.

164. Matyjaszewski, K.; Pyun, J.; Gaynor, S. G. *Macromol. Rapid Commun.* **1998**, *19*, 665-670.

165. Patten, T. E.; Matyjaszewski, K. *Adv. Mater.* **1998**, *10*, 901-915.

166. Hawker, C. J.; Bosman, A. W.; Harth, E. *Chem Rev* **2001**, *101*, 3661-3688.

167. Matyjaszewski, K.; Xia, J. H. *Chem Rev* **2001,** *101*, 2921-2990.

168. Matyjaszewski, K.; Gaynor, S.; Greszta, D.; Mardare, D.; Shigemoto, T. *J. Phys. Org. Chem.* **1995**, *8*, 306-315.

169. Matyjaszewski, K. *J. Phys. Org. Chem.* **1995**, *8*, 197-207.

170. Matyjaszewski, K.; Natagawa, Y.; Gaynor, S. G. *Macromol. Rapid Commun.* **1997**, *18*, 1057-1066.

171. Coessens, V.; Matyjaszewski, K. *J. Macromol. Sci.-Pure Appl.Chem.* **1999**, *A36*, 811-826.

172. Coessens, V.; Nakagawa, Y.; Matyjaszewski, K. *Polym. Bull.* **1998**, *40*, 135-142.

173. Coessens, V.; Matyjaszewski, K. *Macromol. Rapid Commun.* **1999**, *20*, 127-134.

174. Coessens, V.; Matyjaszewski, K. *J. Macromol. Sci.-Pure Appl.Chem.* **1999**, *A36*, 653-666.

175. Coessens, V.; Matyjaszewski, K. *Macromol. Rapid Commun.* **1999**, *20*, 66-70.

176. Bon, S. A. F.; Steward, A. G.; Haddleton, D. M. *J. Polym. Sci., Part A: Polym. Chem.* **2000**, *38*, 2678-2686.

177. Coessens, V.; Pyun, J.; Miller, P. J.; Gaynor, S. G.; Matyjaszewski, K. *Macromol. Rapid Commun.* **2000**, *21*, 103-109.

178. Ando, T.; Kamigaito M.; Sawamoto, M. *Macromolecules* **1998**, *31*, 6708-6711.

179. Ellzey, K. A.; Novak, B. M. *Macromolecules* **1998**, *31*, 2391-2393.

180. Bernaerts, K. V.; Du Prez, F. E. *Polymer* **2005**, *46*, 8469-8482.

181. Becer, C. R.; Paulus, R. M.; Hoppener, S.; Hoogenboom, R.; Fustin, C. A.; Gohy, J. F.; Schubert, U. S. *Macromolecules* **2008**, *41*, 5210-5215.

182. Breland, L. K.; Murphy, J. C.; Storey, R. F. *Polymer* **2006**, *47*, 1852-1860.

183. Takacs, A.; Faust, R. *J. Macromol. Sci.-Pure Appl.Chem.* **1996**, *A33*, 117-131.

184. Breland, L. K.; Storey, R. F. *Polymer* **2008**, *49*, 1154-1163.

185. Hamley, I. *The Physics of Block Copolymers*; Oxford University Press: Oxford, UK, 1998.

186. Hamley, I. W. *Block Copolymers in Solution: Fundamentals and Applications*; Wiley: Hoboken, NJ, 2005.

187. Hamley, I. W. *Development in Block Copolymer Science and Technology*; Wiley: Chichester, UK, 2004.

188. Fredrickson, G. H.; Bates, F. S. *Annu. Rev. Phys. Chem.* **1990**, *41*, 525-557.

189. Khandpur, A. K.; Forster, S.; Bates, F. S. Hamley, I. W.; Ryan, A. J.; Bras, W.; Almadal, K.; Mortensen, K. *Macromolecules* **1995**, *28*, 8796-8806.

190. Matsen, M. W.; Bates, F. S. *J. Polym. Sci., Part B: Polym. Phys.* **1998**, *35*, 945-952.

191. Milner, S. T. *Macromolecules* **1994**, *27*, 2333-2335.

192. Mogi, Y.; Kotsuji, H.; Kaneko, Y.; Mori, K.; Matsushita, Y.; Noda, I. *Macromolecules* **1992**, *25*, 5408-5411.

193. Gido, S. P.; Schwark, D. W.; Thomas, E. L.; Goncalves, M. *Macromolecules* **1993**, *26*, 2636-2640.

194. Jabbarzadeh, A.; Atkinson, J. D.; Tanner, R. I. *Macromolecules* **2003**, *36*, 5020-5031.

195. Pispas, S.; Hadjichristidis, N.; Potemkin, I.; Khokhlov, A. *Macromolecules* **2000**, *33*, 1741-1746.

196. Wang, X.; Xia, J.; He, J.; Yu, F.; Li, A.; Xu, J.; Lu, H.; Yang, Y. *Macromolecules* **2006**, *39*, 6898-6904.

197. Gido, S. P.; Lee, C.; Pochan, D. J.; Pispas, S.; Mays, J. W.; Hadjichristidis, N. *Macromolecules* **1996**, *29*, 7022-7028.

198. Lee, J. S.; Quirk, R. P.; Foster, M. D. *Macromolecules* **2005**, *38*, 5381-5392.

199. Yamaguchi, K.; Takahashi, K.; Hasegawa, H.; Iatrou, H.; Hadjichristidis, N.; Kaneko, T.; Nishikawa, Y.; Jinnai, H.; Matsui, T.; Nishioka, H.; Shimizu, M.; Furukawa, H. *Macromolecules* **2003**, *36*, 6962-6966.

200. Sioula, S.; Hadjichristidis, N.; Thomas, E. L. *Macromolecules* **1998**, *31*, 5272-5277.

201. Huckstadt, H.; Gopfert, A.; Abetz, V. *Macromol. Chem. Phys.* **2000**, *201*, 296-307.

202. Birshtein, T. M.; Polotsky, A. A.; Abetz, V. *Macromol. Theory Simul.* **2004**, *13*, 512-519.

203. Tezuka, Y.; Oike, H. *J. Am. Chem. Soc.* **2001**, *123*, 11570-11576.

204. Wetzel, E. D.; Beyer, F. L. *Self-assembling nanomembranes through electrostatic melt processing of copolymer films*, ARL-TR-2800, U.S. Army Research Laboratory, Aberdeen Proving Ground, MD 2002.

205. Crawford, D. M.; Napadensky, E.; Beck Tan, N.; Sloan, J.; Reuschle, D. A.; Mountz, D. A.; Mauritz, K. A.; Laverdure, K. S.; Gido, S. P.; Liu, W.; Hsiao, B. *Semipermeable Membrane From Ionomeric Self-Assembling Block Copolymer* ARL-TR-2403, U.S. Army Research Laboratory, Aberdeen Proving Ground, MD 2001.

206. Napadensky, E.; Crawford, D.; Sloan, J.; Beck Tan, N. *Viscoelastic and Transport Properties of Sulfonated PS-PIB-PS Block Copolymers* ARL-TR-2482, U.S. Army Research Laboratory, Aberdeen Proving Ground, MD 2001.

207. Mauritz, K. A.; Storey, R. F.; Reuschle, D. A.; Beck Tan, N. *Polymer* **2002**, *43*, 5949-5958.

208. Mountz, D. A.; Storey, R. F.; Mauritz, K. A. *J. Polym. Sci., Part B: Polym. Phys.* **2005**, *43*, 764-776.

209. Kopchick, J. G.; Storey, R. F.; Beyer, F. L.; Mauritz, K. A. *Polymer* **2008**, *48*, 3739-3748.

210. Tuzar, Z.; Kratochvil, P. *Micelles of Block and Graft Copolymers in Solutions in Surface and Colloid Science*; Plenum: New York, 1993.

211. Dongen, S. F. M.; Hoog, H. M.; Peters, R. J. R. W.; Nallani, M.; Nolte, R. J. M.; Hest, J. C. M. *Chem. Rev.* **2009**, *109,* 6212-6274.

212. Adams, M. L.; Lavasanifar, A.; Kwon, G. S. *J. Pharm. Sci.* **2003**, *92*, 1343-1355.

213. Discher, B. M.; Hammer, D. A.; Bates, F. S.; Discher, D. E. *Curr. Opin. Colloid Interface Sci.* **2000**, *5*, 125-131.

214. Discher, B. M.; Won, Y. Y.; Ege, D. S.; Lee, J. C. M.; Bates, F. S.; Discher, D. E.; Hammer, D. A. *Science* **1999**, *284*, 1143-1146.

215. Lee, J. C.; Bermudez, H.; Discher, B. M.; Sheehan, M. A.; Won, Y. Y.; Bates, F. S.; Discher, D. E. *Biotechnol. Bioeng.* **2001**, *73*, 135-145.

216. Photos, P. J.; Bacakova, L.; Discher, B.; Bates, F. S.; Discher, D. E. *J. Controlled Release* **2003**, *90*, 323-334.

217. Merrett, F. M. *Trans. Faraday Soc.* **1954**, *50*, 759-767.

218. Hawker, C. J.; Wooley, K. L. *Science* **2005**, *309*, 1200-1205.

219. Gohy, J. F. *Adv. Polym. Sci.* **2005**, *190*, 65-136.

220. Riess, G. *Prog. Polym. Sci.* **2003**, *28*, 1107-1170.

221. Cameron, N. S.; Corbierre, M. K.; Eisenberg, A. *Can. J. Chem.* **1999**, *77*, 1311-1326.

222. Forder, C.; Patrickios, C. S.; Armes, S. P.; Billingham, N. C. *Macromolecules* **1996**, *29*, 8160-8169.

223. Lutz, J. F. *Polym. Int.* **2006**, *55*, 979-993.

224. Colfen, H. *Macromol. Rapid Commun.* **2001**, *22*, 219-252.

225. Yu, G.; Eisenberg, A. *Macromolecules* **1998**, *31*, 5546-5549.

226. Zhou, Z.; Li, Z.; Ren, Y.; Hillmyer, M. A.; Lodge, T. P. *J. Am. Chem. Soc.* **2003**, *125*, 10182-10183.

227. Lodge, T. P.; Hillmyer, M. A.; Zhou, Z.; Talmon, Y. *Macromolecules* **2004**, *37*, 6680-6682.

228. Kubowicz, S.; Baussard, J. F.; Lutz, J. F.; Thünemann, A. F.; von Berlepsch, H.; Laschewsky, A. *Angew. Chem., Int. Ed.* **2005**, *44*, 5262-5265.

229. Hadjichristidis, N.; Iatrou, H.; Pitsikalis, M.; Pispas, S.; Avgeropoulos, A. *Prog. Polym. Sci.* **2005**, *30*, 725-782.

230. Hadjichristidis, N.; Pispas, S. *Adv. Polym. Sci.* **2006**, *200*, 37-55.

231. Hamley, I. W. *The Physics of Block Copolymers*; Oxford University Press: Oxford, 1998.

232. Zhulina, E. B.; Borisov, O. V. *Macromolecules* **2008**, *41*, 5934-5944.

233. Lutz, J. F.; Laschewsky, A. *Macromol. Chem. Phys.* **2005**, *206*, 813-817.

234. Pispas, S.; Poulos, Y.; Hadjichristidis. N. *Macromolecules* **1998**, *31*, 4177-4181.

235. Li, Z.; Kesselman, E.; Talmon, Y.; Hillmyer, M. A.; Lodge, T. P. *Science* **2004**, *306*, 98-101.

236. Saito, N.; Liu, C.; Lodge, T. P.; Hillmyer, M. A. *Macromolecules* **2008**, *41*, 8815-8822.

237. Saito, N.; Liu, C.; Lodge, T. P.; Hillmyer, M. A. *ACS Nano*, **2010**, *4*, 1907-1912.

238. Brannan A. K.; Bates, F. S. *Macromolecules* **2004**, *37*, 8816-8819.

239. Gomez, E. D.; Rappl, T. J.; Agarwal, V.; Bose, A.; Schmutz, M.; Marques, C. M.; Balsara, N. P. *Macromolecules* **2005**, *38*, 3567-3570.

240. Cui, J., Jiang, W. *Langmuir* **2011**, *27*, 10141-10147.

241. Chance, R. R.; Baniukiewicz, S. P.; Mintz, D.; Ver Strate, G.; Hadjichristidis, N. *Int. J. Polym. Anal. Char.* **1995**, *1*, 3-34.

242. Storey, R. F.; Donnalley, A. B.; Maggio, T. L. *Macromolecules* **1998**, *31*, 1523-1526.

243. Iovu, M. C.; Jeffries-EL, M.; Sheina, E. E.; Cooper, J. R.; McCullough, R. D. *Polymer* **2005**, *46*, 8582-8586.

244. It is common to observe olefinic end groups in $TiCl_4$-co-initiated isobutylene polymerizations at higher temperatures such as those reported here, e.g. -50 °C. These structures result from unimolecular proton transfer to the paired counterion. This process does not cause loss of control over molecular weight, nor does it create any chains without the desired ATRP initiating sites because the eliminated proton cannot initiate a new chain in the presence of proton traps and/or strong bases such as 2,6-lutidine. These concepts are discussed in detail in the following paper: Fodor, Z.; Bae, Y. C.; Faust, R. *Macromolecules* **1998**, *31*, 4439-4446.

245. Balogh, L.; Takacs, A.; Faust, R. *ACS Div. Polym. Chem., Polym. Preprs.* **1992**, *33*, 958-959.

246. Storey, R. F.; Choate, K. R., Jr. *Macromolecules* **1997**, *30*, 4799-4806.

247. Smith, Q. A.; Storey, R. F. *Macromolecules* **2005**, *38*, 4983-4988.

248. Brar, A. S.; Goyal, A. K.; Hooda, S. *J. Mol. Struct.* **2008**, *885*, 15-17.

249. Zhu, Y.; Storey, R. F. *Macromolecules* **2010**, *43*, 7048-7055.

250. Cook, D. *Can. J. Chem.* **1963**, *41*, 522-526.

251. Saied, O.; Bachand, B.; Wuest, J. D. *Can. J. Chem.* **1998**, *76*, 490-497.

252. Faust, R.; Ivan, B.; Kennedy, J. P. *J. Macromol. Sci.-Chem.* **1991**, *A28*, 1-13.

253. Mayr, H.; Roth, M.; Deters, M. *Macromolecules* **1997**, *30*, 3965-3970.

254. Mayr, H.; Striepe, W. *J. Org. Chem.* **1983**, *48*, 1159-1165.

255. Robson F. Storey, Kim R. Choate Jr. *Macromolecular Symposia* **1995**, *95*, 71-78.

256. Schlaad, H.; Kwon, Y.; Faust, R.; Mayr, H. *Macromolecules* **2000**, *33*, 743-747.

257. Faust, R. *Macromol. Symp.* **1994**, *85*, 295-306.

258. Kopchick, J. G.; Storey, R. F.; Jarrett, W. L.; Mauritz, K. A. *Polymer* **2008**, *49*, 5045-5052.

259. Ivan, B.; Kennedy, J. P.; Plamthottam, S. S.; Kelen, T.; Tüdos, F. *J. Polym. Sci., Polym. Chem. Ed.* **1980**, *18*, 1685-1692.

260. Cheon, C. H.; Yamamoto, H. *J. Am. Chem. Soc.* **2008**, *130*, 9246-9247 (Supporting Information).

261. Minisci, F.; Recupero, F.; Cecchetto, A.; Gambarotti, C.; Punta, C.; Paganelli, R.; Pedulli, G. F.; Fontana, F. *Org. Proc. Res. Dev.* **2004**, *8*, 163-168.

262. Liu, R.; Zhang, P.; Gan, T.; Cook, J. M. *J. Org. Chem.* **1997,** *62,* 7447-7456.

263. Chen, X.; Ivan, B.; Kops, J.; Batsberg, W. *Macromol. Rapid. Comm.* **1998**, *19*, 585-589.

264. Suchoparek, M.; Spevacek, J. *Macromolecules* **1993**, *26*, 102-106.